THE APPLICATION OF CONDITIONAL REPROGRAMMING TO DRUG DISCOVERY AND REGENERATIVE MEDICINE

A Dissertation
submitted to the Faculty of the
Graduate School of Arts and Sciences
of Georgetown University
in partial fulfillment of the requirements for the
degree of
Doctor of Philosophy
in Biochemistry, Molecular and Cellular Biology

By

Faris Abdullah Alkhilaiwi., M.S.

Washington, DC
October 30, 2018

THE APPLICATION OF CONDITIONAL REPROGRAMMING TO DRUG DISCOVERY AND REGENERATIVE MEDICINE

Faris Abdullah Alkhilaiwi, M.S.

Thesis Advisor: Richard Schlegel, M.D., Ph.D.

ABSTRACT

The Conditional Reprogramming (CR) method has been shown to induce an in vitro stem-like state allowing for the continuous growth of patient-derived epithelial cells. Due to this new culture system, it has been possible to identify potential therapies for multiple cancer types and to generate differentiated tissue from cultures of normal epithelial cells. Hence, CR has broad applications in the field of drug discovery and regenerative medicine.

Based upon the above findings, we evaluate the ability of CR to identify potential drugs to treat a rare but morbid disease called recurrent respiratory papillomatosis (RRP). A robotic high-throughput screening was performed in collaboration with the National Center for Advanced Technology (NCATS). The conditionally reprogrammed cells, GUMC-403 cells, were screened against two libraries of >4700 drugs. From the two libraries, we identified a total of 13 drugs that induced substantial cytotoxicity in GUMC-403. Furthermore, we validated the efficacy of the drugs in vitro using 2D and 3D models and further polished our list of drugs to panobinostat, dinaciclib and forskolin as potential treatments for RRP patients.

On another front, we investigated the ability of conditional reprogramming to propagate equine keratinocyte cultures for long-term expansion. 3D air-liquid interface culture was used to investigate the ability of CR equine keratinocytes to differentiate and form stratified squamous epithelium that was positive for terminal differentiation markers. These unlimited supplies

of autologous cells could be used to generate skin transplants without the risk of immune rejection.

Our work indicates that conditional reprogramming is a robust method that allows for the rapid and continued in vitro propagation of primary cancer cells or normal equine keratinocytes that can be used for drug discovery or regenerative medicine respectively.

ACKNOWLEDGMENTS

This dissertation is dedicated to Abdullah Alkhilaiwi and Nora AlAwaji.

I would also like to acknowledge and give special thanks to my committee members, Prof. Richard Schlegel, Prof. Amrita Cheema, Prof. Aykut Uren, Dr. Ian Gallacano, Dr. Hang Yuan, for continued guidance, support, and motivation during my ride in Ph.D program. Also, I would like to thank Dr. Craig Thomas, Kelli Wilson, Rajarshi Guha and Marc Ferrer from the NIH for their help in the drug screening project. I would also like to extend my gratitude to the friends who I have worked alongside: Lama Alhawas, Sara Maimouni, Rami Mosaoa, Nouran Abu Alsaud, and Mina Adnani. They have encouraged me, provided insight and reagents that helped me grow and learn more. I must thank the efforts of the students I have mentored who have contributed and assisted me in my projects: Feibai Wang, liqing Wang and Shawn Dziepak. Furthermore, thank you to Dr.Schlegel's lab crew from senior scientists and research specialists who helped me greatly in mastering many skills in order to become a multidisciplinary scientist.

Faris Alkhilaiwi

TABLE OF CONTENTS

LIST OF FIGURES

LIST OF TABLES

ABBREVIATIONS

2D: Two-dimensional

3D: Three-dimensional

AFSC: Amniotic fluid-derived stem cells

ALK: Anaplastic lymphoma kinase

AMP: Adenosine monophosphate

AORP: Adult onset recurrent respiratory papillomatosis

ASC: Adult stem cells

ATCC: American type culture collection

AUC: Area under the curve

BAC: Bacterial artificial chromosome

BPE: Bovine pituitary extract

CAR-T: Chimeric antigen receptors

CDK: Cyclin-dependent kinases

CK: Cytokeratin

CR: Conditional reprogramming

DDTX: Deceased-donor transplantation

DMEM: Dulbecco's modified eagle medium

DMSO: Dimethyl sulfoxide

DNA: Deoxyribonucleic acid

EDTA: Ethylene diaminetetra acetic acid

EGFR: Epidermal growth factor receptor

EK-1547, EK-100: Equine keratinocytes

EMEM: Eagle's minimum essential medium

FACS: Fluorescence-activated cell sorting

FBS: Fetal bovine serum

FDA: Food and drug administration

FISH: Fluorescence in situ hybridization

FISH: Fluorescent in situ hybridization

GAPDH: Glyceraldehyde 3-phosphate dehydrogenase

GIST: Gastrointestinal stromal tumor

GUMC: Georgetown university medical center

HDAC: Histone deacetylases

HER2: Human epidermal growth factor receptor 2

HFK: Human foreskin keratinocyte

HPV: Human papillomavirus

HTS: High-throughput screening

IACUC: Institutional animal care and use committee

IRB: Institutional review board

JORRP: Juvenile onset recurrent respiratory papillomatosis

K9: Canine cells

KSFM: Human keratinocyte medium

LCR: Locus control region

MCTS: Multicellular tumor spheroid

MET: Mesenchymal to epithelial transition

MIPE: Mechanism interrogation plate

MSCs: Mesenchymal stem cells

NCATS: National center for advanced technology sciences

NPC: NCGC pharmaceutical collection

PCR: Polymerase chain reaction

PCR: Polymerase chain reaction

PDs: Population doublings

Prb: Retinoblastoma protein

RAS: Retrovirus-associated DNA sequences

RCA: Rolling circle amplification

RLL: Right lower lobe

ROCK: Rho-associated protein kinase

RRP: Recurrent respiratory papillomatosis

RTCA: Real time cell analysis

SC: Stem cells

TGF-β: Transforming growth factor-beta

eiPSCs: Equine induced pluripotent stem cells

mESCs: Mouse embryonic stem cell

INTRODUCTION

Immortalized Cells vs. Primary Cells

Immortalized cell culture studies offer a treasured complement to *in vivo* experiments, allowing for a more measured manipulation of cellular processes and functions. Almost 70 years ago was the first epithelial immortalized human cancer cell line, HeLa, which was established and isolated from human cervical cancer tissue. Since then Hela cells have been broadly used as a model for cancer research to investigate the pathogenesis and the potential treatments for cervical cancer [1]. Another example is the MCF-7 cell line which was established in 1973 from human breast adenocarcinoma. These cells overexpress estrogen receptors making them a useful model system to investigate the tamoxifen and antiestrogen agents that led to speed breast cancer treatment development and contributed to breast cancer research [2, 3]. For decades, immortalized cell lines have contributed to medical advancements, yet scientists have become progressively thoughtful when interpreting data produced from cell lines only, especially since some of the utilized cell lines have been contaminated or misidentified or don't represent the genetic phenotype properties of primary tumors [4, 5]. In a very "conservative" estimation, scientists have reported an approximate of 32,755 articles to be based on contaminated or misidentified cell lines with a half million papers citing these contaminated literatures [6]. This has sparked interest in primary culture of tumors [4, 5]. Dissimilar to cell lines, primary cells isolated and propagated directly from the tumor or normal tissue as cell suspension or as an explant without genetic manipulation, typically they recapitulate the tumor or original tissue characteristics including genotype and phenotype features [7, 8]. Therefore, primary cells have become a useful tool for regenerative medicine and drug discovery since, compared to immortalized cell lines, they are more reflective of the in vivo condition.

Conditional Reprogramming Culture (CR)

There are numerous challenges to culture human cells in vitro, mainly in comparison to other prokaryotic and mammalian cells. Inconsistency of launching long-term cell culture, elongated population doubling times, Limited lifespan "Hayflick phenomenon", and the high risk of genetic instability in later passages are the most common challenges of primary human cell cultures [9]. Collectively, these limitations deliver a finite capacity for specific human cell lines and limit the number of experiments that can be applied on the same population of cells. In order to obtain long-term, immortalized culture to allow continued studies, the HPV16 E6 and E7 viral oncogenes are frequently used to increase the likelihood of immortalization of human cells in vitro but still present their own restrictions [10]. One of the limitations is the risk of transforming normal human cell lines into atypical malignant human cell lines [9, 11]. Furthermore, scientists have used other methods also to immortalized cells in culture such as radiation, carcinogenic reagents, and viral oncogenes large T antigen SV 40 [12–15]. Nevertheless, the debate on whether the oncogenic transformation of human cell lines is theoretically considered biologically normal remains to be settled, resulting in questionable outcomes in relation to in vitro treatment efficacy. Also, it should be understood that, although immortalization procedures can generate cells with a wanted phenotype, the cells are transformed and unpredicted results can be obtained when working with such cell lines. For instance, when the ras oncogene was introduced into Schwann cells that are not expressing SV40 LT Ag, the ras oncogene induced a rapid growth halt. However, when the same ras oncogene was introduced in Schwann cells expressing SV40 LT Ag that changed these cells from growth factor dependent slow growing cells into rapidly dividing cells that are able of growing in a mitogen-free medium [16].

Conditional reprogramming (CR) is a novel method in cell culture arena that allows for establishing and propagating cells forever from tumor and normal tissues without any genomic manipulation such as transduction of cellular genes or exogenous viral. Moreover, in disparity to the selection of rare stem-like cells, the conditional reprogramming (CR) can generate almost two million cells in less than a week from needle biopsies, and can generate cultures from fresh or cryopreserved tissue. This system also competently established cell cultures from rodent and human tumors.

It utilizes two essential factors: 1) irradiated mouse fibroblast (Swiss 3T3 J2) and 2) Rho kinase inhibitor (Y-27632) (Figure I). Recently, it has been shown that conditional reprogramming can indefinitely propagate nonkeratinocyte epithelial cells (e.g., liver, prostate, lung, and breast) and human keratinocytes in vitro by culturing with a Rho kinase (ROCK) inhibitor, Y-27632 and irradiated fibroblast feeder cells. Since both tumor and normal cells can be cultured using the method, conditional reprogramming is providing opportunities for phenotypic and genetic characterization, including chemosensitivity testing [9, 14].

Because of the conditional stimulation of cell propagation, these cultures are named conditionally reprogrammed cells (CRCs) and deliver many opportunities for regenerative and personalized medicine.

A

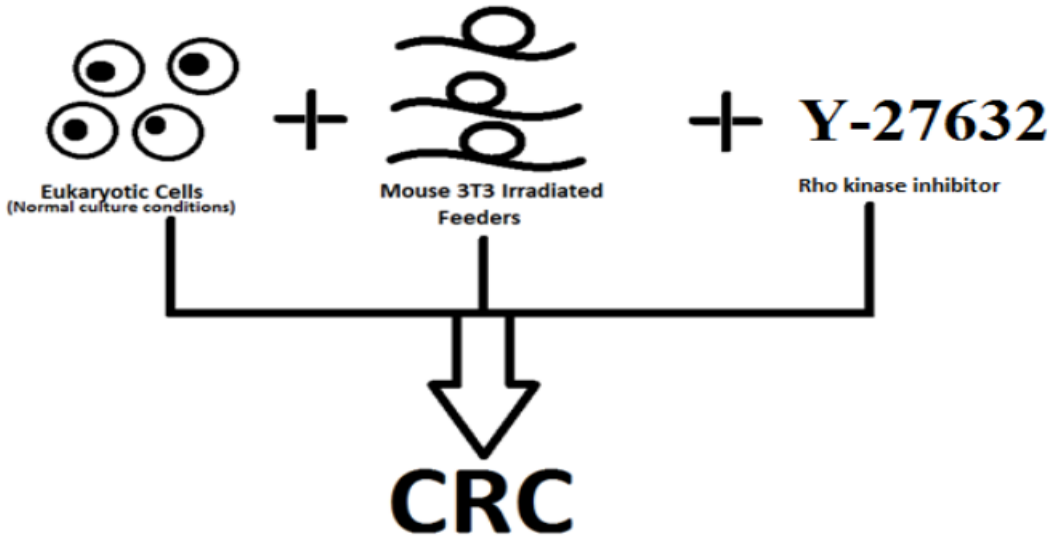

B

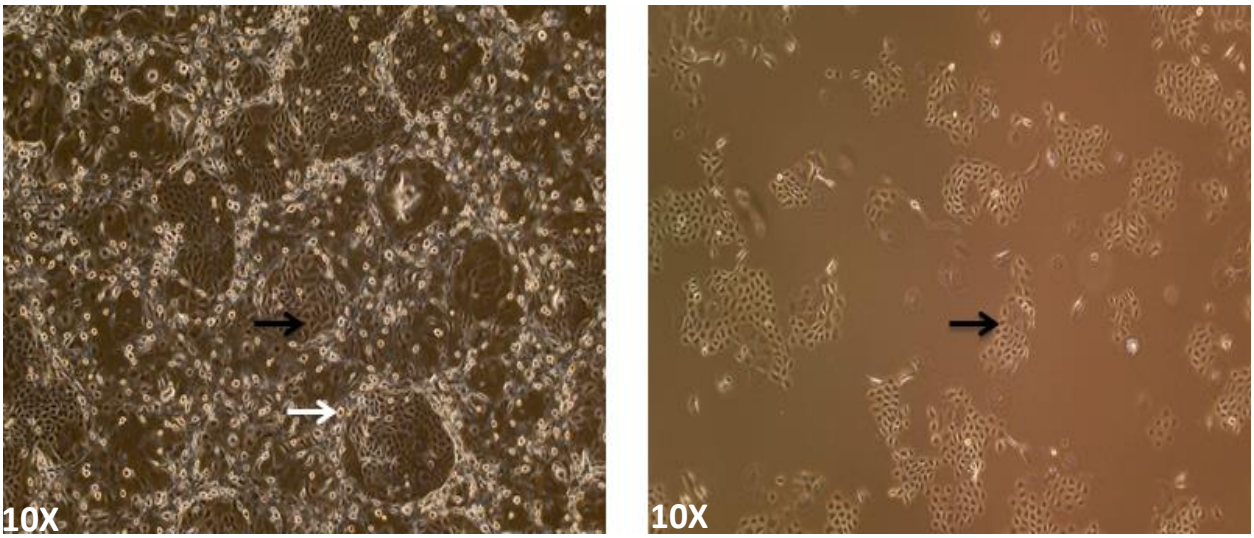

Figure I. Schematic diagram of conditional reprogramming (CR) culture. (A) Essential components in CR condition where feeders and Y compound are needed. (B) Human foreskin cells in full CR conditions in presence of feeders and the Y compound (left) or in conditioned media without the feeders (Right). (Magnification is 10X) white arrows indicate irradiated j2 and black arrows indicate keratinocytes.

The first factor is the use of irradiated mouse fibroblasts (feeders). The feeder cells need to be irradiated to halt their proliferation and avoid their overgrowth in co-culture with the epithelial cells [9, 17, 18]. Also, irradiation is critical to produce factors in the feeders that promote epithelial growth [9]. The feeders contribute to the maintenance of telomeres in mouse embryonic stem cells (mESCs), and when cells are cultured without feeders, they often display aneuploidy, chromosomal fusion and telomere loss with increasing passages [19]. However, the feeder cell's contact with the epithelial cells is not mandatory for the conditional reprogramming method. Epithelial cells can grow in a conditioned media, prepared from irradiated feeder cells, and display a similar growth rate when compared to co-culture conditions in the presence of feeders [20]. Replacing feeders with conditioned media allows for conducting some experiments where feeders might interfere with the results such as chemosensitivity assays [21, 22].

The second factor in the conditional programming is Y-27632 rho kinase inhibitor (Figure I). ROCK signaling is involved in gene expression, cell motility, cell cycle progression and cytoskeleton regulation [23]. Y-27632 rho kinase inhibitor was the first to show an increase in cloning and sub-cloning efficacy and a decrease in the apoptosis of human embryonic cells [24]. Additionally, Y-27632 increases the expression of stem cell markers and proliferation in human-skin-derived keratinocytes [25]. However, the effect of Y-27632 on cell differentiation and growth is reversible when Y-27632 is withdrawn from the culture [26]. Consequently, when CRCs from tracheal epithelium or ectocervical epithelium are transferred to a three-dimensional air-liquid interface culture system to test their ability to differentiate, a ciliated airway epithelium was formed from the tracheal cells, while a fully differentiated stratified squamous epithelium was formed from the cervical cells [26].

Table I. CR cell growth conditions for different types of tissues.
Adapted from Liu et al 2017 [18].

Tissue type	Conditional reprogramming components		
	F media	Y-27632	Irradiated feeders
Prostate (N,T)	+	+	+
Breast (N,T)	+	+	+
Cervix (N,T)	+	+	+
Lung (N,T)	+	+	+
Ovary (N,T)	+	+	+
Oral (N,T)	+	+	+
BX-795 (N,T)	+	+	+
Salivary (N,T)	+	+	+
Skin (N,T)	+	+	+
Kidney (N,T)	+	+	+
Thyroid (N,T)	+	+	+
Pancreas (N,T)	+	+	
Colon (N)		+	
Colon (T)	+	+	
Neuroendocrine (T)	+	+	
Schwannomas		+	
GIST cells (T)	+	+	

Normal (N) and tumor (T)

Drug Discovery and Precision Medicine

Drug discovery efforts are initiated to treat clinical conditions or diseases that lack appropriate medical interventions. The early research, regularly happening in academia, produces data to develop an assumption that the activation or inhibition of a pathway or a protein will result in a therapeutic outcome in a disease condition. Such a process will be followed by target selection with further validation before advancement into the lead discovery phase. Throughout lead discovery, there is a rigorous search effort to find a biological therapeutic agent or a small molecule that progresses into preclinical, and if effective, into clinical development and eventually be a marketed drug [27]. Although the drug discovery process costs almost $1.8 billion in US dollars and 10 to 15 years of intensive research per drug, not all drugs succeeded in reaching the market [28]. The main two reasons for failure and attrition are the lack of clinical efficacy and the safety concerns of the developed drug [29, 30]. In recent years, there has been arising interest in drug repositioning, which is driven by various factors. Repositioned drugs have the benefit of reduced time and development costs to market than the typically discovered drugs; this is due to the availability of previously collected safety, pharmacokinetic, and toxicology data [31]. Therefore, it has been projected that 3 to 12 years is the time needed for the development of a repositioned product with markedly lower costs [32].

One of the first successful stories in the field of repurposed drugs is sildenafil's story, which was repositioned to erectile dysfunction from angina. Another story is thalidomide repurposing to multiple myeloma from morning sickness [33].

Precision medicine is an old concept that has gained desirability recently with the advancement in technologies. By definition, precision medicine is treating patients with therapies

to meet their specific needs using psychosocial, phenotypic characteristics, biomarker and genetic tools that discriminate a given patient from other patients with identical clinical manifestation [34]. The earliest reported case was for blood transfusion case when the donor's blood was tested for type match before transfused into the patient [35]. More recently in oncology, the treatment and classification of cancer have changed because of the genetic testing. For example, genes like MET, EGFR, ALK, RAS, and other genetic markers have been tested and added to the traditional classification of lung cancer that was based previously only on histologic and anatomic criteria. Less than 5% of non–small-cell lung cancer has ALK fusion genes, yet using crizotinib (targeted ALK inhibitors) has led to a significant inhibitory effect on this tumor type [36]. Avoiding treating patients with no such abnormalities in ALK genes will save them from costly and potentially toxic therapies that yield no therapeutic effect. Immunotherapies for cancer have targeted specific pathways with antibodies such as tyrosine kinase ERBB2 [HER2] by trastuzumab, immune checkpoint pathways by nivolumab or antigens such as CD19 with engineered CAR -T cells [37–39]. Thus, the standard of matching diagnostics and therapeutics will also be a key feature of the future of immunotherapy.

Regenerative Medicine

Regenerative medicine (RM) designates the regeneration or replacement of human organs, tissue or, cells to reestablish normal function [40]. Precisely, this term "regenerative medicine" was used by Leland Kaiser in 1992 for the first time, when he listed the tools which would influence the hospital's future [41]. However, the phrase "regenerative medicine" is broadly considered to be invented by William Haseltine at a Lake Como conference in 1999, in the effort to define a developing field, which merges knowledge deriving from different topics: cell transplantation, biomechanics prosthetics, biochemistry tissue engineering (TE), stem cell

biology, and nanotechnology [42]. Before that Nevertheless, Charles Lindbergh and Alexis Carrell, a Nobel Prize laureate for his work on vascular anastomosis, worked together during the 1930s at Rockefeller Institute for Medical Research. There, they generated an artificial perfusion pump enabling the perfusion of the organs during surgery outside the body. Their effort was the foundation for the development of the artificial heart [43].

Due to the increasingly aging population, regenerative medicine will be progressively needed to restore end-stage diseased organs damaged by age-related illnesses. For instance, waiting times for kidney transplantation from deceased donor have significantly increased. So half of the candidates who were listed in 2006 through 2007 and older than 60 years old are estimated to die before receiving a deceased-donor transplant (DDTx) [44]. However, regenerative medicine has the potential to deliver new substitutes for donor organs. In the last 30 years, researchers have tried to engineer tissues, design treatment modalities and grow stem cells using regenerative medicine methods for almost every human organ or tissue [45].

Cell-based therapy involves injecting healthy cells in pathologic and diseased tissues, and it can depend either on undifferentiated stem cells or on differentiated cells. For example, the primary cells can be isolated from any tissue of a patient and without any further manipulations; these cells are ready to be implanted. However, difficulties of growing large quantities of primary cells limit their use in regenerative medicine [45]. Conversely, stem cells (SCs), which have the self-renewing capacity, can grow extensively without losing the undifferentiated state, until they are triggered to differentiate into a definite cell type [46]. Embryonic stem cells (ESCs), adult stem cells (ASCs), induced pluripotent stem cells (iPSCs), and amniotic fluid-derived stem cells (AFSCs) have been studied intensely to unleash their potential in regenerative medicine with pros and cons of each cell type [42]. Thus, regenerative medicine and tissue

engineering have the potential to solve many of the unsolvable problems of the current therapeutic options.

Human Papillomavirus and Cancer

Human Papillomavirus (HPV) is a 55 nm, icosahedral, non-enveloped virus that belongs to the family of papillomaviridae [47]. Although Human Papillomavirus (HPV) can infect humans only, other Papillomaviruses can infect the mucosa and keratinocytes of the skin of diverse vertebrate species [48–50]

HPV viruses contain a circular, double-stranded DNA which is 8-kb. The HPV DNA encodes eight genes coding for proteins and has a regulatory noncoding long control region (LCR) that controls the expression of the viral proteins [51]. The two structural proteins L1, (major basic protein) and L2 (minor basic protein) are encoded by the late transcribed genes L1 and L2 (L-genes) respectively. Five L1 proteins and one L2 protein make each of the 72 pentameric capsomeres that form the icosahedral capsid of the HPV (Figure II) [52, 53]. The early genes (E1, E2, E4, E5, E6, and E7 (E-genes) are coding for viral proteins that regulate DNA replication, RNA transcription, and cell transformation [52]. The progression to cancer preceded by the malignant transformation resulting from the high expression of E6 and E7 when the integration of the viral DNA into the human genome occurs [54]. The loss of the inhibitory effect of E2, due to viral integration, on the expression level of E6 and E7 leads to the deregulation of the viral oncogenes E6 and E7. E6 oncoprotein will cause the tumor suppressor protein p53 to be damaged while E7 will bind and degrade the retinoblastoma protein (pRB), tumor suppressor protein, leading to genomic instability, DNA damage and allowing HPV DNA synthesis. Moreover, increasing replication of viral genome is mediated by E1 [52, 55, 56]. From

the perspective of oncology, HPV can be classified into low risk or high risk types. The non-oncogenic low-risk HPVs such as 6, 11, 40, 42, 43, 44, 54, 61, 70, 72, and 81 are linked to some forms of cutaneous warts, recurrent respiratory papillomatosis (RRP) and anogenital warts (AGWs) [49, 57]. Almost 90% of external anogenital warts and RRP are caused by HPV types 6 and 11[54, 58]. On the other hand, HPV 16, 18, 31,33, 35, 39, 45, 51, 52, 56, 58, 59, 66, 68, 73, and 82 are oncogenic high-risk HPVs in which HPV 16 and 18 are contributing to the majority of anal dysplasia, high-grade cervical cancer and invasive carcinoma [58, 59].

Based on the L1 DNA sequence, there are more than 180 distinctive genotypes that have resulted from the analysis of HPV sequences [47]. HPV-6 and HPV-11 are accountable for almost 90% of patients with recurrent respiratory papillomatosis (RRP) [60]. Although RRR is a rare and benign condition of the larynx, if extra laryngeal extension to bronchus and trachea has occurred, it becomes a life-threatening condition [61, 62]. Although 5% of the population is infected with laryngeal HPV, only a trivial fraction develops RRP [63]. Previous studies have shown that changing the innate immune response and twisting adaptive immunity to a T_H2-like phenotype can be mediated by HPV E6 [64, 65]. Furthermore, the absence of certain HLA alleles and specific innate immune receptors could also affect disease severity and predispose an HPV infected person to RRP development [66, 67]. Regarding the severity of the disease, it was reported that HPV-11 is associated with an aggressive form of RRP comparing to HPV-6 [68]. More importantly, 2 % of the RRP cases develop malignant degeneration in which the condition becomes difficult to treat [69]. The cost of treatment per case of RRP patient for a lifetime is almost $198,500, mainly to cover the surgical expenses [70].

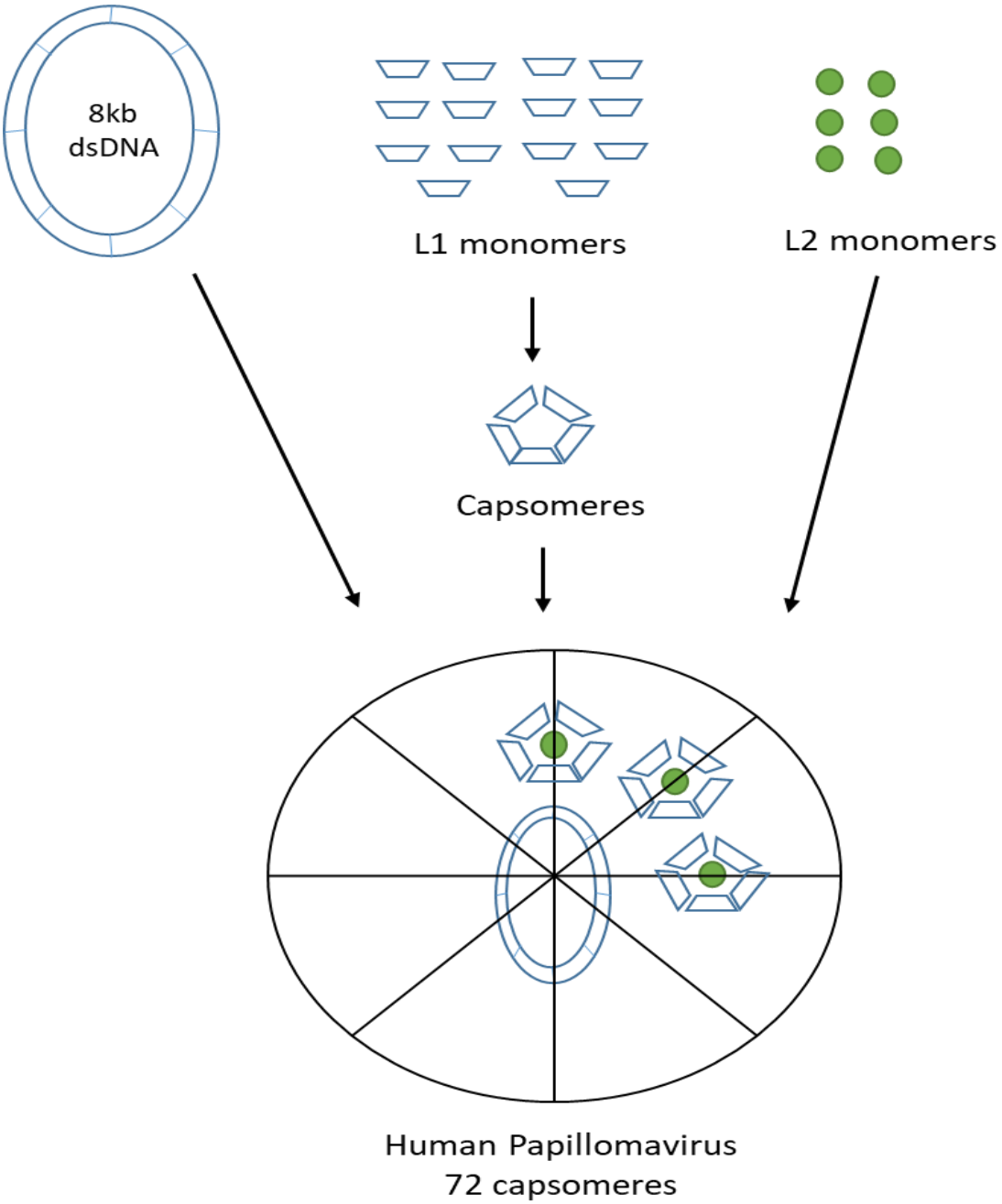

Figure II. Graphic illustration of human papillomavirus (HPV) virion. 72 capsomeres covering capsid of HPV that contain the circular viral DNA.

Wound Healing in Horses

The skin is a vital organ that performs crucial functions including insulation, sensation, physical protection and temperature regulation. It is composed of two components; the epidermis which is populated with 95% keratinocytes and the dermis in which the fibroblast is the main sort of cell found in (Figure III). Equine skin injuries are major challenges for every equine practitioner and are responsible for a substantial financial effect on the equine industry, which is accounting for $140 billion in the USA's gross domestic product as in 2010[71]. In the UK, a study found that half of all injuries reported by owners were wounds and more than 21% of veterinary treatments of polo ponies were related to wounds [72, 73]. A similar situation is found in Australia and New Zealand where wounds are ranked third and second respectively as the most common reason for euthanasia or death [77, 75]. Horses are prone to injuries and traumas because of their "flight" instinct in reaction to fright. The whole healing process is compromised by excessive scaring leading to poor esthetic and functional outcomes. A large study conducted by the National Animal Health Monitoring System reported that traumas and injuries are the most frequent health condition affecting horses [71]. For instance, wounds cause 7% of injuries that lead to the retirement of racehorses [76]. The majority of healing problems develop basically in wounds located on the horses' limbs, probably due to anatomic distinctions such as (i) higher wound contamination due to proximity to the earth; (ii) the limited vascular support due to the lack of sufficient soft tissue coverage; (iii) high motion due to the existence of several highly movable joints; and (iv) the absence of panniculus carnosus muscle leading to a reduced wound contraction [71]. There are four phases in the equine wound healing process: first is the hemostasis phase in which bleeding is controlled by peripheral vasoconstriction and activation of the coagulation cascade leading to clot formation that covers the vessel [77, 78]. The second

phase is the inflammatory phase, where neutrophils and monocytes are recruited by chemoattractants to play a major role by eliminating dead tissue and alien substances [78, 79]. In the third phase, proliferation of the epithelial, endothelial and fibroblasts cells enter the wound to form the granulation tissue and form a new epithelial cover [78]. The last phase consists of remodeling of the extracellular matrix during which glycosaminoglycans, proteins, and polysaccharides undergo certain modifications to guarantee function, integrity, and strength of the replacement tissue [78, 80].

When it comes to treating wounds in horses, there are many choices depending on the phase of healing. Recently, many novel therapies have been investigated such as hyperbaric oxygen therapy, vacuum-assisted closure and cell therapies including the practice of induced pluripotent stem cells (iPSC), platelet-rich plasma (PRP) as well as adult mesenchymal stem cells [81]. Nevertheless the full-thickness grafting was limited to smaller wounds due to the lacking of enough donor skin in horses; additionally, graft failure is fairly common in equine patients as a result of motion, inflammation, infection, and fluid accumulation below the graft [81].

Tissue engineering and cell therapy have emerged as multidisciplinary fields with the aim to regenerate new biological material for replacing damaged or diseased organs or tissues. The final goal is to promptly create a construct that effects the comprehensive regeneration of structural and functional skin, including all its layers similar to that witnessed in the natural epidermis [81].

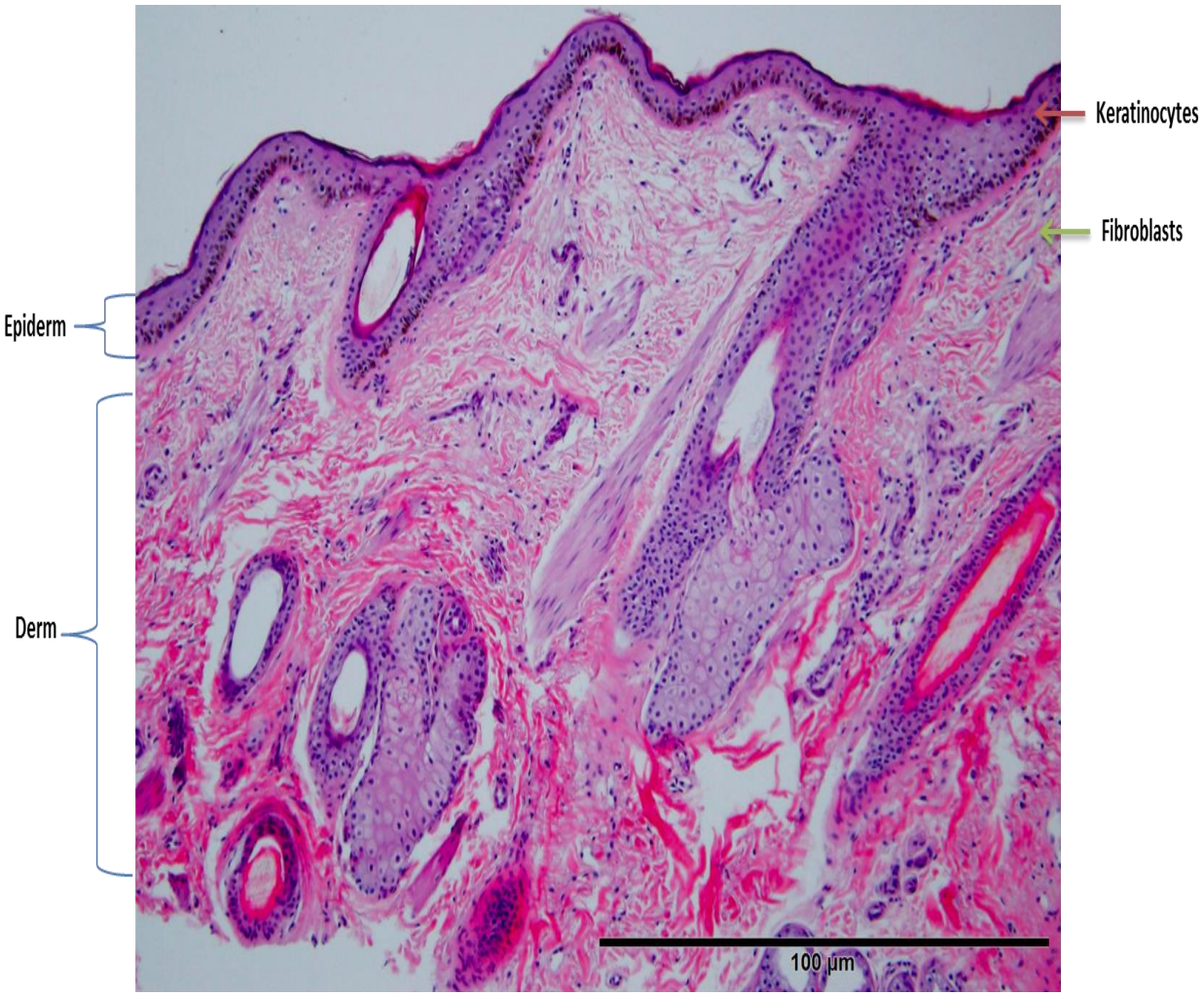

Figure III. Photomicrograph of equine skin tissue. Epidermis has keratinocytes cells and is attached with basement membrane to derm that has the fibroblasts cells. (Magnification is 10X, scale bar is 100 uM) the green arrow indicates fibroblasts and the red arrow indicates keratinocytes.

Specific Aims

Aim I

To determine the ability of conditional reprogramming to ex vivo culturing and expanding recurrent respiratory papillomatosis cells and to use the generated cells for high throughput screening (HTS) to identify an appropriate therapy for the recurrent respiratory papillomatosis (RRP).

Aim II

To evaluate conditional reprogramming for culturing normal equine keratinocytes and investigate the ability to differentiate the generated epithelial cells into stratified epithelium to treat horse wounds.

CHAPTER ONE

High-throughput Screening Identifies Candidate Drugs for Treatment of Recurrent Respiratory Papillomatosis

Summary

Recurrent papillomatosis (RRP) is a benign neoplasm of the larynx caused mainly by human papillomavirus type 6 or 11 and its standard treatment involves repeated surgical debulking of the laryngeal tumors. However, significant morbidity and occasional mortality due to multiple recurrences occur. Conditional reprogramming (CR) was used to establish a stable, HPV-6 positive culture from an RRP patient, named GUMC-403. High-throughput screening was performed at the National Center for Advanced Technology Sciences (NCATS) to identify potential drugs to treat this rare but morbid disease. GUMC-403 cells were screened against the NPC library of >2,800 approved drugs and the MIPE library of >1900 investigational drugs to identify new uses for FDA-approved drugs or drugs that have undergone significant research and development. From the two libraries, we identified a total of 13 drugs that induced significant cytotoxicity in RRP cells at IC50 values that were clinically achievable. We validated the efficacy of the drugs in vitro using CR and 3D models and further refined our list of drugs to panobinostat, dinaciclib and forskolin as potential therapies for RRP patients. We conclude that the present drug repurposing approach has the potential to identify drug therapies for RRP patients and possibly for different types of cancer. In addition, our cell-based therapy model can be used to personalize therapy for RRP patients using screening technology in a timely efficient manner.

Background

Recurrent respiratory papillomatosis (RRP) is a rare disease with an actual incidence of approximately 20,000 cases in the United States [82]. RRP is marked by the proliferation of tumors in the respiratory tract caused by the human papillomavirus type 6 or 11 (HPV-6 or -11) and generally classified into two subtypes: juvenile-onset RRP (JORRP) and adult-onset RRP (AORRP) [83, 84]. JORRP cases, which develop before the age of 14, are more recurrent and aggressive than their AORRP counterpart [85]. Despite the fact that RRP primarily occurs on and around the laryngeal vocal cords, these growths can spread downward and affect the bronchi, the trachea and intermittently the lung parenchyma [83, 84]. Life-threatening breathing complications such as acute respiratory distress can result from untreated papilloma. When progression to the lung occurs there are limited treatment options, and the disease is fatal [86].

Presently, there is no "cure" for RRP, and no single adjuvant treatment has reliably been shown to be effective in eliminating RRP [87]. The backbone of RRP therapy is surgical excision to debulk the papilloma without injuring the normal tissues [88]. A characteristic feature of this disease is the tendency for the papilloma to reappear after surgical excision, causing JORRP patients to have an average of 4.4 surgeries per year [9, 82, 87].

One of the limitations for investigating RRP treatment has been the lack of a suitable cell culture system. As reported previously, conditional reprogramming (CR) allows rapid and efficient isolation and propagation of primary tumor cells [9, 19]. In contrast to existing conventional cancer cell lines, the conditionally reprogrammed (CR) tumor cells maintain the cancer-specific mutations and phenotypic heterogeneity typically seen in the primary tumor [26, 89, 80]. Therefore, CR cells represent an advanced cancer model for preclinical drug development. In the past, we isolated and propagated CR cultures from an HPV-11-positive

RRP patient. We utilized the generated cell line to detect an HPV-11 mutation that may have been responsible for the observed aggressive clinical phenotype. We also used the patient's cells for a limited drug screening and identified vorinostat, an HDAC inhibitor, as a potential treatment and subsequently showed that vorinostat was effective for arresting tumor growth in the patient [91].

To extend this line of work, we have used high-throughput screening to identify potential new drugs effective against RRP. The RRP CR cells, which contained episomal HPV-6 DNA, were screened by the National Center for Advanced Translational Sciences against the NPC library of 2,816 approved drugs and the MIPE library of 1912 investigational drugs. From approximately 4,700 drugs we have identified three that might be clinically actionable (Figure 1.1).

Methods

Cell isolation and propagation of normal and tumor tissue samples

Lung tissue (right lower lobe) was obtained at surgery with the patient's written consent according to the Georgetown University Hospital IRB. The sample was digested with collagenase and trypsin, and the obtained cells were propagated using the conditionally reprogrammed (CR) system that includes the use of a bed of irradiated murine fibroblasts and an F medium supplemented with Y-27632 Rho-kinase inhibitor (Enzo Life Sciences) as described previously [9, 18]. The cells, named as GUMC-403, were used for HTS, 2D and 3D cell viability assays. Previously a laryngeal sample from another patient was used to generate normal cells, named GUMC-228 (HPV negative), which used as a control in the 2D cell viability assay.

DNA isolation, cloning, and sequencing

DNA was isolated and purified from the cultured cells, GUMC-403, or directly from the tissues using the DNeasy Blood and Tissue Kit (Qiagen) and was amplified with specific primers for HPV-6, HPV-11 or general primers for HPVs or with the Rolling Circle Amplification (RCA) kit (Illustra TempliPhi, GE Healthcare Life Sciences), as published previously [91]. The products of RCA were digested with EcoR I, BamHI, Hind III, Nde I and EcoR V. Two DNA fragments from the digestion were isolated from agarose gel, and cloned into pUC19 separately and sequenced from two directions with the use of Primer Walking Services (Genewiz).

Chemotaxis/cell migration assay

Cell migration experiments were performed using the xCELLigence RTCA (ACEA Biosciences Inc.) system as described before [92]. xCELLigence allows the examination of the cell migration process in real time by measuring electrical impedance. Experiments were carried out in 16-well plates (CIM-16, ACEA Biosciences Inc.). Briefly, 160 µL of cell culture medium with and without serum were dispensed in the lower chambers while 50 µL serum-free medium was added to the upper chamber followed 1 hour incubation. Next, the background was read. The experiment was paused and the plate removed from the RTCA-DP device. Then, 1.0 x 10^5 of GUMC-403 cells or Human Foreskin Keratinocytes (HFK) cells in a total volume of 50-µL serum-free medium/well were seeded on the upper chamber. The plate was placed back in the RTCA system and incubated for 27 hours, performing measurements every 10 minutes. The electrical impedance is a reflection of cell number and software was used to generate the migration activity of each condition. The graph represents the average of triplicates.

High throughput screen (HTS) assay

GUMC-403 cells were plated at a density of 700 cells/well in 5 µL of (F+Y medium) into white tissue culture treated polystyrene plates (Corning Cat. 7464) using a MultiDrop Combi dispenser with small volume cassette. All plates were covered with a stainless steel gasketed lid and placed into an incubator at 37°C/95% RH/5% CO_2 overnight. The next day, 23 nL of MIPE 4.0 library, NPC library, and control compounds were added to each plate using a pin tool dispenser [93, 94]. Controls included bortezomib at 9.2 µM, DMSO only, and empty wells. Plates were then returned to the incubator for 48 hours. To assess cell viability, 3 µL of CellTiter-Glo reagent (Promega) was added to each well of the plates using a solenoid value dispenser. Plates were then incubated at room temperature for 15 minutes and then, luminescence signal was read using a ViewLux (PerkinElmer) with a 2 second exposure time. Data normalization was done using DMSO as 100% cell viability and empty wells as 0% viability.

Cell viability assay for 2D and 3D

GUMC-403 cells (5.0 x 10^3 cells/well in 100 µl of F+Y medium) were seeded in a 96 wells plate for 2D monolayer (VWR, Radnor, PA) or (5.0 x 10^3 cells/well in 50ul of F+Y medium) in a 96-well ULA round-bottomed plates for 3D spheres culture (CLS3474, corning). Seeded cells were incubated overnight at 37°C in a cell culture incubator with 5% CO2 levels. For 2D drug culture treatments, the medium was replaced with fresh medium that has 7 different concentrations of the 13 drugs (drugs are listed in Table 1.1). For the 3D drug culture treatments, 7 different concentrations of panobinostat, dinaciclib or forskolin were added in 50 ul to make up the volume to 100 ul. Cell viability assay was conducted using The Veritas microplate luminometer turner Biosystems. The CellTiter-Glo® Luminescent Cell Viability

Assay (G7570, Promega, Madison, WI) kit for 2D culture or CellTiter-Glo® 3D Cell Viability Assay (G9681, Promega, Madison, WI) kit for 3D culture and GloMax®-96 Microplate Luminometer Software (Promega) were used for data analysis according to the manufacturer's protocol. The cell viability reading was measured after 3 days for 2D culture or 5 days for 3D culture and the treated cells luminescence reading was normalized to that of vehicle (DMSO) treated cells. For statistical significance, the experiment including was carried in 3 technical replicates and conducted at three independent times.

Xenograft assay

To determine *in vivo* tumorigenicity for the GUMC-403, 1×10^6 cells were suspended in 200 µL of Matrigel HC (BD-growing Biosciences). The Matrigel-suspended cells were injected subcutaneously into the left and right flanks of 6-week-old male mice with severe combined immunodeficiency (Taconic, Germantown, NY). The growth of xenografts was measured weekly with callipers. Animals were housed at the Georgetown University animal care facility according to institutional guidelines. Animal protocol #14-033-100171 was approved by Institutional Animal Care and Use Committee (IACUC) at Georgetown University. All experiments were performed in accordance with the protocol relevant guidelines and regulations.

Statistical analysis

Unpaired student's t-test was used to compare drug treatment response in primary cells. Data (mean ± s.e.m.) were calculated and plotted using GraphPad Prism 6.0 (La Jolla, CA).

Results

Generation and characterization of HPV-6 positive CR cultures from RRP patient

The patient was a 29 year old female with more than 26-year history of recurrent respiratory papillomatosis. She had undergone more than 90 laryngeal ablation surgeries to control viral-induced tumors and had been additionally treated with intralesional cidofovir. However, the treatment was not able to slow tumor growth or its progression into the lung. Computed Tomographic (CT) scanning revealed that there were multiple pulmonary nodules that had accelerated in growth. Bronchoscopy was performed and papillomas from the right lower lobe (RLL) were excised and submitted for both pathologic examination and cell isolation. Histology of the tumor revealed squamous papillary proliferation (Figure 1.2A, Left) and intraepithelial mucocytes (Figure 1.2A, Right). To facilitate the analysis of molecular alterations and drug screening in RRP, we established a stable cell culture (GUMC-403) from a right lower lobe papilloma biopsy using conditional reprogramming [18]. The cells could be observed as early as 2 days after isolation, and the primary culture reached confluence in 10 days (Figure 1.2B). The cells were maintained for more than 28 population doublings (52 days) with an average growth rate of 45 hours/doubling.

HPV typing using specific primers for HPV-6 or HPV-11 or general primers for HPV was conducted. Only bands with primers for HPV-6 and general HPV were detected in the biopsy and GUMC-403 (Figure 1.3A). The amplified bands were isolated and cloned. Sequencing of the PCR products showed that all the products matched HPV-6 DNA. HPVs can exist in two forms in the infected cells either episomal form or integrated form [95]. To confirm the anticipated episomal form of the HPV-6 DNA in GUMC-403, we performed rolling circle amplification (RCA) followed by digestion by a set of restriction enzymes [96]. The expected

number and size of bands for HPV-6 were detected in the biopsy and GUMC-403 (Figure 1.3B). HPV-6 from the lung tissue and GUMC-403 cells exhibited no bands with EcoR I enzyme, one band (8000 kb) with BamHI, one band (8000 kb) with Hind III, 3 bands (3200kb, 1300kb, 800kb) with NdeI and 2 bands (6000kb, 1000kb) with EcoR V. To determine if the HPV-6 genome might contain significant mutations, the whole viral genome was cloned and sequenced. Unlike in our previously reported RRP case, we did not detect any mutations in the viral genome [91]. This cell line represents the first stable HPV-6 cell culture containing episomal viral DNA.

GUMC-403 cells maintain RRP characteristics

The capacity of tumor cells to migrate is a critical property for cancer metastasis [97]. Therefore, a transwell migration assay was used to measure the chemotaxis of GUMC-403 cells by electric impedance in response to a chemoattractant fetal bovine serum (FBS). GUMC-403 cells showed higher migration potential compared to human foreskin keratinocytes (HFK, negative control) in the presence or the absence of fetal bovine serum (FBS) during a 27 hours period (Figure 1.4A). We further analyzed GUMC-403 for in vivo tumorigenicity. Cells were trypsinized from a culture at passage 5 and injected subcutaneously into immunodeficient mice. The tumors were measurable as early as 8 weeks post-injection. Xenograft experiments were performed three times independently, with a total of 11 out 12 xenograft sites producing tumors. Similar to the primary tumor (Figure 1.2A), the xenografts were composed of atypia squamous papillary proliferation with focal koilocytotic (Figure 1.4B, Left) and intraepithelial mucocytes (Figure 1.4B, Right). These results demonstrate that the cell line GUMC-403 maintains the tumorigenic phenotype in vitro and in vivo and mimic the original tumor.

High throughput screening assay for RRP cells

Drug screening was performed at the National Center for Advancing Translational Sciences (NCATS) using 1536 well plates. Drugs from the NPC library (8 *point dilutions*, 1:5 dilutions) and MIPE library (*11 point dilutions*, 1:3 dilution) were evaluated at concentrations ranging from 0.5 nM to 50 μM [93]. Survival curves with an area under the curve (AUC) less than 425 for MIPE or less than 460 for NPC and Curve Class of -1.1 were selected [98]. Out of 4728 drugs, 45 drugs matched the criteria, and 13 were selected for further validation in 2D and 3D cultures. Priority was given to compounds based on their degree of cell killing, clinical status, and FDA approval.

2D and 3D drug sensitivity validation

The 13 potential candidates from NCASTS screening (Figure 1.5, Table 1.1) were further evaluated using 2 and 3-dimensional culture systems. For the validation assays and to further narrow down the potential candidates, we used normal laryngeal cells isolated from a second RRP patient, named GUMC-228 (HPV negative), since the GUMC-403 patient did not provide normal tissue. $5.0x10^3$ cells/well of GUMC-403 and GUMC-228 were seeded in 96 well plates, allowed to attach for 24 hours. The cell monolayer was then treated for 72h with (Figure 1.6A,I) verteporfin, (Figure 1.6A,II) fomepizole, (Figure 1.6A,III) carlfilzomib, (Figure 1.6A,IV) flavopiridol, (Figure 1.6A,V) AT-7519, (Figure 1.6A,VI) SNS-032, (Figure 1.6A,VII) romidepsin, (Figure 1.6A,VIII) PF-04691502, (Figure 1.6A,IX) sertindole and (Figure 1.6A,X) crenolanib in concentrations ranging from 50 uM to .5 nM. The cell viability assays revealed higher selective cytotoxicity toward GUMC-403 compared with GUMC-228 when treated with panobinostat (Figure 1.6B, I), dinaciclib (Figure 1.6B, II) and forskolin (Figure 1.6B, III), depicted by an IC50 of 0.035 uM for panobinostat, 0.010 uM for dinaciclib

and 5.157 uM for forskolin (Table 1.2). The cytotoxic effect of these drugs induced morphological changes within 3 days of treatment and ultimately a decreased cell viability compared to DMSO treated control (Figure 1.6C I, II, III and IV).

In recent years, the use of 3D cell culture systems has been increasingly used as an in vitro model for drug discovery. Therefore testing drug candidates for efficacy and tissue distribution can be enhanced through 3D culture such as multicellular tumor spheroids (MCTS) due to the in vivo like microenvironment [99]. $5.0x10^3$ cells/well of GUMC-403 and GUMC-228 were seeded in low attachment plates and incubated overnight. GUMC-403 cells formed spheres around the sizes of 200-400 uM (Figure 1.7A left) while GUMC-228 cells failed to form spheres (Figure 1.7A right). The RRP cells were treated for 5 days with panobinostat, dinaciclib or forskolin. In the 3D culture, the IC50 of panobinostat, dinaciclib or forskolin were 0.030 uM, 0.010 uM and 1.920 uM respectively, as calculated from dose-response curves (Figure 1.7B, Table 1.2). Thus, we found that panobinostat, dinaciclib, and forskolin have a similar cytotoxicity for RRP Cells in 2D and 3D in vitro models.

Conditional reprogramming tests candidates for treating an RRP patient in a time-efficient manner

To investigate the RRP platform generated from the HTS, a female patient sample was received from Georgetown university hospital with a history of the RRP disease. Tissue was processed using CR method to generate cells (named GUMC-1695) then subjected to HPV typing, and 3D chemosensitivity assay using HTS derived RRP platform drugs panobinostat and dinaciclib. The bands corresponding with HPV 11 and general HPV were detected in agarose gel (Figure 1.8A bottom panel). More importantly, GUMC-1695 cells were sensitive to panobinostat and dinaciclib with IC50 26.9 nM and 9.1 nM respectively, and the

chemosensitivity result was provided to the oncologist within 14 days from delivering the tissue sample. We conclude CR method was timely efficient to establish patient-derived cells from an RRP patient (HPV-11) and test the sensitivity of the patient-derived cells to panobinostat and dinaciclib.

Discussion

Recurrent respiratory papillomatosis is a fatal disease once it has metastasized to the lung and there are limited therapeutic options since no single adjuvant therapy has been shown to be effective in eliminating RRP [83]. A major limitation to study RRP tumor progression and treatment is the lack of an appropriate cell culture system. Recently CR culture has shown to maintain and imitate the ordinary biology of their primary tissue such as tracheal epithelium, ectocervical epithelium or breast tumors [26, 89]. Additionally, intra-tumoral heterogeneity was maintained in CR cells suggesting the oligoclonality of these cultures [90]. In an earlier study, we isolated and established a continuous CR cell culture from a patient with recurrent respiratory papillomatosis. The HPV-11 positive CR cell culture helped us to detect a unique and important mutation in the viral genome. More importantly, the primary patient's RRP cells enabled us to run a limited-scale drug screening and identified an effective therapy for the patient in less than two weeks [91]. In this study, we successfully established the first long-term RRP cell culture system that contains episomal HPV-6. Unlike in the earlier HPV-11 positive RRP cells, we did not detect any significant mutations of the HPV6 viral genome in this cell line. In xenograft assays, measurable tumors were observed as early as eight-weeks post injection into immunodeficient mice. The original cellular characteristics of the RRP tumor, as well as HPV genome, were maintained in the xenografts.

Recently, CR cells have been used in translational research for drug discovery. Using small scaled high-throughput drug screening with 306 clinical and emerging cancer drugs on CR cells, Saeed et al., (2017) have identified Bcl-2 family inhibitor navitoclax as a potential treatment for castration-resistant prostate cancer (currently is being tested in a clinical trial) [22]. Chen et al., (2017) have used CR to grow cells from rare salivary gland cancers and identify regorafenib as a potential therapeutic drug [100]. Recently, Alamri et al., (2018) have shown that allosteric AKT inhibitor MK2206 can inhibit the growth of mucoepidermoid carcinoma (MEC) cells in 2d and 3d CR culture [21]. Formerly, we have used CR method to identify vorinostat as an effective treatment for an HPV-11 positive RRP case; the appropriate therapy was identified in less than two weeks [91]. In contrast of the limited, small-scale drug screening in our earlier HPV-11 case using 96-well plates, the drug repurposing study in this HPV6 case was done in a high throughput format with thousands of drugs using 1536-well plates. The rapid expansion of 35 million cells of the RRP CR cells met the demand for a large number of testing cells.

Drug repurposing has emerged a novel approach in finding new treatments for unmet health conditions due to the well-defined side-effect profiles and the established bioavailabilities of drugs that led to FDA approval [32, 101]. Here we identified three drugs cytotoxic to RRP cells and all of them have IC 50s that are within the safe range of therapeutic use. In this study, we found HDAC inhibitors panobinostat and romidepsin, were cytotoxic for HPV-6 positive RRP cells. Panobinostat and romidepsin have been approved for multiple myeloma and cutaneous T-cell lymphoma, respectively [102, 103]. Additionally, the pan-deacetylase inhibitor, panobinostat (Farydac®, LBH589) is under clinical investigation for a range of hematological and solid tumors worldwide in both oral and intravenous formulations [102, 104].

Panobinostat represses tumor cell growth by interacting with nonhistone and histones proteins as well as autophagy-mediated targets, apoptotic and tumorigenesis pathways involved in the development of cancer [105].

Our drug screening also found CDK inhibitors that had potent cytotoxicity against RRP cells. For instance, dinaciclib is an inhibitor of CDK1, CDK2, CDK5, and CDK9, and is active in a broad range of cancer cell lines originating from leukemia, melanoma, osteosarcoma and pancreatic cancer [106–109].

The mechanism by which dinaciclib inhibits RRP cells is unknown but previous study has shown that it inhibits RB phosphorylation in cancer cells at concentrations between 12 and 500 nM [110, 111]. The IC50 from this study is 10nm from 2D and 3D cell validation assays. Interestingly, the combination of HDAC and CDK inhibitors is a new leukemic and melanoma strategy since in combination they activate caspase; induce mitochondrial damage, and alter cell cycle regulation [112, 113]. Therefore, we will explore the potential synergy of HADCi and CDKi present for RRP treatment.

Unlike panobinostat and dinaciclib, forskolin is a natural product that has been isolated from the roots of plant Coleus Forskohlii [114]. Forskolin exhibits a wide range of pharmacological properties such as anti-obesity, asthma, and glaucoma by the stimulation of the adenylyl cyclase activity and increases intracellular levels of the cyclic AMP [115–117]. It has also been reported forskolin has anti-cancer activity. Treatment of colon cancer line KM12C with the adenylyl cyclase activator Forskolin completely inhibits their growth at the concentration of 50uM [118, 119]. In the present study, we demonstrated that forskolin was cytotoxic to RRP cells at concentrations as low as 1.67 uM.

The use of three-dimensional (3D) cellular systems for drug discovery has been explored in drug discovery. A recent study, using the same HTS screen platform, showed similar drug responses between cancer cell lines growing as 2D monolayers and 3D spheres [120]. In this study, we developed the first 3D tumor model of RRP using patient's primary CR cells. Interestingly we were able to validate drug sensibility in our 3D sphere system, and IC50s for the three drugs were similar in 2D and 3D systems. However, the 3D RRP culture does have the potential to discover novel mechanisms and targets and to accelerate target identification and validation, given that the gene expression patterns found in 3D models can better mimic physiological conditions [99].

Figures and Tables

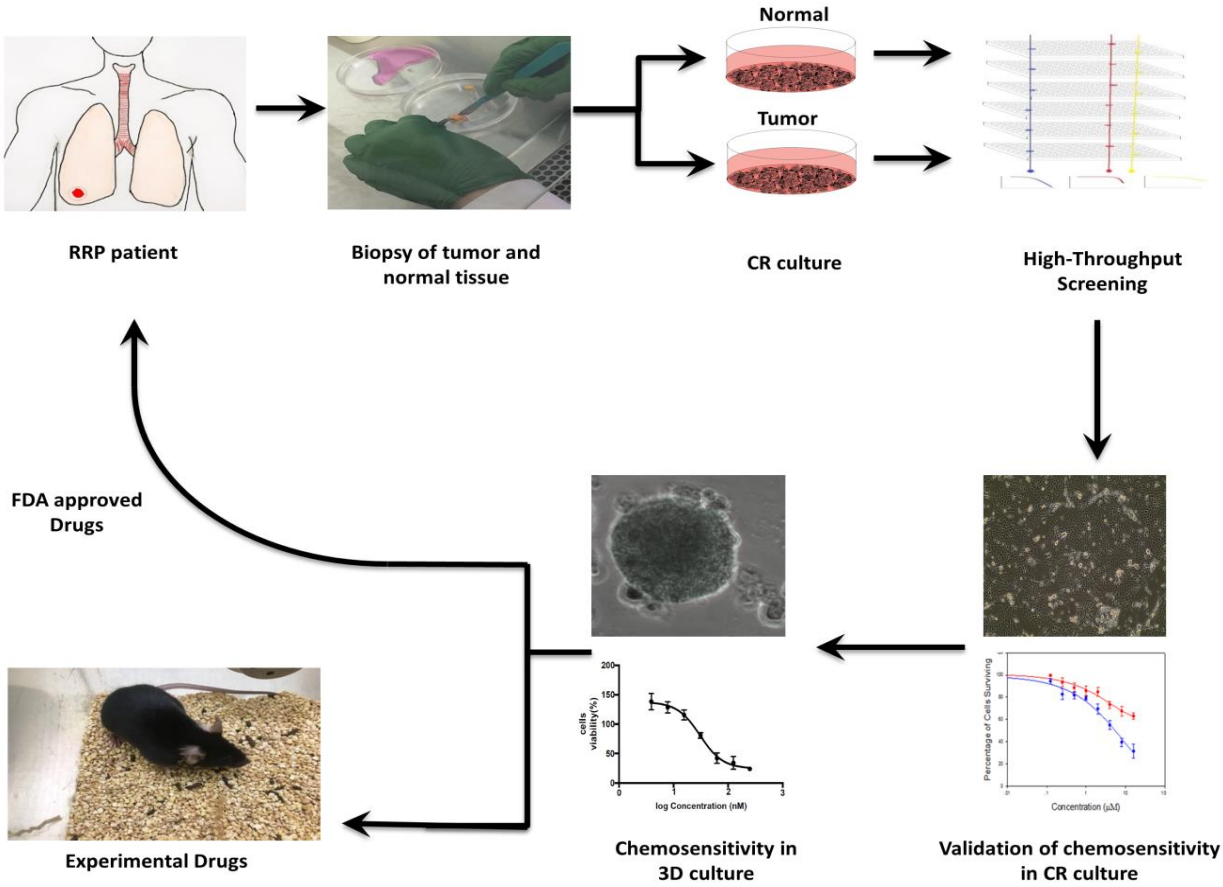

Figure 1.1. Outline for screening conditional reprogrammed cells by high throughput screening. Patient biopsies were collected from patient and examined by pathology, followed by tumor and normal cell lines establishment and propagation using conditional reprogramming method (CR). Next, Reprogrammed cells were tested against different drugs libraries using NCATS HTC platforms. Drugs were selected based on efficacy, safety, and specificity towards tumor cells over normal cells. In vitro 2d and 3d models were used to perform chemo sensitivity tests and to select the most effective chemo agents that inhibited cell proliferation of the tumor cells. Tumor/ Normal samples were collected according to the Georgetown University Institutional Review Board protocols with the informed consent of the patient.

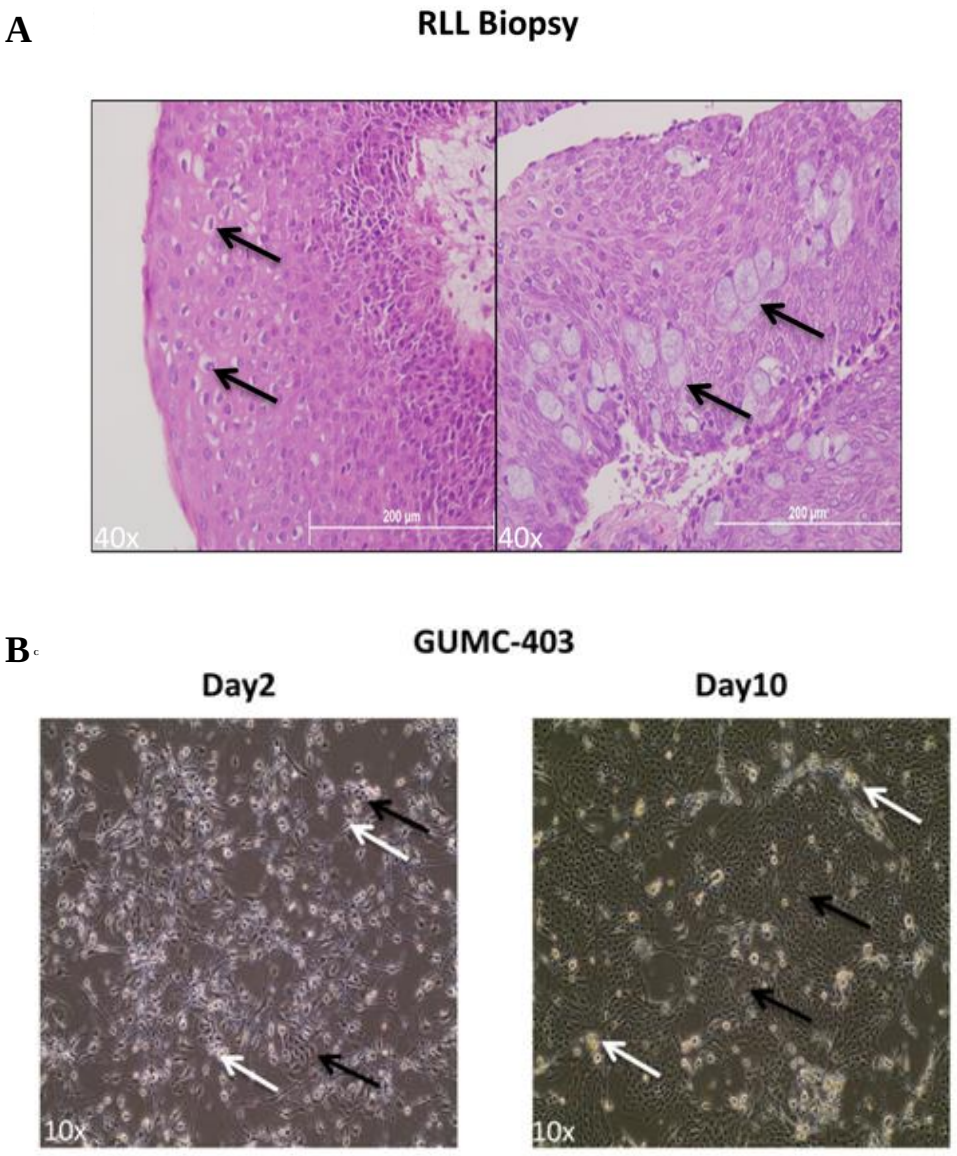

Figure 1.2. Generation and HPV typing of conditionally reprogrammed recurrent respiratory papillomatosis (RRP) cells from a neoplastic lung biopsy. (A) Lung biopsy H&E staining is displaying koilocytotic atypia (Left, black arrow) and intraepithelial mucocytes (Right, black arrow). (B) Phase contrast images of GUMC-403 (black arrow) cocultured with irradiated feeders (white arrow) on day 2 (Left) and day 10 (Right). (40X magnification. Size bars= 200µm in (A) and 10X magnification in (B).

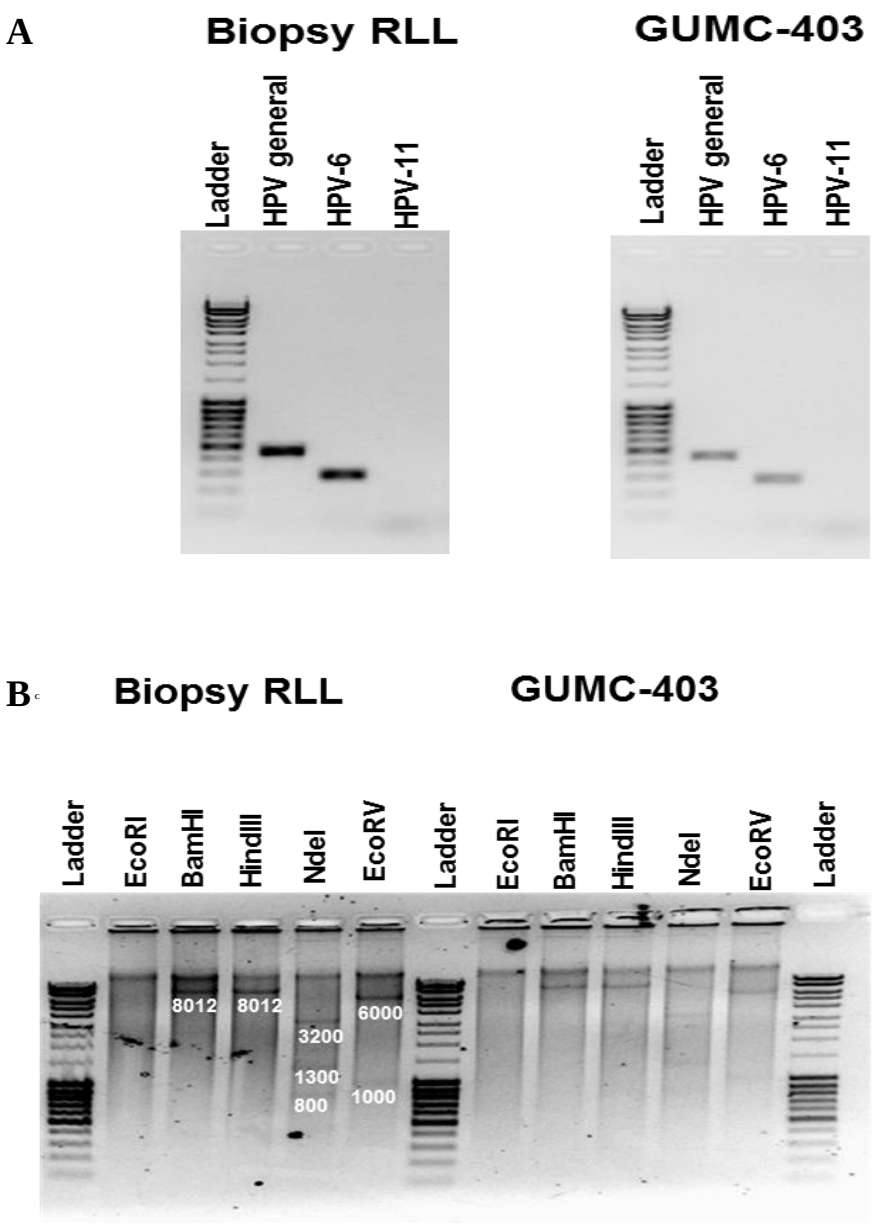

Figure 1.3. HPV typing of conditionally reprogrammed recurrent respiratory papillomatosis (RRP) cells from a neoplastic lung biopsy. (A) Genotyping with HPV-6 and HPV-11 primers showing PCR Results indicates the exclusive presence of HPV-6 DNA in RLL biopsy and GUMC-403 samples. (B) Enzyme-restriction pattern using EcoRI, BamHI, HindIII, Ndel, and EcoRV in the HPV-6 genome after rolling circle amplification, HPV-6 from RLL biopsy and GUMC-403 show one band with BamHI, one band with HindIII, three bands with Ndel and two bands with EcoRV suggesting the episomal nature of the viral DNA.

A

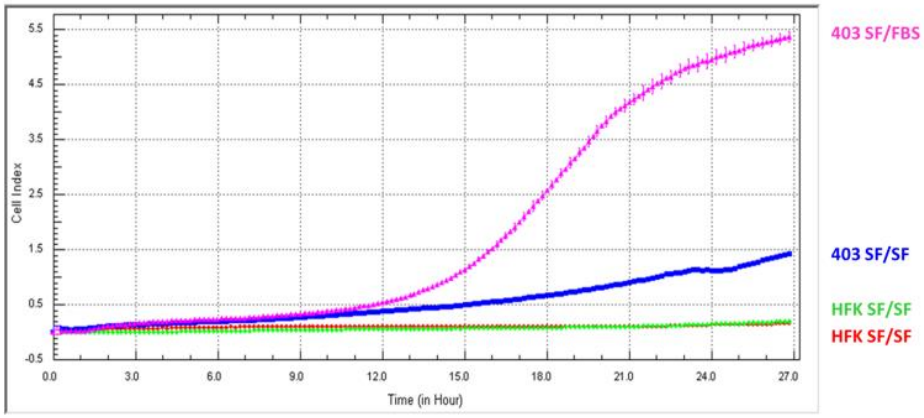

B

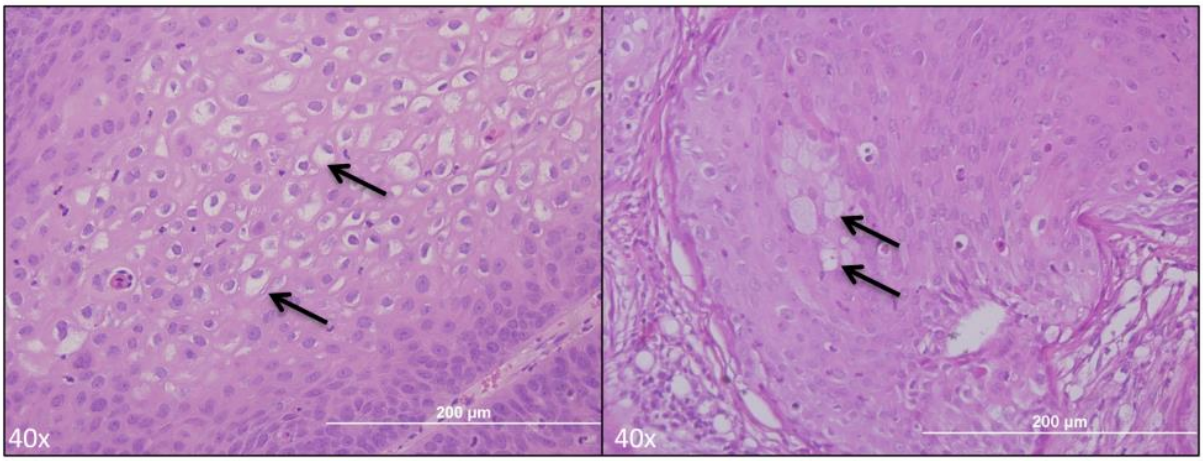

Figure 1.4. GUMC-403 cells maintain invasive and tumorigenic properties. (A) GUMC-403 cells exhibit a higher migration capacity in either the presence or the absence of FBS compared with HFK (The graph is the average of triplicates). (B) Xenograft H&E staining is displaying koilocytes (Left, black arrow) and intraepithelial mucocytes (Right, black arrow). (40X magnification. Size bars= 200µm).

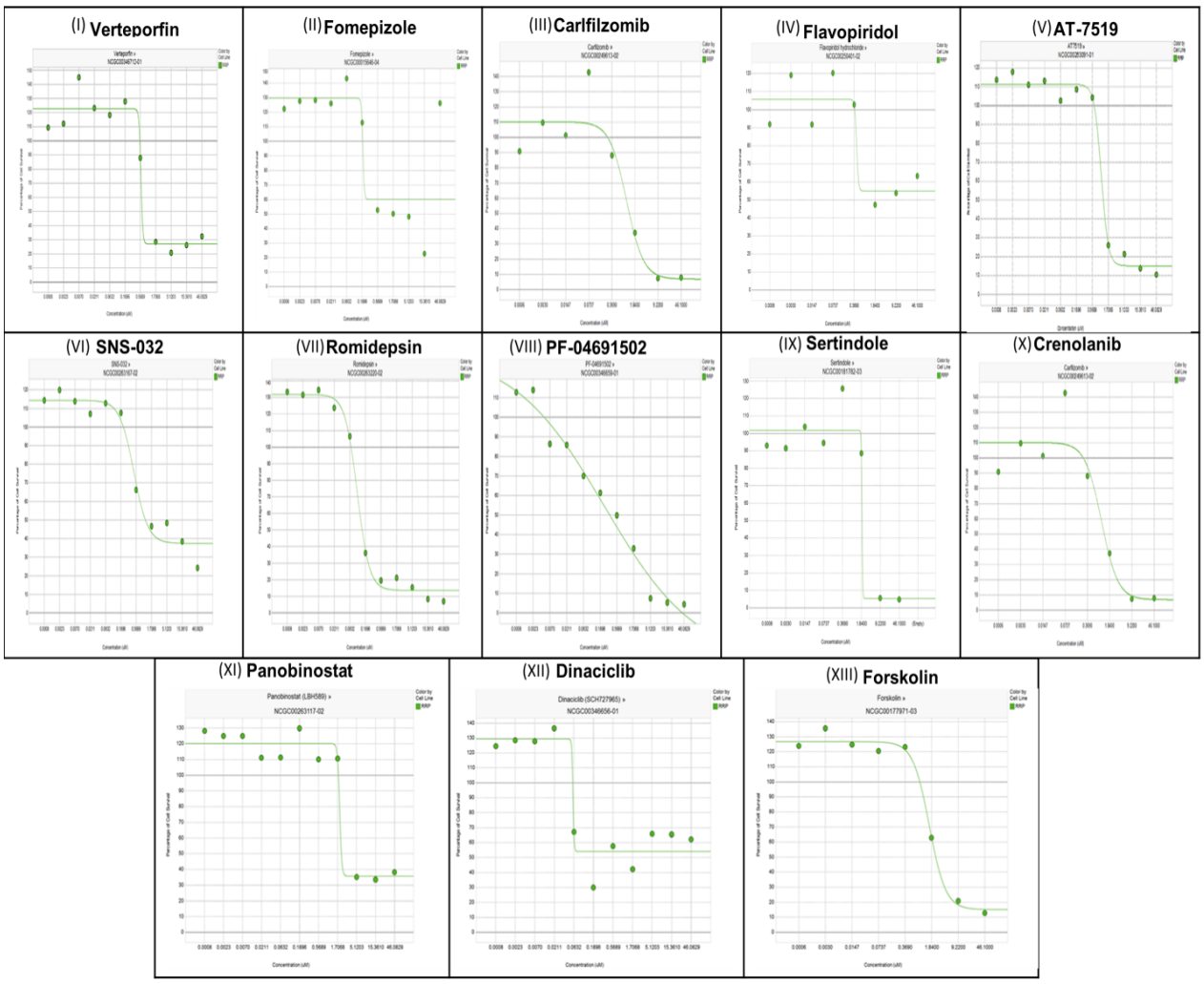

Figure 1.5. HTS drugs cytotoxicity on GUMC-403 culture. Dose-response curves for (I) verteporfin, (II) fomepizole, (III) carlfilzomib, (IV) flavopiridol, (V) AT-7519, (VI) SNS-032, (VII) romidepsin, (VIII) PF-04691502, (IX) sertindole, (X) crenolanib, (XI) panobinostat, (XII) dinaciclib and (XIII) forskolin demonstrate a significant cytotoxic effect on GUMC-403 with durable IC-50 (Table 1.2).

A

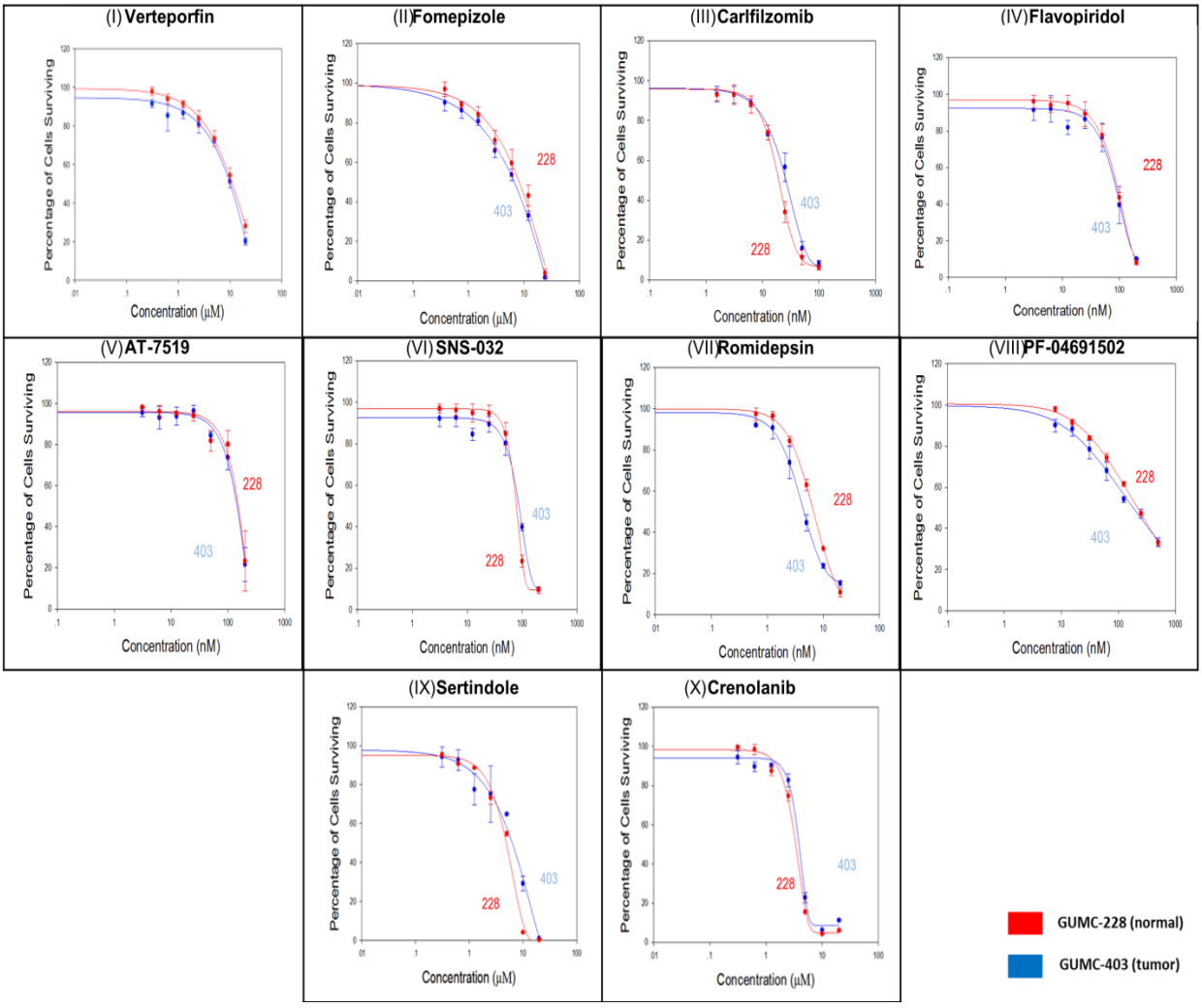

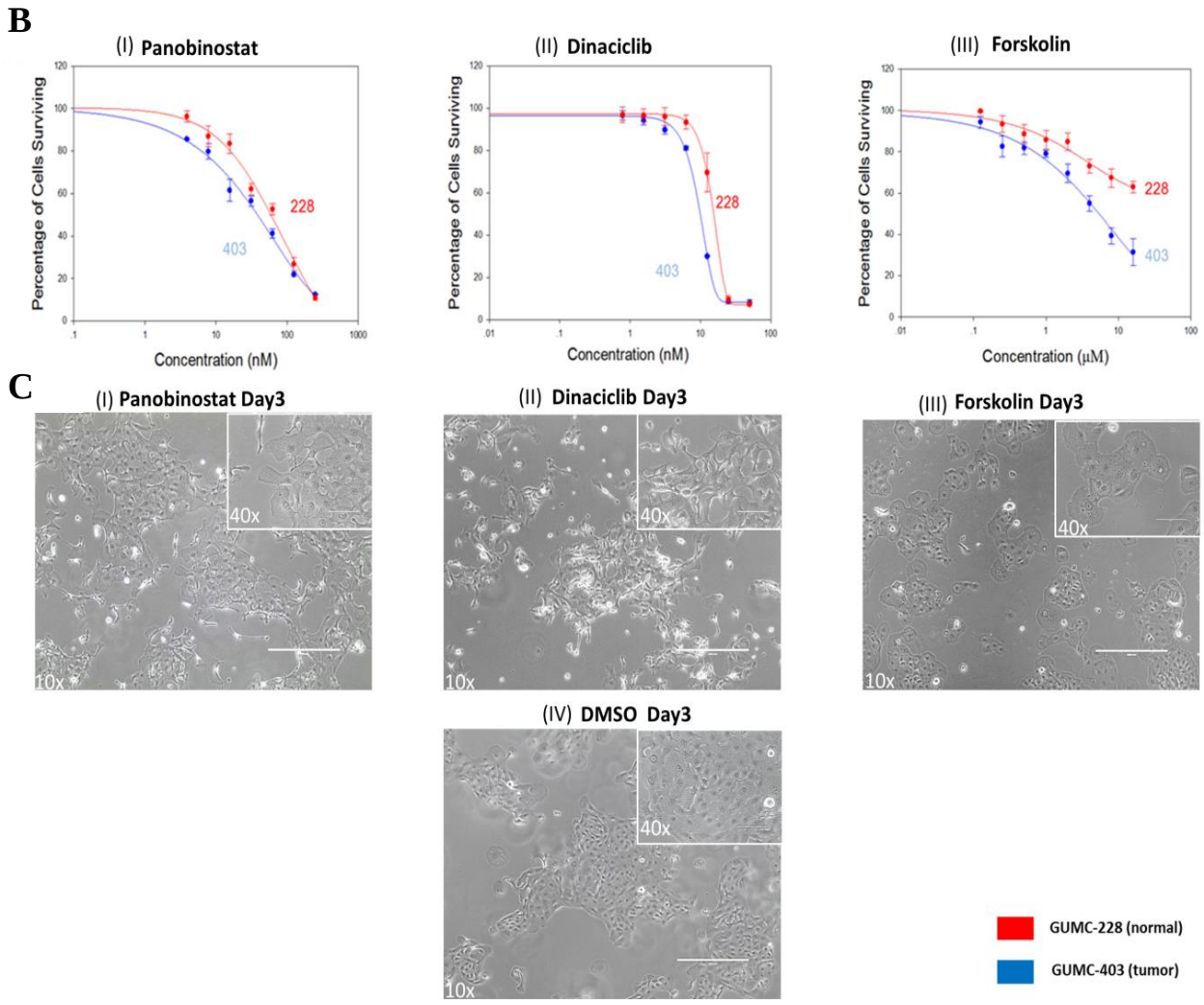

Figure 1.6. Validation of drugs cytotoxicity on 2D culture of GUMC-403 and GUMC-228. (**A)** Dose–response curves for (I) verteporfin, (II) fomepizole, (III) carlfilzomib, (IV) flavopiridol, (V) AT-7519, (VI) SNS-032, (VII) romidepsin, (VIII) PF-04691502, (IX) sertindole, (X) crenolanib. (B) Dose–response curves for (I) panobinostat, (II) dinaciclib and (III) forskolin show differential toxicity toward GUMC-403 over GUMC-228 (P value is 0.0014, 0.0018 and 0.000005 for panobinostat, dinaciclib and forskolin respectively). (C) Phase contrast images of GUMC-403 cells treated with (I) panobinostat, (II) dinaciclib (III) forskolin show evidence of abnormal stressed cells compared to the vehicle control (IV) DMSO treated cells (right) (10X magnification. Size bars= 400μm). Top right images show enlarged magnification (40X magnification, size bars= 100μm). Data represents mean ± s.d. from 3 independent measurements, each in triplicate. Unpaired student T test was performed on the data and *p* value < 0.05 was considered statistically significant.

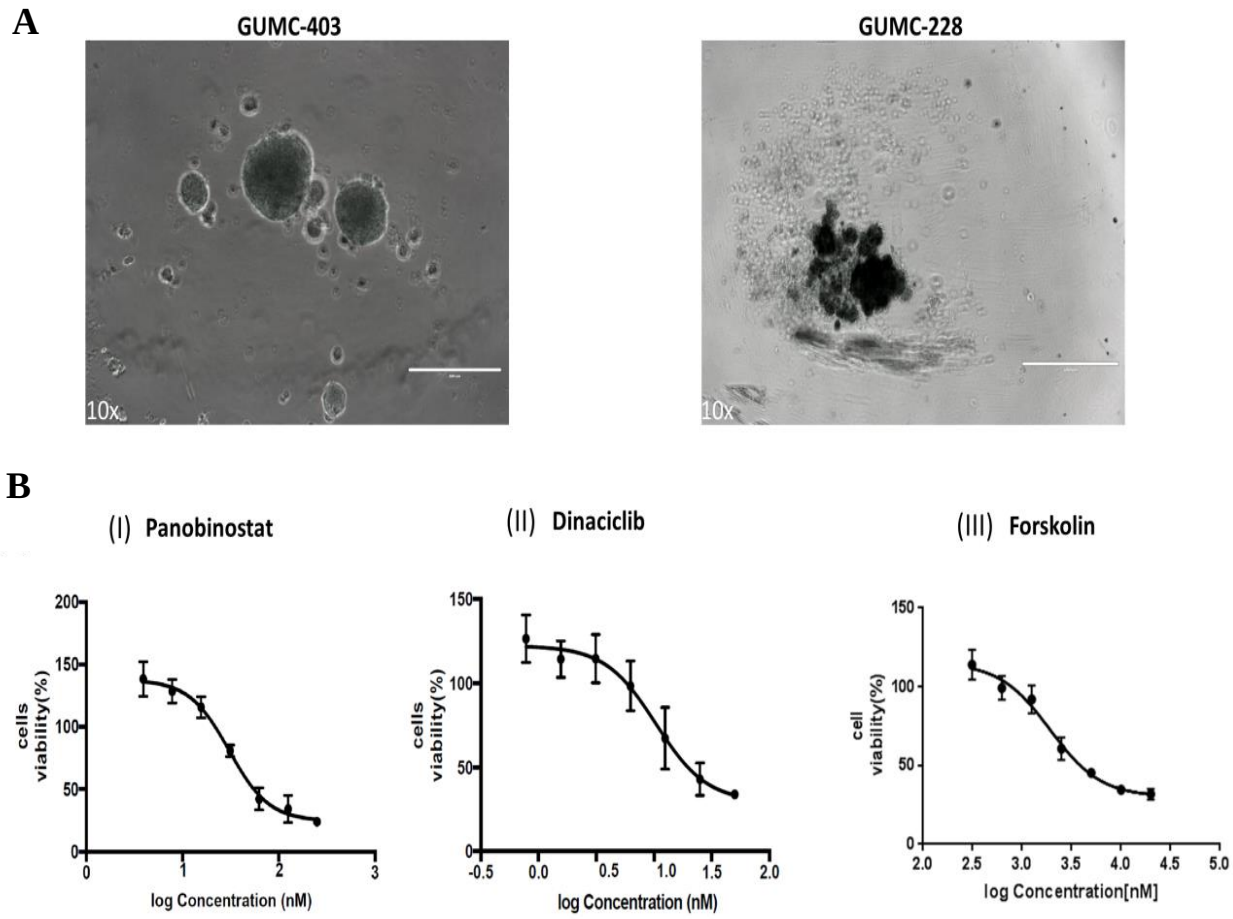

Figure 1.7. Validation of cytotoxicity of panobinostat, dinaciclib and forskolin on the GUMC-403 3D culture. (A) Morphology of GUMC-403 spheres in ULA round-bottomed plates (left) and GUMC-228 (right). (B) Dose–response curves for (I) panobinostat, (II) dinaciclib and (III) forskolin show similar cytotoxicity to 2D on 3D culture of GUMC-403. (10X magnification. Size bars= 400μm). Data represents mean ± s.d. from 3 independent measurements, each in triplicate.

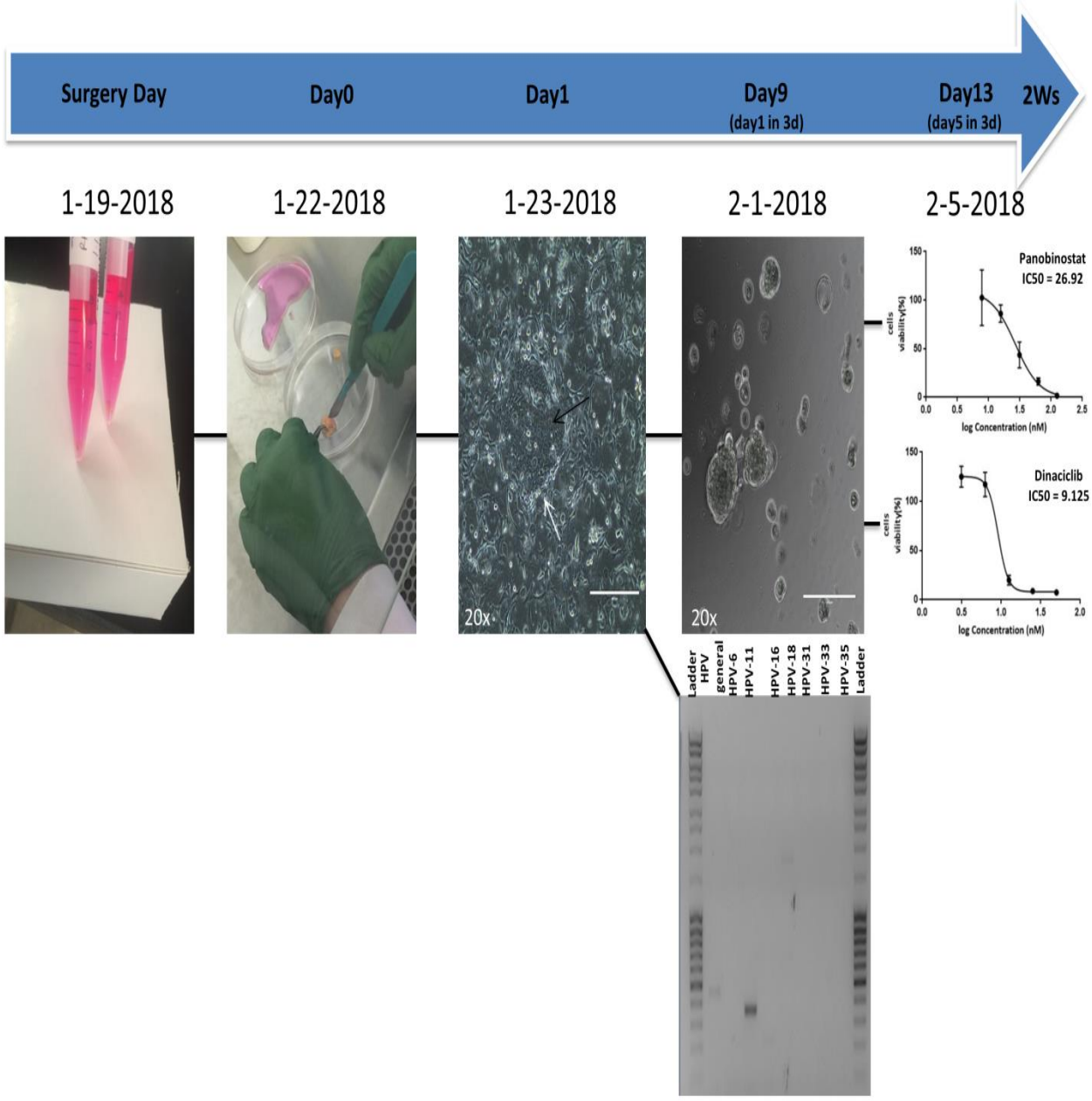

Figure 1.8. Roadmap from receiving a patient sample to test different drugs on patient-derived cells within 14 days. HPV typing and 3D chemosensitivity assay using HTS derived RRP platform drugs panobinostat and dinaciclib. The bands corresponding with HPV 11 and general HPVs were detected in agarose gel (bottom panel). More importantly, GUMC-1695 cells were sensitive to panobinostat and dinaciclib with IC50 26.9 nM and 9.1 nM respectively.

Table 1.1. The best 13 drugs from NCATS screening.

Drugs	Name	Mode of Action	Diseases Treated	Library
Drug 1	Panobinostat	HDAC inhibitor	Multiple myeloma(approved),HIV-HAART combination (in trial)	MIPE
Drug 2	Dinaciclib	CDK2, CDK5, CDK1 and CDK9 inhibitor	In clinical trial for various cancer	MIPE
Drug 3	Forskolin	ubiquitous activator of eukaryotic adenylyl cyclase	Glaucoma	NPC
Drug 4	Verteporfin	Photo-sensitizing agent derived from porphyrin in endothelial cells.	Photodynamic therapy for abnormal blood vessels	MIPE
Drug 5	Fomepizole	Inhibitor of the enzyme alcohol dehydrogenase.	Antidote for methanol or ethyl alcohol poisoning	MIPE
Drug 6	Carlfilzomib	Selective proteasome inhibitor	Multiple myeloma	MIPE &NPC
Drug 7	Flavopiridol	Inhibitor of CDKs including CDK1, CDK2, CDK4 and CDK6	Acute myeloid Leukemia	MIPE &NPC
Drug 8	AT-7519	Multi CDK inhibitor	Metastatic Tumors, Multiple myeloma	MIPE
Drug 9	SNS-032	CDK inhibitor	Chronic lymphocytic leukemia. (In phase I trial)	MIPE
Drug 10	Romidepsin	HDAC1and HDAC2 inhibitor	Cutaneous T-cell Lymphoma (CTCL)	MIPE
Drug 11	PF-04691502	PI3K(α/β/δ/γ)/mTOR dual inhibitor	Solid Tumors	MIPE
Drug 12	Sertindole	5-HT_2 serotonin and D_2 dopamine receptor antagonist and antipsychotic.	Antipsychotic in schizophrenia	NPC
Drug 13	Crenolanib	selective inhibitor of PDGFRα/β, and FLT3 inhibitor	In clinical trials for leukemia, glioma, NSLCC	MIPE

Table 1.2. IC50 comparison between NCATS and CR 2D, 3D chemosensitivity.

No.	Drugs	NCATS IC50 (µM) 2D	CRC center IC50 (µM) 2D	CRC center IC50 (µM) 3D
1	Panobinostat	2.600	0.035	.0304
2	Dinaciclib	0.046	0.010	.0104
3	Forskolin	1.670	5.157	1.920
4	Verteporfin	0.660	8.898	
5	Fomepizole	0.330	5.406	
6	Carlfilzomib	1.180	0.024	
7	Flavopiridol	0.130	0.079	
8	AT-7519	1.040	0.133	
9	SNS-032	0.460	0.083	
10	Romidepsin	.1040	0.005	
11	PF-04691502	0.265	0.188	
12	Sertindole	2.600	5.460	
13	Crenolanib	0.008	3.674	

CHAPTER TWO

Long-term Expansion of Primary Equine Keratinocytes that Maintain the Ability to Differentiate into Stratified Epidermis

Summary

Equine skin conditions have been ranked as the third most common health condition in domestic equine populations. Skin injuries in horses frequently lead to chronic wounds that lack a keratinocyte cover essential for healing. The limited proliferation of equine keratinocytes using current protocols has limited their use for regenerative medicine. Previously, equine induced pluripotent stem cells (eiPSCs) have been produced, and eiPSCs could be differentiated into equine keratinocytes suitable for stem cell-based skin constructs. However, the procedure is technically challenging and time-consuming. The present study was designed to evaluate whether conditional reprogramming (CR) could expand primary equine keratinocytes rapidly in an undifferentiated state but retain their ability to differentiate normally and form stratified epithelium similar to that witnessed in natural epidermis.

Conditional reprogramming was used to isolate and propagate two equine keratinocyte cultures. Polymerase chain reaction (PCR) and fluorescence in situ hybridization (FISH) were employed to evaluate the equine origin of the cells and karyotyping to perform the chromosomal count. Fluorescence-activated cell sorting (FACS) analysis and immunofluorescence were used to determine the purity of equine keratinocytes and their proliferative state. Three-dimensional air-liquid interface method was used to test the ability of cells to differentiate and form stratified squamous epithelium.

Conditional reprogramming was an efficient method to isolate and propagate two equine keratinocyte cultures. Cells were propagated at the rate of 2.39 days/doubling for more than 40 population doublings. A feeder-free culture method was also developed for long-term expansion. Rock-inhibitor is critical for both feeder and feeder-free conditions and for maintaining the proliferating cells in a stem-like state. Polymerase chain reaction (PCR) and fluorescence in situ hybridization (FISH) validated equine-specific markers in the cultures. Karyotyping showed normal equine 64, XY chromosomes. Fluorescence-activated cell sorting (FACS) analysis using pan-cytokeratin antibodies showed a pure population of keratinocytes. When ROCK inhibitor was withdrawn, and the cells were transferred to a 3D air-liquid culture, they formed a well-differentiated stratified squamous epithelium which was positive for terminal differentiation markers involucrin and filaggrin.

Our results prove that conditional reprogramming is the first method that allows for the rapid and continued in vitro propagation of primary equine keratinocytes. These unlimited supplies of autologous cells could be used to generate transplants without the risk of immune rejection. This offers the opportunity for treating recalcitrant horse wounds using autologous transplantation. This original culturing system could offer a very resourceful tool for studying drug testing, modeling skin diseases, and, possibly, equine regenerative medicine [121].

Faris Alkhilaiwi1,2,3,4*, Liqing Wang1, Dan Zhou1, Terje Raudsepp5, Sharmila Ghosh5, Siddartha Paul1, Nancy Palechor-Ceron1, Sabine Brandt6, Jennifer Luff7, Xuefeng Liu1, Richard Schlegel1* and Hang Yuan1* 2018**. "Long-term expansion of primary equine keratinocytes that maintain the ability to differentiate into stratified epidermis."** Stem Cell Research & Therapy**.**2018 Jul 4; 9(1):181.[121] doi.org/10.1186/s13287-018-0918-x**.**

Background

For thousands of years, humans have depended on horses (Equus caballus) for transportation in different places of the world [122]. As in 2013, there were more than 60 million horses registered globally, and almost ten million in the United States with a tremendous economic value [123]. Epidermal tumors such as squamous cell carcinomas as well as other epidermis diseases such as pemphigus foliaceus and seborrhea are identified regularly in horses [124, 125]. Furthermore, wound healing in horses is a very complicated process due to the vigorous granulation tissue formed [126]. Therefore, horse skin injuries often lead to the development of chronic non-healing wounds that lack a keratinocyte cover, essential for healing. The pathophysiology of delayed healing in horse wounds has been poorly studied, but the transforming growth factor-beta (TGF-β) expression changes may contribute [127]. While several treatments have been developed for speeding wound healing and inhibiting hyper granulation tissue in horses, the majority of these are of unverified efficacy [128, 129]. In *vivo* Equine wound healing studies and experiments are traumatic and costly for horses [130]. Therefore, a feasible, convenient and effective *in vitro* equine keratinocyte model is needed. Optimally the model would allow for the investigation of the wound pathophysiology and be applicable to skin transplantation.

Stem cell therapy is being increasingly used in horses [131]. For example, mesenchymal stem cells (MSCs) have been used to treat tendon injuries in horses. However, these cells have shown to mediate their effect as trophic cells rather than differentiated cells [132, 133]. Recently, equine induced pluripotent stem cells (eiPSCs) have been generated from equine fibroblasts by overexpressing reprogramming factors Klf4, Sox2, Oct4, and c-Myc by using either transposons or retroviral vectors method [134–136]. The generated eiPSCs have provided

a valuable source for researchers to generate different types of somatic cells. More relevant, equine iPSCs could be differentiated into equine keratinocytes (eiPSC-KC) with characteristics suitable for stem cell-based skin constructs to repair damaged or lost skin [137].

It has been difficult to propagate equine keratinocytes in vitro long-term using conventional two-dimensional (2D) culture systems [123, 138, 139]. Recently a new cell culture technique, conditional reprogramming (CR), was developed to efficiently and rapidly establish patient-derived cell cultures from both diseased and normal cells, including tumor cells [9, 18]. With this technique, approximately 1 million epithelial cells can be generated in within seven days [18]. Additionally, these epithelial cells can be propagated indefinitely in vitro, yet maintain the capability to become fully differentiated when transferred into conditions that mimic their biological environment [14, 26].

The objective of our study was to establish primary equine keratinocyte using CR method and to evaluate their potential for transplantation. We demonstrated the equine cells were rapidly reprogrammed and acquired characteristics of adult stem cells. During this process, the cells became less differentiated and begin to divide rapidly. More importantly, when removed from CR conditions, these cells reverted to their normal differentiated state and organized into structures similar to stratified epithelium from which they were derived. Thus these cultures appear to have a potential for regenerative medicine. The equine CR cultures may also have applications to generate iPSC, drug screening and transdifferentiation into different somatic cells (Figure 2.1).

Methods

Equine cell harvesting and culturing

Primary horse epidermal keratinocytes and fibroblasts were isolated from two different normal horse tissues (named 1547, 100) using conditional reprogramming method (CR) as described and used previously [9, 18]. Keratinocytes were cultured under different conditions: (i) In co-culture with irradiated 3T3 fibroblasts (J2 strain) in F media with or without 10 uM Y-27632 Rho-kinase inhibitor (Enzo Life Sciences), (ii) In F media with or without 10 uM Y-27632 with no J2, (iii) In CnT-09 media supplemented with A and B supplements (CELLnTEC, Switzerland) with or without 10 uM Y-27632, (iv) In Keratinocyte Serum-Free Medium (KSFM) supplemented with Bovine Pituitary Extract (BPE) and Epidermal Growth Factor 1-53 (EGF 1-53) (KSFM; Invitrogen) with or without 10 uM Y-27632.

Equine fibroblast cells were purchased from ATCC and cultured in Eagle's Minimum Essential Medium EMEM as recommended; primary equine fibroblasts EF-1547 and EF-100 were grown in complete Dulbecco's Modified Eagle Medium DMEM (supplemented with 10% penstrep, 10% L-glutamine and 10% fetal bovine serum). All cells were incubated in 37°C with 5% CO. 4.0×10^3 cells/cm^2 were seeded per passage and split when at 80% confluency was reached. Time in days versus population doubling was plotted to generate a growth curve. All growth conditions are summarized in (Table 2.1).

DNA Isolation and PCR Amplification

DNA was isolated from human foreskin keratinocyte, dog cells (k9), 3T3 murine fibroblasts (J2 strain), equine keratinocytes (EK-100/EK-1547) and equine fibroblasts (EF-100/EF-1547) using DNeasy kit (Qiagen, Germantown, MD). PCR condition for amplification

of ATPase6/ATPase8 gene using sense CTATCCGACACACCCAGAAGTAAAG and anti sense GATGCTGGGAAATATGATGATCAGA primers was described before [140]. Amplification of human housekeeping gene GAPDH by using sense TCCCTGCCTCTACTGGCGCTGCCAAGGCTG and antisense TCCTTGGAGGCCATGTGGGCCATGAGGTCC primers followed published method [141].

Karyotyping

Monolayer primary cultures of equine keratinocyte lines EK1546 and EK100 were grown in CNTY or FY media in T75 cell culture flasks. Semi-confluent (~ 70%) cultures with many mitotic cells were harvested with colcemid (Sigma) following standard procedures [142]. The cells were treated with Optimal Hypotonic solution (Rainbow Scientific) following the manufacturer's protocol, and fixed in methanol:acetic acid (3:1). Chromosome preparations were made on pre-cleaned wet glass slides and stained with Giemsa for initial counting. The sex chromosomes were identified by CBG-banding , and refined chromosome analysis and karyotyping were done by GTG-banding [143, 144]. A minimum of 10 cells were captured and analyzed for each technique using an Axioplan2 microscope (Zeiss) and Ikaros (MetaSystems GmbH) software.

Fluorescence in situ hybridization (FISH)

Additional verification that the primary keratinocyte cultures EK1547 and EK100 were of pure equine origin and not mixed with other cell lines was done by FISH. We used horse bacterial artificial chromosome (BAC) clones (CHORI-241: http://bacpac.chori.org/equine241.htm) containing select chromosome-specific markers (Table 2.2). BAC DNA was isolated by Plasmid Midiprep kit (Qiagen), labeled with biotin-16-dUTP or digoxigenin-11-dUTP using Biotin- or DIG-Nick Translation Mix (Roche), and hybridized to

metaphase chromosomes. Hybridizations and signal detection were carried out according to standard protocol [142]. The results were examined with Zeiss Axioplan2 fluorescence microscope and at least 10 images were captured and analyzed for each experiment using Isis V5.2 (MetaSystems GmbH) software.

Flowcytometry

3×10^5 cells were permeabilized with 0.1% v/v Triton X-100 after fixing with 2% PFA.0.5% BSA solution was used for blocking for 30 mins. EK-1547, HFK, and J2 cells were stained with Alexa Fluor (R) 488 Conjugate Pan-Keratin (C11) Mouse mAb (Cell Signaling #4523S,1:100) for overnight at 4c followed by washing twice with 1X PBS/.5 BSA then resuspend in 1x PBS for flow cytometric analysis. 30000 cells were analyzed on an LSRFFortessa (BD). Cells were gated by light scatter (FSC vs SSC) to remove debris. Data analysis on population B was done utilizing FCSExpress 5 (DeNovo software) and the percentage of cells staining positive was determined by setting a marker on the unstained sample (1% positive) of each cell line. HFK cells and J2 fibroblast cells were used as a positive and negative control to confirm antibody specificity. Analysis of data from three independent cell cultures was conducted by the flow-cytometry and cell sorting shared facility at Georgetown University.

Immunofluorescence staining

Immunofluorescence staining of equine cells on coverslips was performed for CK14 using kits from Vector Labs and Dako according to manufacturer's instructions. Briefly, slides were treated with 3% hydrogen peroxide and with an avidin/biotin blocking kit (Invitrogen). The slides were exposed to 10% normal horse serum and to a primary antibody for CK14 (Abcam #ab7800, 1:300) diluted in Tris Buffered Saline with 0.5% Tween (TBST) for 1 hour at

room temperature. Slides were exposed to a biotin-conjugated rabbit secondary antibody (Vector Labs) diluted in an anti-mouse conjugated-horseradish peroxidase labeled polymer from Dako (K4001). The CK14 was visualized with TSA-488 (Life technology, REF T20948). Slides were mounted with Pro-Long Antifade with DAPI. TBST was used for washing throughout. Consecutive cells with the omitted primary antibodies were used as negative controls.

Immunohistochemistry

Hematoxylin and eosin (H&E) staining and immunohistochemical staining of normal human skin, normal horse skin, breast cancer tissue and insert's membranes were performed for filaggrin, involucrin, and CK-14. Five-micron sections from formalin fixed paraffin embedded tissues were rehydrated through a graded alcohol series and de-paraffinized with xylenes. Heat-induced epitope retrieval (HIER) was conducted by immersing the tissue sections at 98^{o}C for 20 minutes in Tris/EDTA (pH 9.0). Immunohistochemical staining was performed using a horseradish-peroxidase labeled polymer from Dako K4001 according to manufacturer's instructions. In summary, slides were treated with 10% normal goat serum and 3% hydrogen peroxide for 10 minutes each and exposed to primary antibodies for 1hour at room temperature. Slides were exposed to the appropriate HRP labeled polymer for 30min and DAB chromagen (Dako) for 5 minutes. Slides were counterstained with Hematoxylin (Fisher, Harris Modified Hematoxylin), blued in 1% ammonium hydroxide, dehydrated, and mounted with Acrymount. Consecutive sections with the primary antibody omitted were used as negative controls.

Following antibodies were used: anti-cytokeratin 14 (Abcam#ab7800, 1:600, 1:5000), anti-involucrin (Santa Cruz Biotechnology sc-28557, 1:300, 1:600), anti-filaggrin 14 (Abcam #ab17808, 1:150)

3D Air-liquid-interface culture

0.4 um PCF inserts (CELLnTEC, Switzerland) were placed in 24 wells plates (Falcon) and 3×10^5 EK-1547 or HFK cells were seeded inside the insert using 400ul CNT+Y or F+Y medium correspondingly while 600 ul of medium were added outside the insert. On day 3, all medium was aspirated and 400 ul of differentiation media CnT-Prime 3D Barrier (CELLnTEC, Switzerland) were added inside the insert and 600 ul outside to allow cells to form intercellular adhesion structure. Plates were incubated for additional 16h overnight at 37°C 5% CO2. On day 4, all media was removed, and inserts were transferred to 60 x 15 mm dishes (Falcon) and 3.2 ml CnT-Prime 3D Barrier were added outside of the insert to start the airlift culture. Media was changed every 2-3 days. On day 14 inserts were fixed overnight at 4C using 4% (w/v) paraformaldehyde. Membrane inserts were then placed in 70% Ethanol and submitted for H&E staining and sectioning.

Results

Establishing equine keratinocytes with the CR method

Two skin biopsies containing epidermis and dermis were obtained aseptically from two different horses (Equus caballus): One strip of scrotal skin was obtained during castration of a Lipizzaner stallion (GUMC-100) and the other one from the neck area of a second horse (GUMC-1547). Approximately 1 x 2 cm biopsies were taken and transferred into DMEM media supplemented with pen/strep mix, gentamicin, amphotericin B and nystatin as described previously [18]. Tissues were transported and stored at 4 °C and processed by incubating them in a mixture of dispase and collagenase to enable physical separation of epithelium and dermal tissue. Later, the epithelium was dispersed into single cells by digestion with collagenase/trypsin), and the resulting cells were plated on a bed of irradiated Swiss 3T3 J2 cells

(feeder cells) and F medium supplemented with 10 µM Y-27632 (ROCK inhibitor) as previously described [18]. Cobble-stone shaped keratinocyte colonies (Figure 2.2A, B black arrows) were readily visible after 2 days, and cultures reached confluence in 5 days. After the first plating, the keratinocytes were seeded at 4.0 x 10^3 cells/ cm^2 and passaged every 6-8 days. As reported previously the irradiated feeders inhibited the outgrowth of fibroblasts in the CR culture conditions [17, 18]. In order to establish fibroblasts from the same equine tissue, some of the single cell suspension was plated in DMEM with 10 µM Y-27532. Spindle-shaped fibroblasts were visible after 2 days (Figure 2.2C, D).

ROCK Inhibitor Y-27632 is required for equine keratinocytes proliferation

To define the optimal in vitro conditions to cultivate and propagate equine keratinocytes, we compared F, KSFM and CnT09 mediums with or without ROCK inhibitor. We also evaluated F medium with or without feeder cells. The full CR conditions, feeders + F medium + Y-27632, supported equine keratinocyte (EK-1547) growth beyond 40 population doublings (PDs) with an average growth rate of 2.39 days/doubling (Figure 2.3A). Without ROCK inhibitor cell proliferation ceased at 16 population doublings (Figure 2.3A). J2 feeder cells were also optimal for cell proliferation since F medium + Y-27632 supported limited cell expansion 25 pds with a decreased rate of 4.18 days/doubling (Figure 2.3A). In this feeder-free system, ROCK inhibitor played a critical role since F medium alone did not support cell growth (Figure 2.3A). Equine keratinocytes were not able to proliferate in the synthetic human keratinocyte medium (KSFM) with or without ROCK inhibitor, but rather became rapidly senescent (Figure 2.3B, C bottom panel). CnT09, an animal keratinocyte medium, could extend the cell growth to 20 population doublings but only when Y-27632 was added (Figure 2.3A). The importance of ROCK inhibitor was also demonstrated with the second Equine keratinocytes (EK-100)

(Supplementary figure 2.1). Thus, equine keratinocytes were able to survive and proliferate indefinitely only under complete CR conditions.

Verification of equine origin and chromosomal stability

To verify the equine species identity of the isolated cells, DNAs were extracted from monolayer cultures of the two horse primary keratinocytes lines (EK-1547 and EK-100), as well as from human foreskin keratinocyte (HFK), canine cells (K9) and mouse fibroblasts (J2). Equine-specific mitochondrial ATPase6/ATPase8 gene primers were used to confirm equine origin of the keratinocytes and the expected equine specific band 153 bp was detected only in the two horse primary keratinocyte preparation (EK-1547 and EK-100) (Figure 2.4A). Pan-species GAPDH primers were used as loading control (Figure 2.4B). Furthermore, we applied FISH with BAC clones specific for select horse autosomes (chrs 9 and 29, Table 2.2) where two red signals (CREM, chrs 29) and two green signals (LCORL, chrs 9) were detected, which is expected and normal for horse samples (Figure 2.4C). Cytogenetic analysis was carried out to corroborate that both cell lines had a normal diploid chromosome number (2n=64) for the horse and normal chromosome morphology as revealed by karyotyping Giemsa stained and G-banded chromosomes (Figure 2.5A, B). Both cell lines were confirmed to be genetically male with XY sex chromosomes, as revealed by C-banding (Figure 2.5A, B). We did not observe any chromosome abnormalities or any other signs of chromosomal instability, such as breaks, unstained gaps, or abnormal chromosome configurations. These results demonstrate that the cell lines EK1547 and EK100 originate from male horses and carry normal diploid horse karyotypes.

Pure population of highly proliferative basal keratinocytes

When growing keratinocytes from skin tissues, fibroblast contamination represents a common challenge [138]. To determine the purity of the grown keratinocytes, FACS analysis was used. EK-1547 cells at passage 5 were collected and stained with conjugated pan-Keratin antibody. Consistently more than 96% of the total cells were positive for pan-Keratin indicating a very high level of keratinocytes (from three independent cell cultures) (Figure 2.6A, B). Human foreskin keratinocytes and mouse fibroblasts were used as positive and negative controls respectively (Supplemental figure. 2.2A, B and 2.2C, D). To confirm the basal nature of the equine keratinocytes, cells were stained for cytokeratin 14 and analyzed using immunofluorescence. The resulting images confirmed that both cell lines EK1547 and EK100 displayed a positive cytoplasmic signal with CK-14 (Figure 2.7A, B).

Equine keratinocytes retain differentiation potential

In order to test whether these proliferating adult stem cell-like equine keratinocytes retained the ability to differentiate, cells were transferred to a 3D air-liquid interface culture in medium lacking Y-27632 [26, 145]. EK-1547 cells were seeded in 0.4 um PCF polycarbonate inserts with 2D medium CnT09+Y. The cells were incubated at 37°C with 5% CO2. To induce differentiation, on day 3, medium was replaced with differentiation medium CnT-PR-3D. On day 4, medium on the top of the cells was removed, and cells began to be exposed to air. Hematoxylin and Eosin staining of the 3D equine culture (Figure 2.8 2nd column) revealed that the cells formed an organized differentiated stratified squamous epithelium including a cornified layer similar to equine skin tissue (Figure 2.8A, 1st column). Morphological analysis was complemented by immunohistochemistry for the basal cell marker CK14 (Figure 2.8B) and the terminal differentiation markers involucrin (Figure 2.8C) and filaggrin (Figure 2.8D). The 3D

human foreskin keratinocytes culture was used as positive control (Figure 2.83rd column A-D). Breast cancer tissue and equine skin tissue were used to test the specificity and the reactivity of CK-14 to horse tissue (Supplemental figure 2.3A, B).

Discussion

Primary equine keratinocytes have limited growth potential in vitro thereby limiting their use for expansion and regenerative medicine [138]. Despite the high incidence of skin cancer and high rate of granulation in horses' wound, the complex interaction of keratinocytes with other cells in the inflamed wound such as neutrophil and fibroblast have not been fully investigated, due to the lack of a reliable in vitro research system [146]. Dahm et al. were the first to isolate and cultivate primary equine keratinocytes from lip epithelium using equine fibroblast feeders or with collagen type I culture coating. However, the equine keratinocytes growth was limited only to a low number of passages, and their growth rate was very slow needing on average 38 days to reach confluence [137]. Another study showed that equine keratinocytes were isolated from lip epithelium and propagated on collagen type I coated substrate. The cells could be sub-cultured to passage 6 without significant loss of cell character [139]. More recently isolation of primary equine keratinocytes was accomplished by enzymatic dissociation or with explant culture method [123]. Both methods led to a heterogeneous primary culture comprised of keratinocytes and fibroblasts. There was no evidence of high proliferation rate or long lifespan of the developed keratinocytes. Using a similar explant culture technique, equine keratinocytes were isolated and propagated using matrigel coated dishes. These cells were proliferating up to six passages [147]. Using the CR technology, we were able to isolate pure primary equine keratinocyte and efficiently propagate them at the rate of 2.39 days/doubling for 40 PDs.

To the best of our knowledge, this is the first report that shows that primary equine keratinocytes can be propagated indefinitely in an undifferentiated status using an *in vitro* 2D system. Similarly, we were also able to successfully propagate these cells for long-term using a feeder-free system F medium supplemented with the Rho-Kinase inhibitor Y-27632.

ROCK inhibitor, Y-27632, was first identified as being capable of increasing the cloning efficiency of human embryonic stem (ES) cells [24]. Later studies showed that Y-27632 increased the viability of human keratinocyte stem cells [25]. Here, our study shows that the exposure to Y-27632 appears to be required for continued equine keratinocytes proliferation since the removal of Y-27632 in any culture condition led to cell senescence. The exact mechanism of Y-27632 on cell immortalization is still unknown. However, it is known that Y-27632 disrupts the actin cytoskeleton, inactivates Rho, and inhibits apoptosis [148]. Interestingly, the effects of Y-27632 are completely reversible, in that equine keratinocytes stopped proliferating and terminally differentiated after its removal when the cells were moved into an air-liquid interface culture.

Among the earlier studies, it was controversial whether calcium concentration of the medium for equine keratinocytes needed to be low. Dahm et al. showed a low concentration of 0.6 mM was required, whereas Michelle et al. suggested higher concentration 1.8 Mm as optimum concentration [138, 139]. In our culturing system, high calcium concentration 1.8 mM in CNT media or 1.36 mM in F media supported the growth of equine keratinocytes in presence of 10 uM Y-27632. In contrast, KGM with low calcium concentration was not able to support the growth of equine keratinocytes with or without Y-27632. This agrees with the earlier study that skin keratinocytes are able to proliferate at a higher calcium concentration, as long as suitable media and substrate conditions are present [139]

Figures and Tables

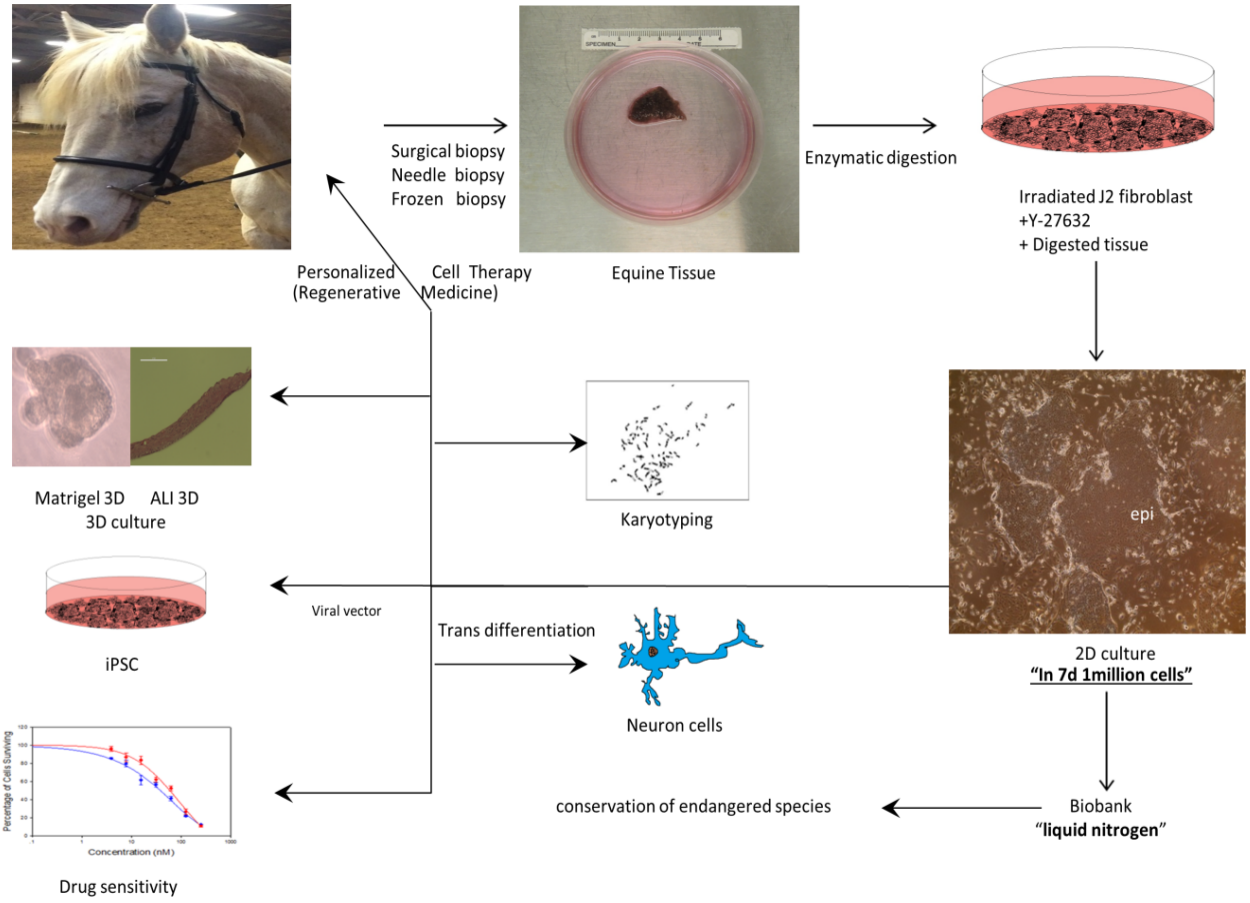

Figure 2.1. Outline of the CR method for establishing Equine keratinocytes cultures and potential uses of generated cells. Equine tissues were obtained from different horses; tissues were digested enzymatically followed by initiation of cells growth and propagation using irradiated mouse fibroblast and ROCK inhibitor. Cells were cryopreserved in liquid nitrogen. The generated equine keratinocytes can be used in numerous applications, including -but not limited to- induced reprogramming stem cells generation (iPSC), transdifferentiating into somatic cells, drug screening and regenerative medicine.

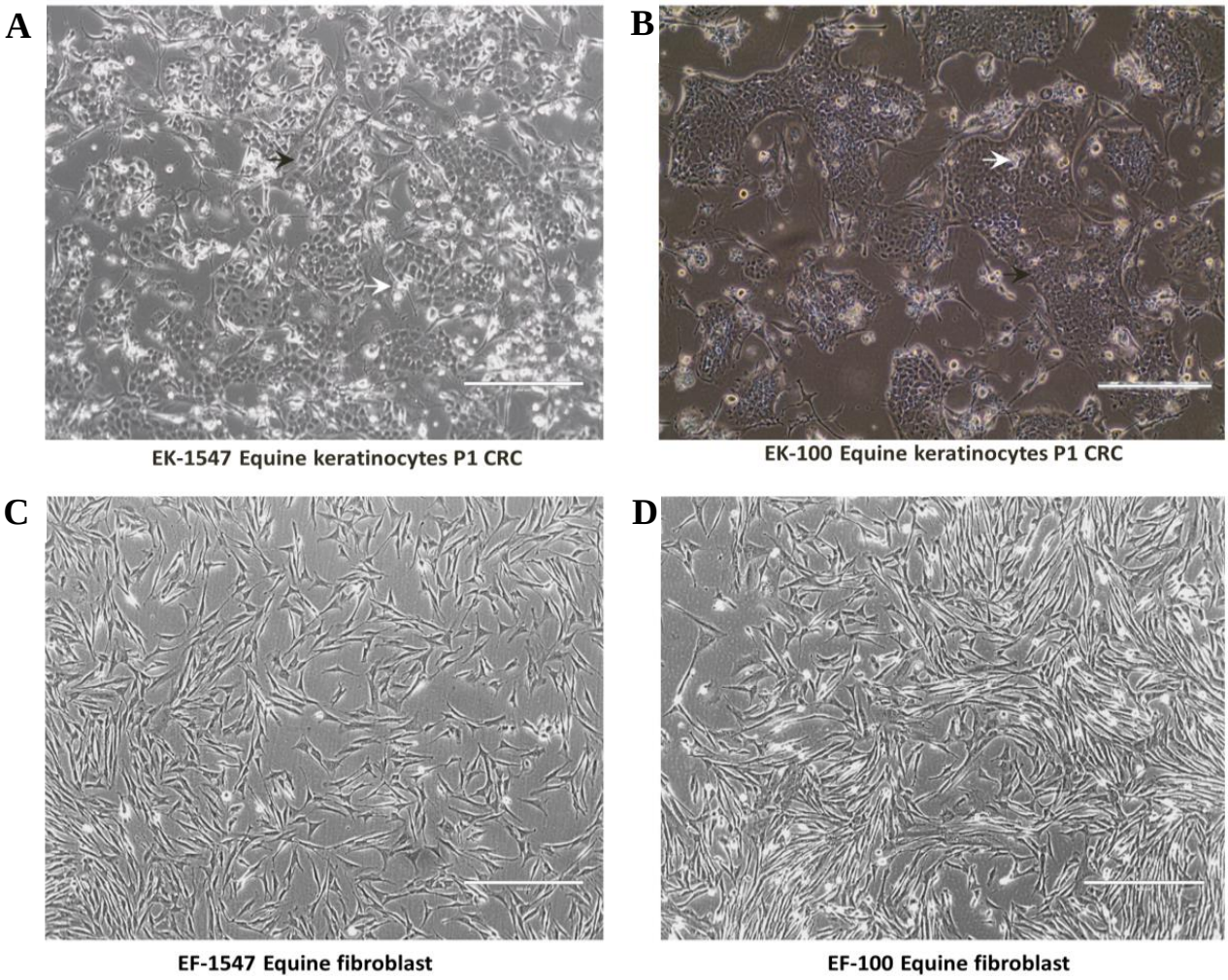

Figure 2.2. Phase contrast photomicrograph of primary equine keratinocytes and fibroblasts from two different tissues. Cells from horse skin (horse 1) in (A) and (C) and ones from scrotal skin (horse 2) in (B) and (D). (A) Equine keratinocytes-1547 (B) Equine keratinocytes-100 (C) Equine fibroblasts-1547 (D) Equine fibroblasts-100. (Magnification is 10X scale bar is 400 µm) white arrows indicate irradiated j2 and black arrows indicate keratinocytes.

A

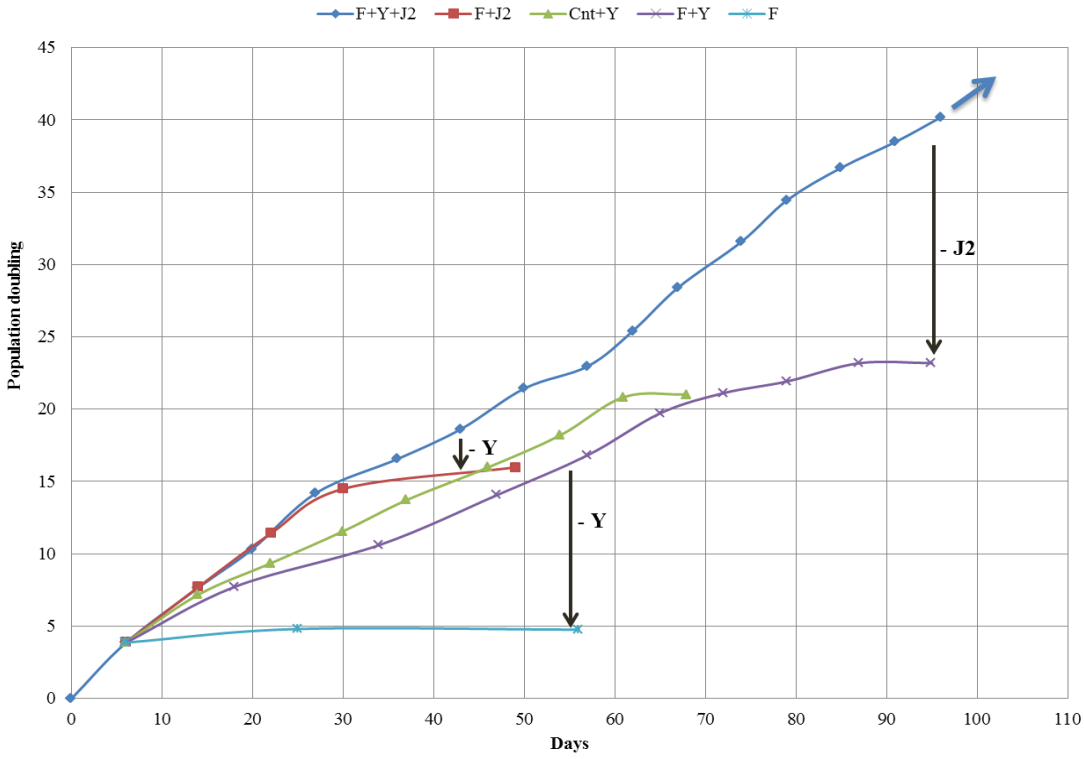

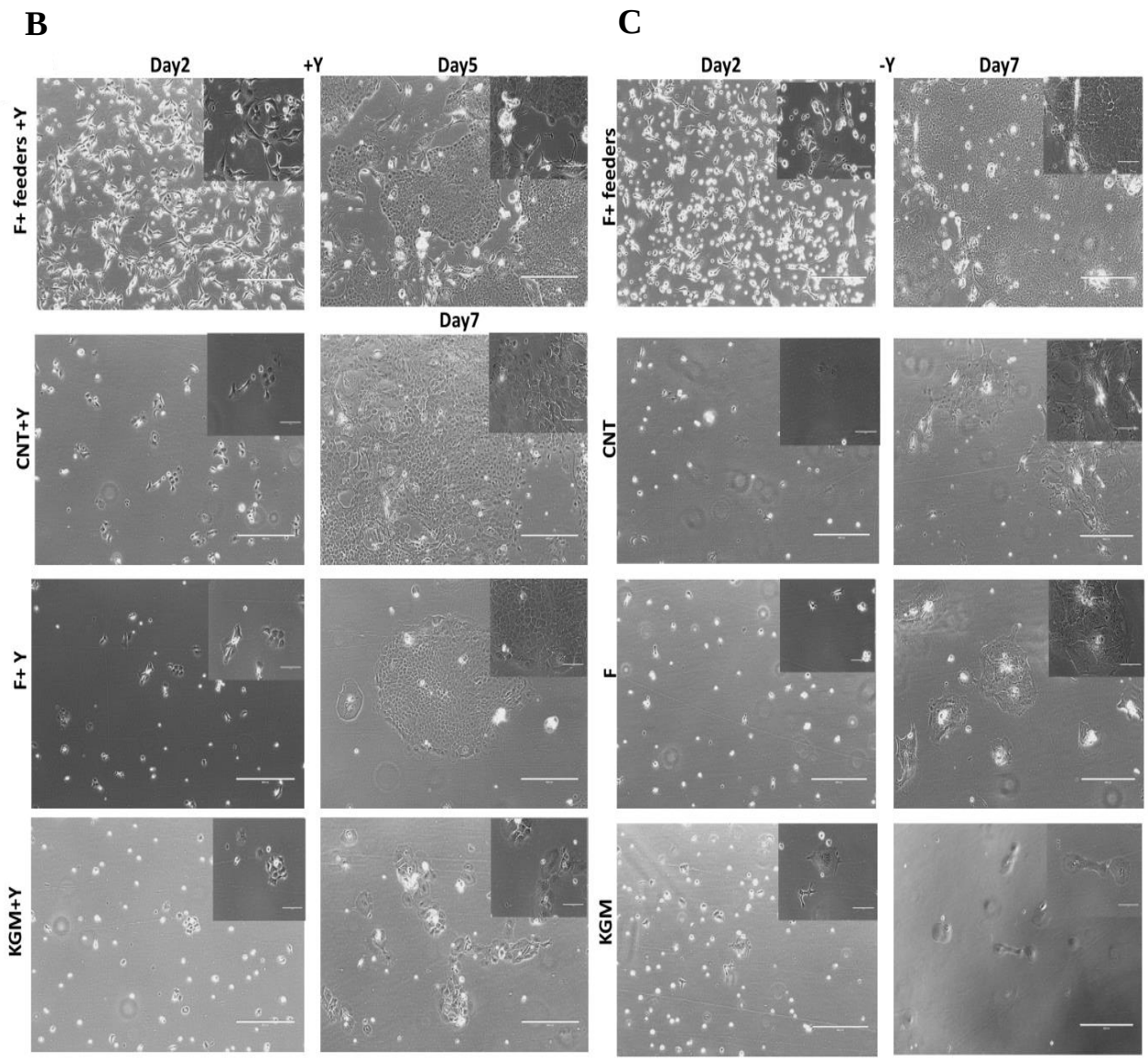

Figure 2.3. Equine keratinocyte growth was tested in various culture conditions with or without 10 uM Y-27632. (A) Growth curve was generated to represent growth rate by plotting population doubling over days in time (graph shows the average of replicates). The arrow indicates cells that continued to divide indefinitely. Phase contrast images of primary equine keratinocytes (EK-1547) cultured in co-culture with irradiated fibroblasts, CNT, F and KSFM with (B) or without Y-27632 (C). All images were taken on day2 and day7 following initial culture without passage (day 5 for feeders+Y condition due to 95% confluency) (10X magnification. Size bars= 400μm). Top right images show enlarged magnification (40X magnification, size bars= 100μm).

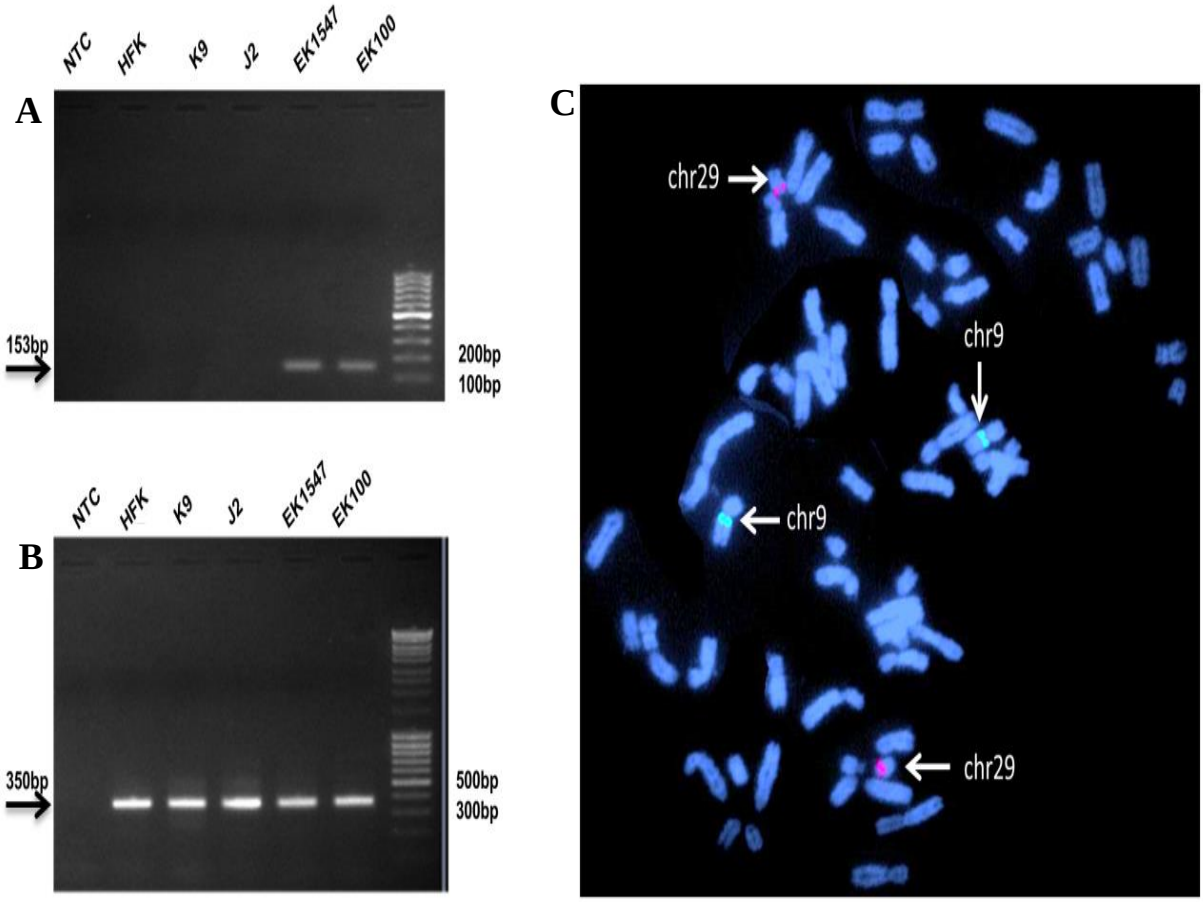

Figure 2.4. Validation and genotyping of Equine keratinocyte cell lines. (A,B) PCR amplification with equine MT-ATP6/MT-ATP8 (top)and GAPDH (bottom) primers; NTC – no template control, HFK -human foreskin keratinocytes, K9 - dog cells, J2 - mouse fibroblasts, EK100 – equine keratinocytes, EK1547- equine keratinocytes;(C). FISH with BACs 49H16 (chr9, green) and 76H13 (chr29, red) in EK1547.

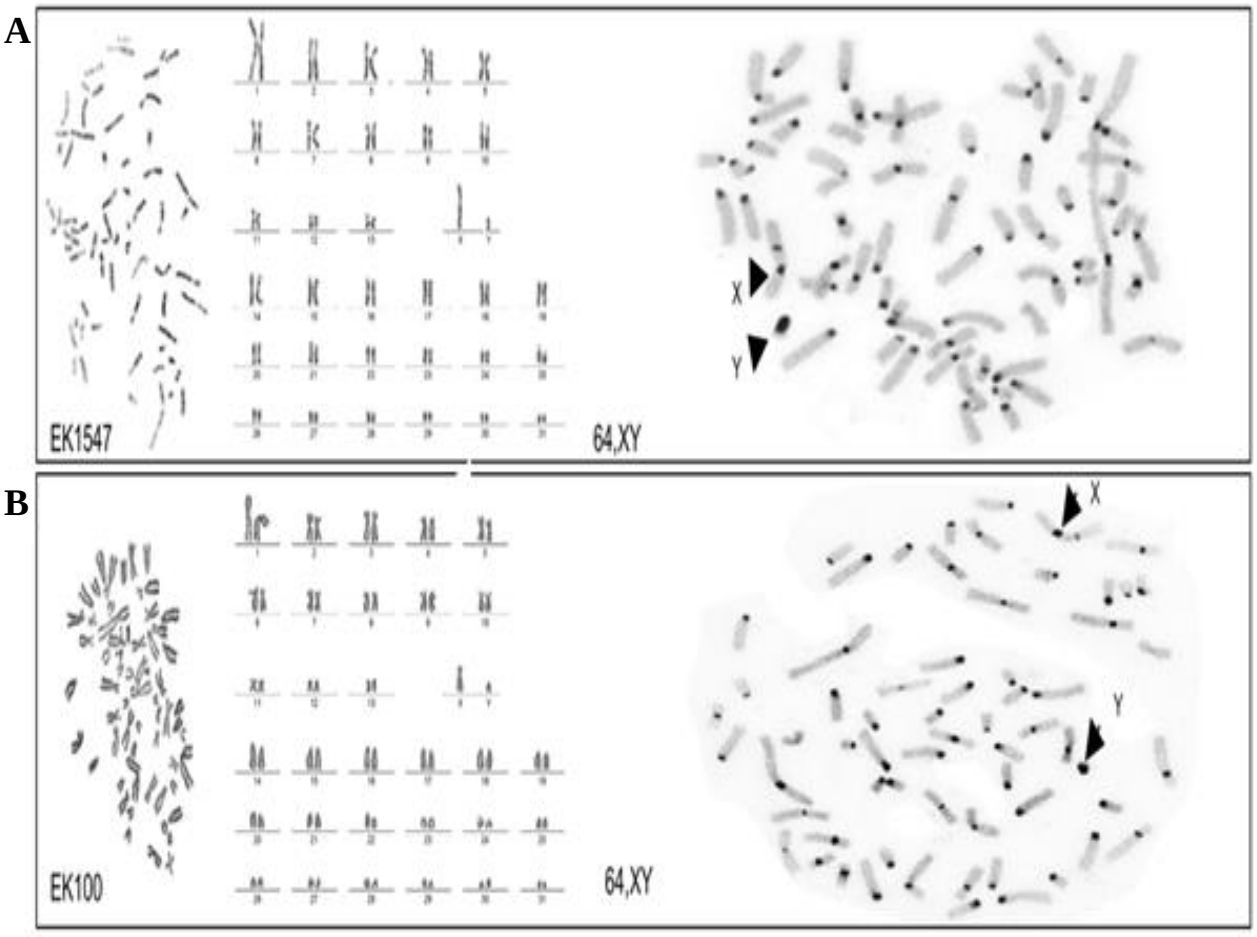

Figure 2.5. Chromosomal stability of Equine keratinocyte cell lines. (A) (Cytogenetic analysis of EK1547: G-banded metaphase (left), G-banded karyotype (middle), C-banded metaphase (right); (B) Cytogenetic analysis of EK100: Giemsa stained metaphase (left), Giemsa stained karyotype (middle), C-banded metaphase (right).

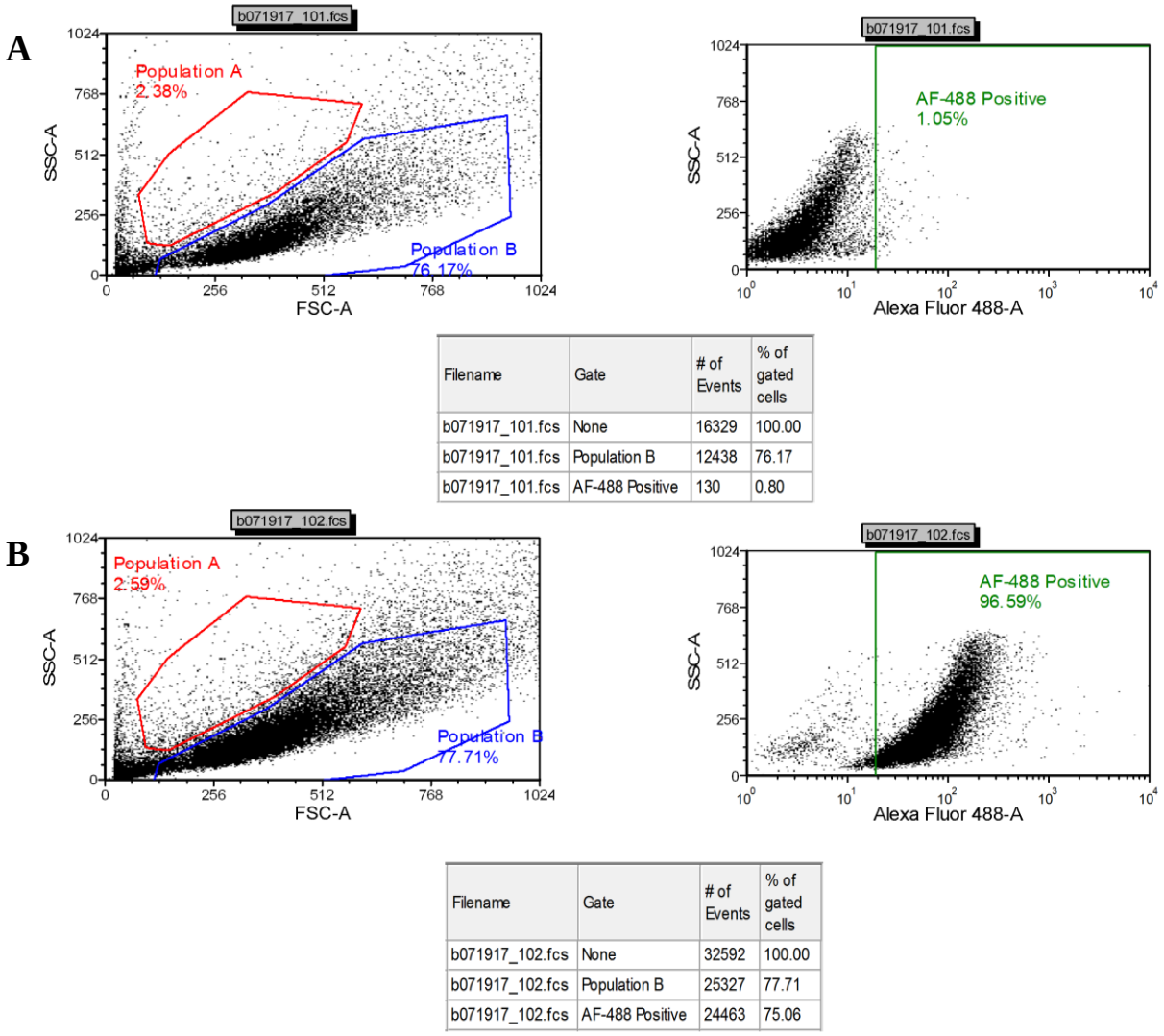

Filename	Gate	# of Events	% of gated cells
b071917_101.fcs	None	16329	100.00
b071917_101.fcs	Population B	12438	76.17
b071917_101.fcs	AF-488 Positive	130	0.80

Filename	Gate	# of Events	% of gated cells
b071917_102.fcs	None	32592	100.00
b071917_102.fcs	Population B	25327	77.71
b071917_102.fcs	AF-488 Positive	24463	75.06

Figure 2.6. Highly pure population of highly proliferative basal equine keratinocytes. Fluorescence-activated cell sorting (FACS) analysis with pan-cytokeratin antibodies was performed on equine keratinocytes. (A) EK-1547 cells without Pan-CK antibody as control or (B) EK-1547 cells with Pan-CK antibody.

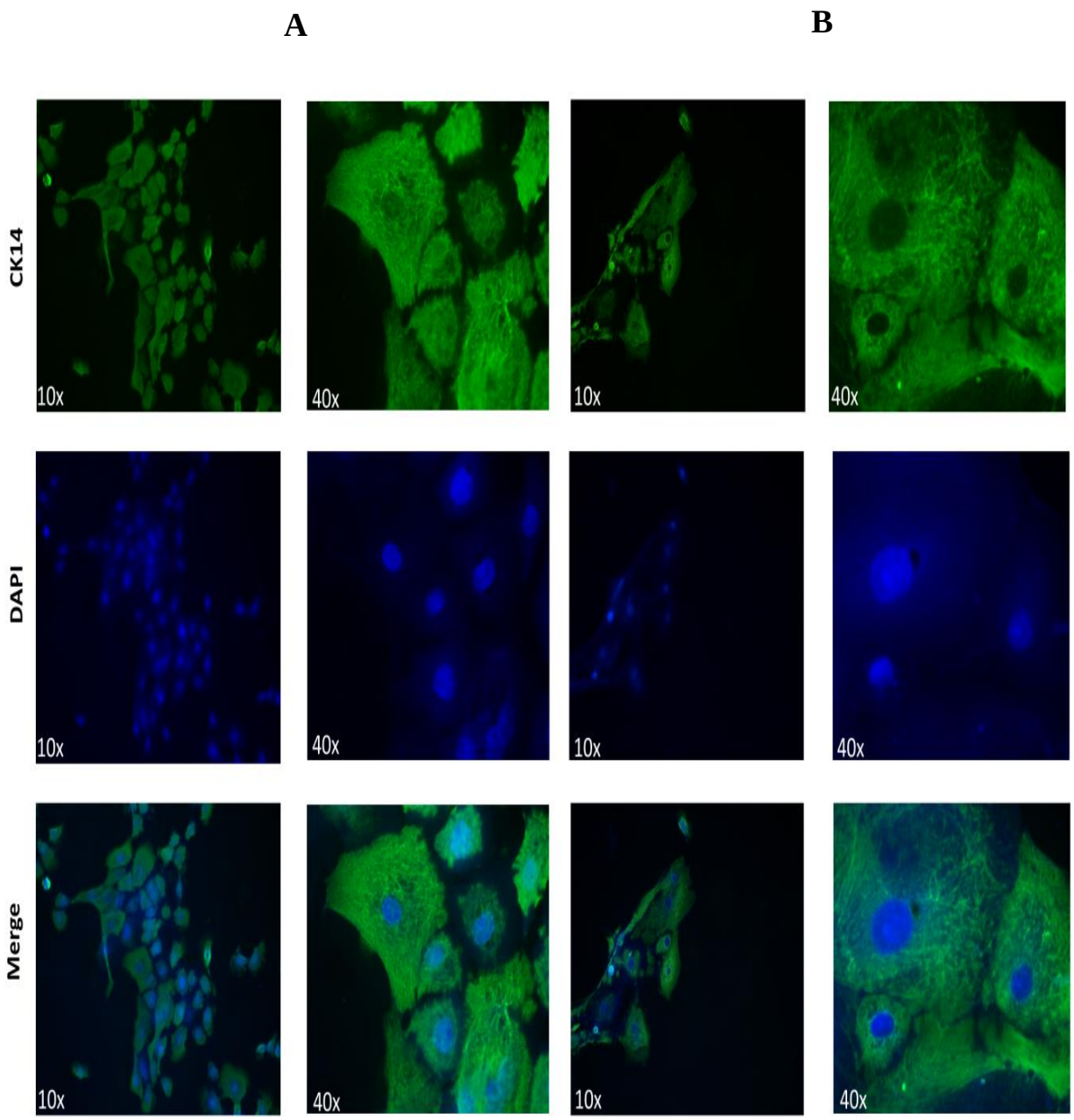

Figure 2.7. CK-14 Immunofluorescence staining of equine keratinocytes cells. (A) EK-1547 Cells and (B) EK-100 cells were stained for cytokeratin 14 which is localized on the cytoplasm. Fluorescent photomicrographs from three experimental replicates using 10X and 40X magnification were captured.

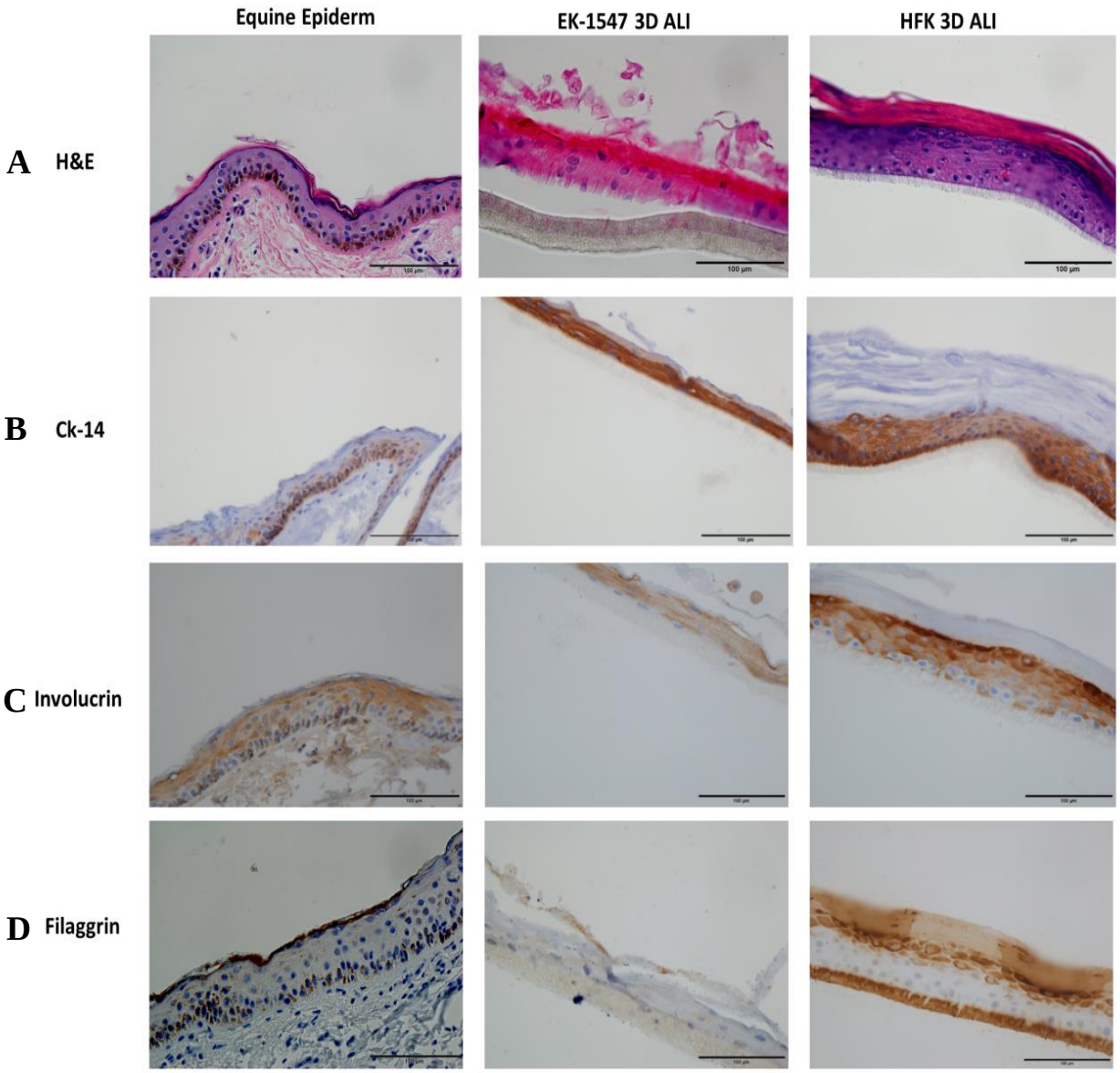

Figure 2.8. The air-liquid interface of primary equine epithelial cells recapitulate the In vivo skin epithelium. To assess the ability of equine keratinocytes to form a stratified epidermis in ALI (middle panel) morphology was compared to normal equine skin (left panel) by Hematoxylin and Eosin (H&E) (A) and stratification marker CK14 (B) Involucrin (C) and Filaggrin (D). HFK in ALI was used as technical control. All images (40x magnification, scale bar= 100μm) are representative of three experimental repeats.

Table 2.1. Culture conditions were used for growing equine keratinocytes.

Growth Media	Calcium Concentration* (mM)	Y-27632 Concentration (uM)	FBS Concentration	Survival	Ability to passage
KSFM+[suppa]	0.1	No	No serum	No	No
KSFM+[suppa]	0.1	Yes	No serum	No	No
CnT-09+[suppb]	1.8	No	10%	yes	No
CnT-09+[suppb]	1.8	Yes	10%	Yes	Yes
Fmedia	1.36	No	7.40%	Yes	Yes (1 passage)
Fmedia	1.36	Yes	7.40%	Yes	Yes
Fmedia + irradiated feeders	1.36	Yes	7.40%	Yes	Yes

suppa Epidermal Growth Factor 1-53 (EGF 1-53) and Bovine Pituitary Extract (BPE)
suppb Supplements A and Supplements B (200mM L-Glutamine)
* Calcium concentration in FBS is not included.

Table 2.2. Horse chromosome specific BAC clones used for FISH.

BAC ID	Horse chromosome	Known gene content	Reference	Label&detection
049H16	**9**	**LCORL**	**Staigeret al. 2016**[149]	**Biotin-FITC**
076H13	**29**	**CREM**	**Ghosh et al. 2014**[150]	**Digoxigenin_Rhodamine**

Conclusion

By using conditional reprogramming and high throughput screen platforms in the first study, we identified and validated panobinostat, dinaciclib or forskolin as effective drugs for recurrent respiratory papillomatosis therapy in 2D and 3D culture. Moreover, we have shown the feasibility to test drugs based on high throughput screen (the RRP platform) in a very short time providing a tool for personalized medicine. Unlike our previous study with the RRP patient in which drugs were tested based on known drugs for RRP condition, we used candidates from the high throughput drug screening results (RRP-platform) in GUMC-1695 drug screening. Therefore, The GUMC-1695 drug screening was undoubtedly a successful application of the CR method in a clinical setting and can serve as a model for personalized medicine.

In the second study, we were able to isolate and propagate pure primary equine keratinocytes rapidly. We also demonstrated that the cells preserved the ability to regenerate a fully stratified epithelium sheet with appropriate spatial and temporal expression of differentiation markers in a short-term in vitro organotypic culture system.

The first study provides support that the CR method can make substantial contributions by providing a valuable method to identify, repurpose and personalize therapy for different types of cancer, especially where lacking funding is an issue facing researchers focusing on orphan diseases like recurrent respiratory papillomatosis. Additionally, in the second study, conditional reprogramming is setting the groundwork for a model system to study wound healing products, regeneration processes and more importantly the possibility of grafting the keratinocytes in horses. This system can be used for autologous skin regeneration therapy for horses which will potentially satisfy a huge unmet medical need.

Overall, these set of experiments demonstrated that the CR method was successfully applied to the fields of regenerative medicine, drug discovery and personalized medicine. In conclusion, there is an expanding potential for the application of conditional reprogramming to a wide variety of fields such as, but not limited to, regenerative medicine and drug discovery.

Appendix A: Chapter One Supplementary Figures and Data

Supplementary Methods

DNA was isolated and purified from the cultured cells, GUMC-403, or directly from the tissues using the DNeasy Blood and Tissue Kit (Qiagen) and was amplified with specific primers for HPV-6 or HPV-11 for typing. Genomic DNA was extracted from RLL-403 and GUMC-403 and diluted with nuclease-free water to 10 µg/ml then used for all ddPCR experiments. ddPCR, probes were designed to amplify products of 100-300bp as recommended. The reaction mixtures contained ddPCR Probe Supermix (Bio-Rad Laboratories, Hercules, CA, USA), template DNA (1µl) and primers (final concentration, 25 nM) in a final volume of 20 µl. Each reaction was then loaded into a sample well of an eight-well disposable cartridge (DG8™; Bio-Rad Laboratories) along with 70 µl of droplet generation oil (Bio-Rad Laboratories). A QX200™ Droplet Generator (Bio-Rad Laboratories) was used to generate the droplets as per the manufacturer's directions. Droplets were then transferred to a 96-well PCR plate, heat-sealed with foil and amplified using a conventional thermal cycler to the end point (95 °C × 5 mins (1 cycle), 95 °C × 30 s, 56 °C × 30 s and 72 °C x 30 s (40 cycles), followed by 4 °C x 5 mins (1 cycle), 90 °C x 5 mins (1 cycle), and lastly 4 °C hold). A QX200 Droplet Reader (Bio-Rad Laboratories) was used to read the resulting products, and QuantaSoft™ software (Bio-Rad Laboratories) to analyze data. Thresholds bar was set based on the value of the no template control (NTC), and the copy number was calculated based on the ratio of HPV-6: RNaseP. RNaseP copy number reference assays were purchased commercially (Applied Biosystems). The HPV6-L1 Tagman assay used is forward primer 5′-(TGG AAG ATG TAG TTA CGG ATG C) -3′, reverse primer 5′-(AGC CCA GGG ACA TAA CAA TG) -3′, and probe 56-FAM/AC CAC ACG C/ZEN/A GTA CCA ACA TGA CA/3IABkFQ. The HPV6-E6 Tagman assay used is forward primer 5′-

(CCACGTCTGCAACGACCATA)-3′,(reverseprimer)5′-(TTCCATGAAATTCTAGGCAGCA) -3′, and probe FAM-5'- CCTG TTTCGAGGCGGCTATCCA-3'-TAMRA.The HPV6-E2 Tagman assay used forward primer 5′-(AAAAGTATGGGAGCACCAAACA-) -3′, (reverse primer) 5′-(GCTGGTCGTGATTGTTAGTGATG)-3′,and probe FAM-5'-TGGACCCGTGGACAGTGGAAACC-3'-TAMRA. The same protocol was followed for E6: E2 ratio assay except for a melting point of 61 °C×30 s. For chemosensitivity assay, GUMC-403 cells (5.0 x 10^3 cells/well in 100 µl of F+Y medium) were seeded in a 96 wells plate for 2D monolayer (VWR, Radnor, PA). Seeded cells were incubated overnight at 37°C in a cell culture incubator with 5% CO2 levels. The medium was replaced with fresh medium that has 7 different concentrations of the 13 drugs (drugs are listed in Table 1.1.). Cell viability assay was conducted using the veritas microplate luminometer turner Biosystems. The CellTiter-Glo® Luminescent Cell Viability Assay (G7570, Promega, Madison, WI) kit for 2D culture was used for data analysis according to the manufacturer's protocol. The cell viability reading was measured after 3 days and the treated cells luminescence reading was normalized to that of vehicle (DMSO) treated cells. For statistical significance, the experiment including was carried in 3 technical replicates and conducted at three independent times.

Supplementary Results

HPV-6 DNA loads were measured with HPV-6 L1 and RNaseP assays using RRL-403 and GUMC-403 genomic DNA. 13 copies per cell in RRL-403 and single copy per cell in GUMC-403 (Supplementary figure 1.1). To investigate the existence of integrating of viral DNA into the cellular genome, HPV-6 E6/E2 ratios were used and value more than 2 suggest the presence of integrated HPV-6 [151]. E6/E2 ratios were .89 and .94 for RLL-403 and GUMC-

403 respectively indicating lacking of integration of viral DNA into cellular DNA (Supplementary figure 1.2).

To investigate the cytotoxicity of the 13 drugs on another RRP cells, we used the previously established cells in our lab GUMC-429 and GUMC-228 (matched pair). HPV typing using specific primers for HPV-11 was conducted. Only bands with primers for HPV-11 were detected in GUMC-429, not in GUMC-228 (Supplementary figure 1.3). All drugs have shown significant toxicity on both GUMC-429 and GUMC-228. Interestingly, differential cytotoxicity toward GUMC-429 over GUMC-228 was detected with romidepsin but not with panobinostat, dinaciclib or forskolin (Supplementary figure 1.4-1.9).

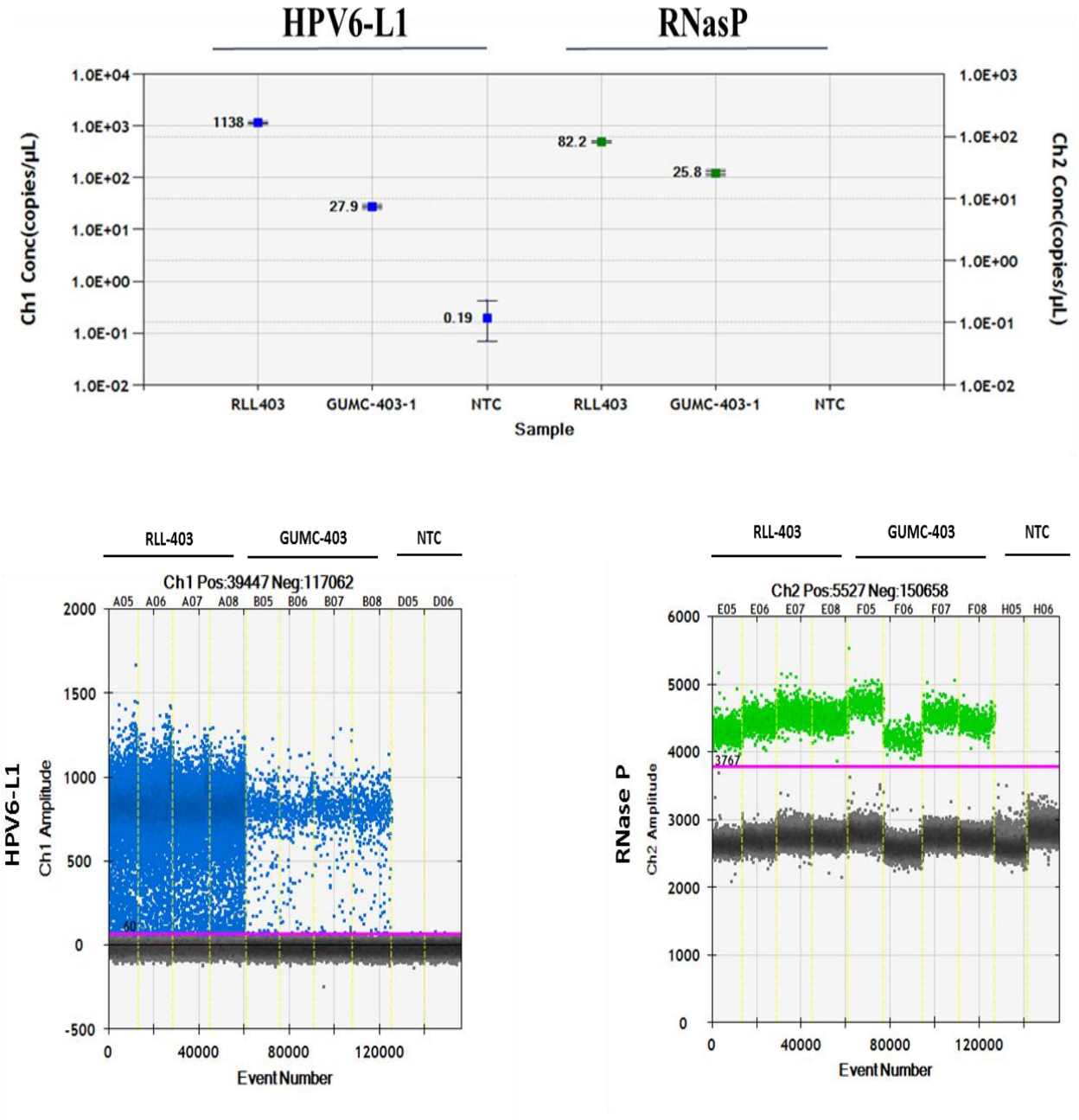

Figure S1.1. Quantification of HPV-6 copy number by digital droplet PCR using HPV6 L1 and RNasP assays.

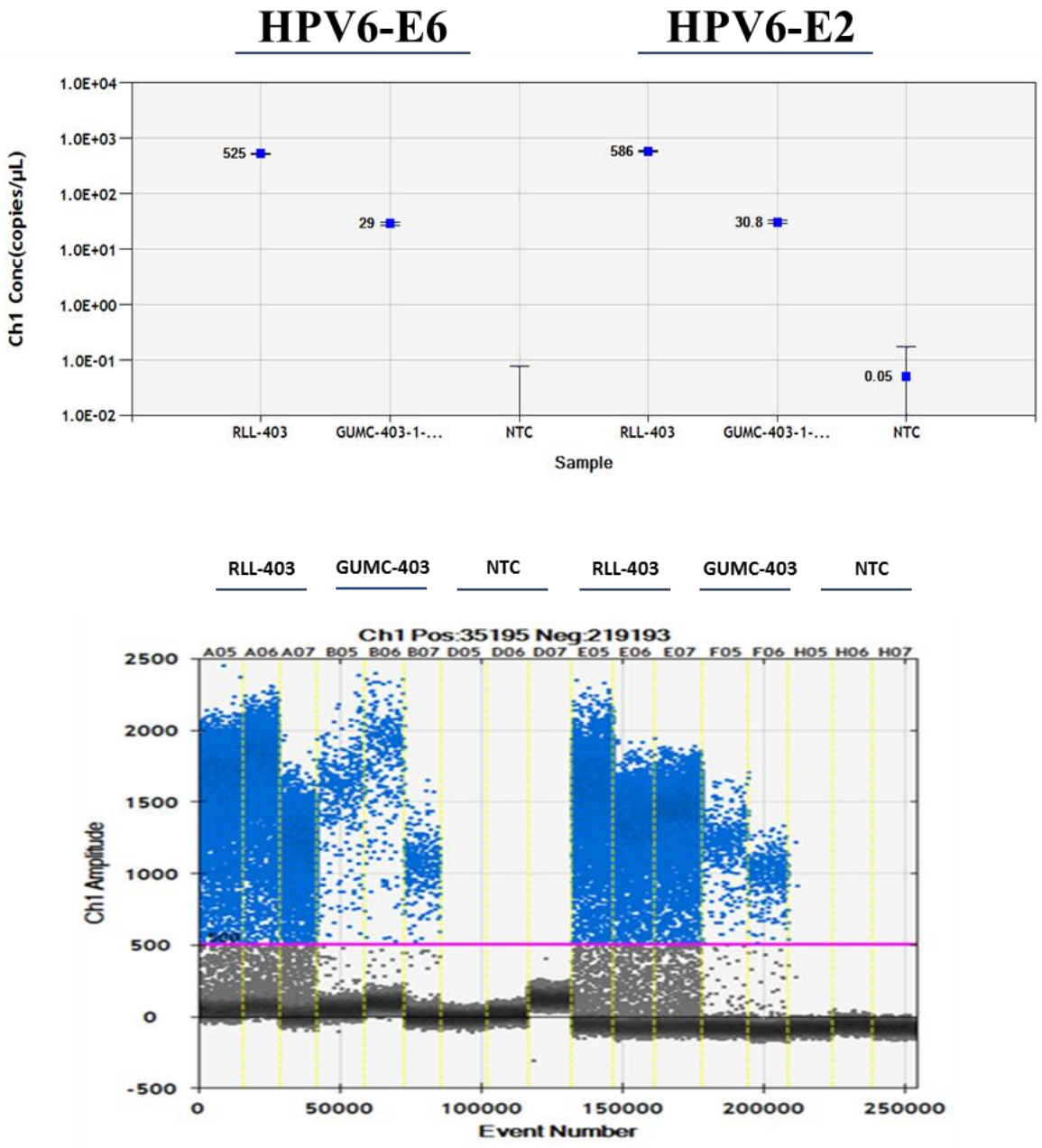

Figure S1.2. Quantification of HPV-6 E6 and E2 by digital droplet PCR using HPV6 E6 and E2 assays.

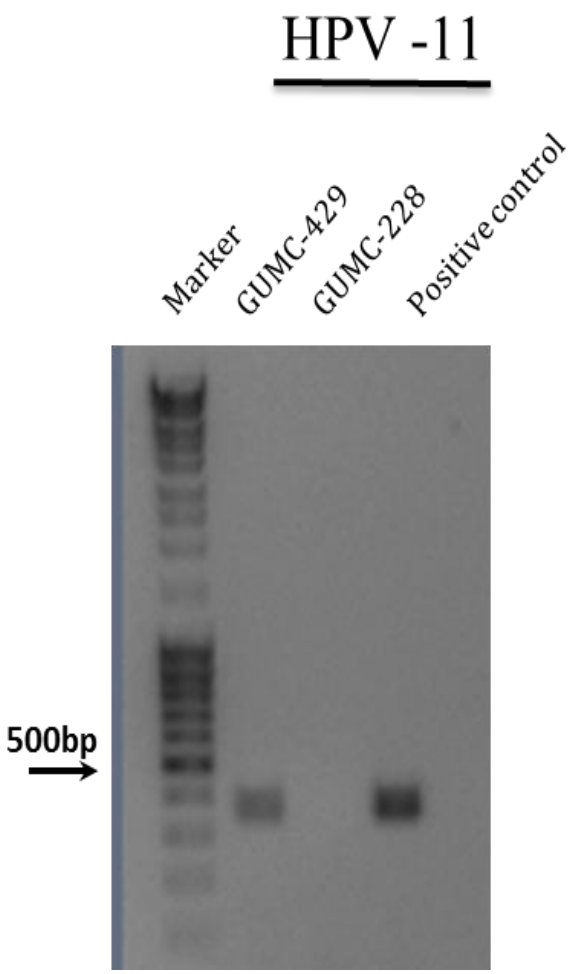

Figure S1.3. HPV typing of conditionally reprogrammed recurrent respiratory papillomatosis (RRP) GUMC-429 and GUMC-228 cells. Genotyping with HPV-11 primers showing PCR results indicates the exclusive presence of HPV-11 DNA in GUMC-429 but not in GUMC-228 cells.

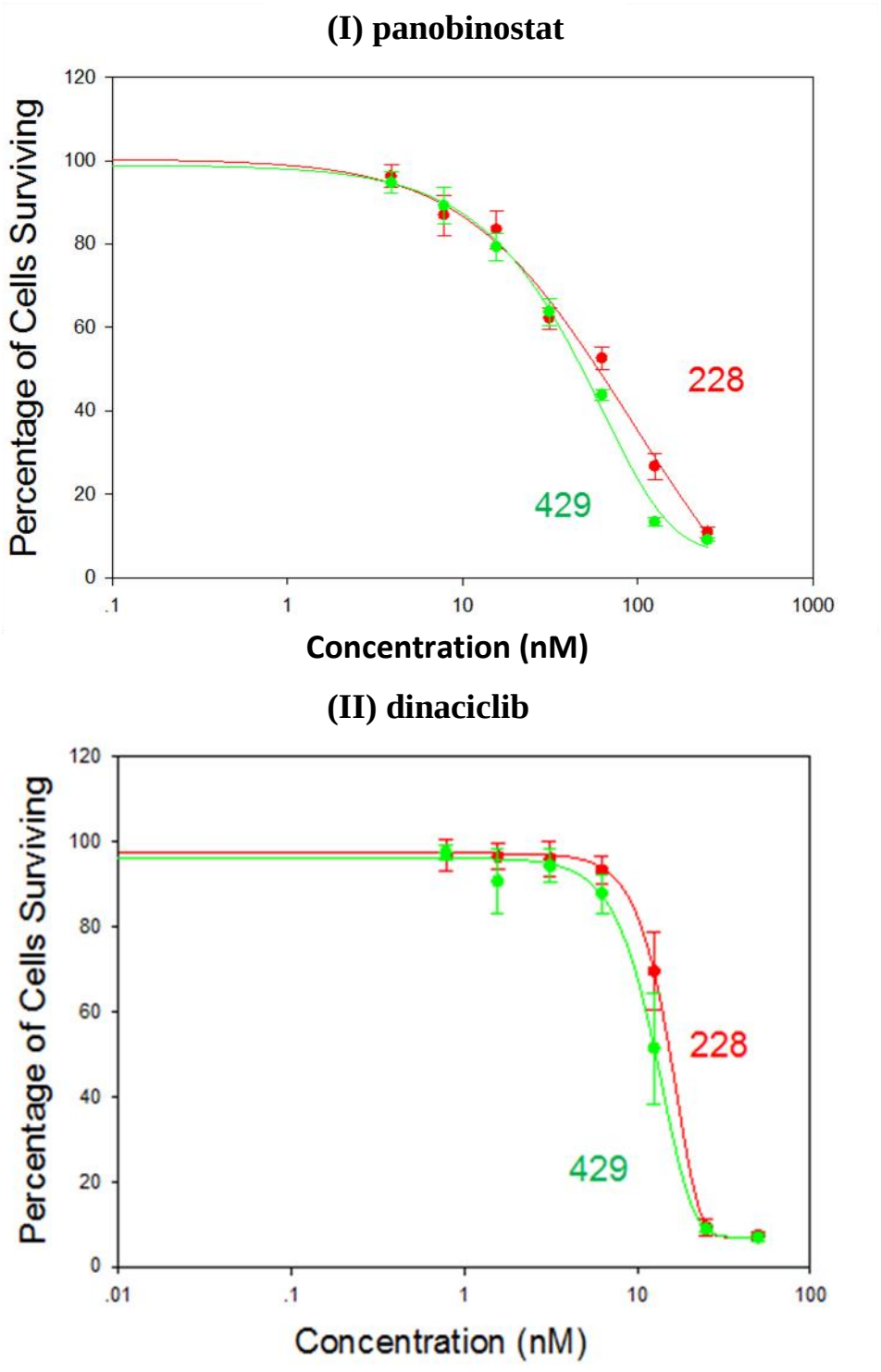

Figure S1.4. Validating of panobinostat, and dinaciclib on GUMC-429 and GUMC-228 cells. Dose–response curves for (I) panobinostat, (II) dinaciclib.

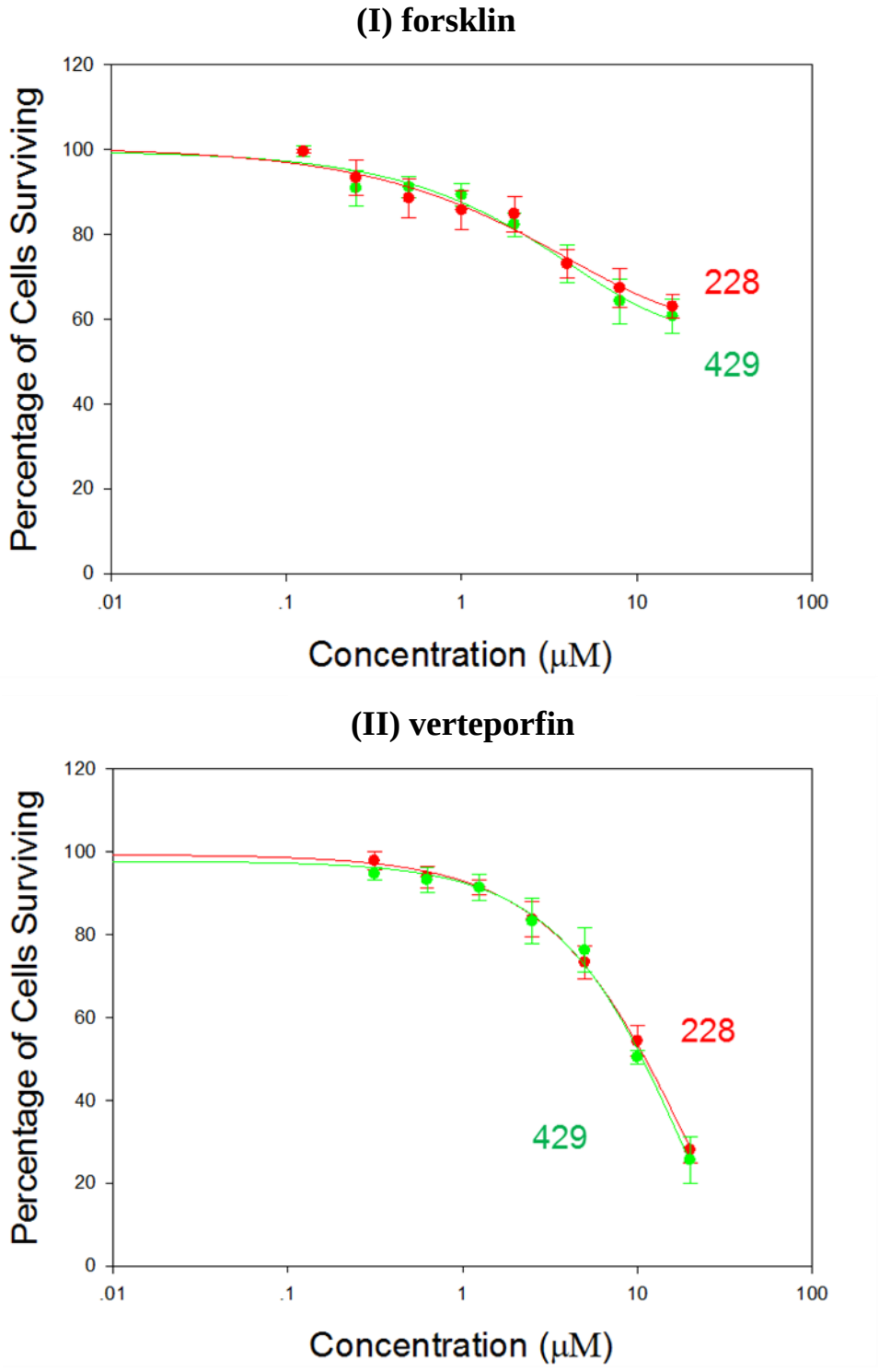

Figure S1.5. Validating of forskolin, and verteporfin on GUMC-429 and GUMC-228 cells. Dose–response curves for (I) forskolin, (II) verteporfin.

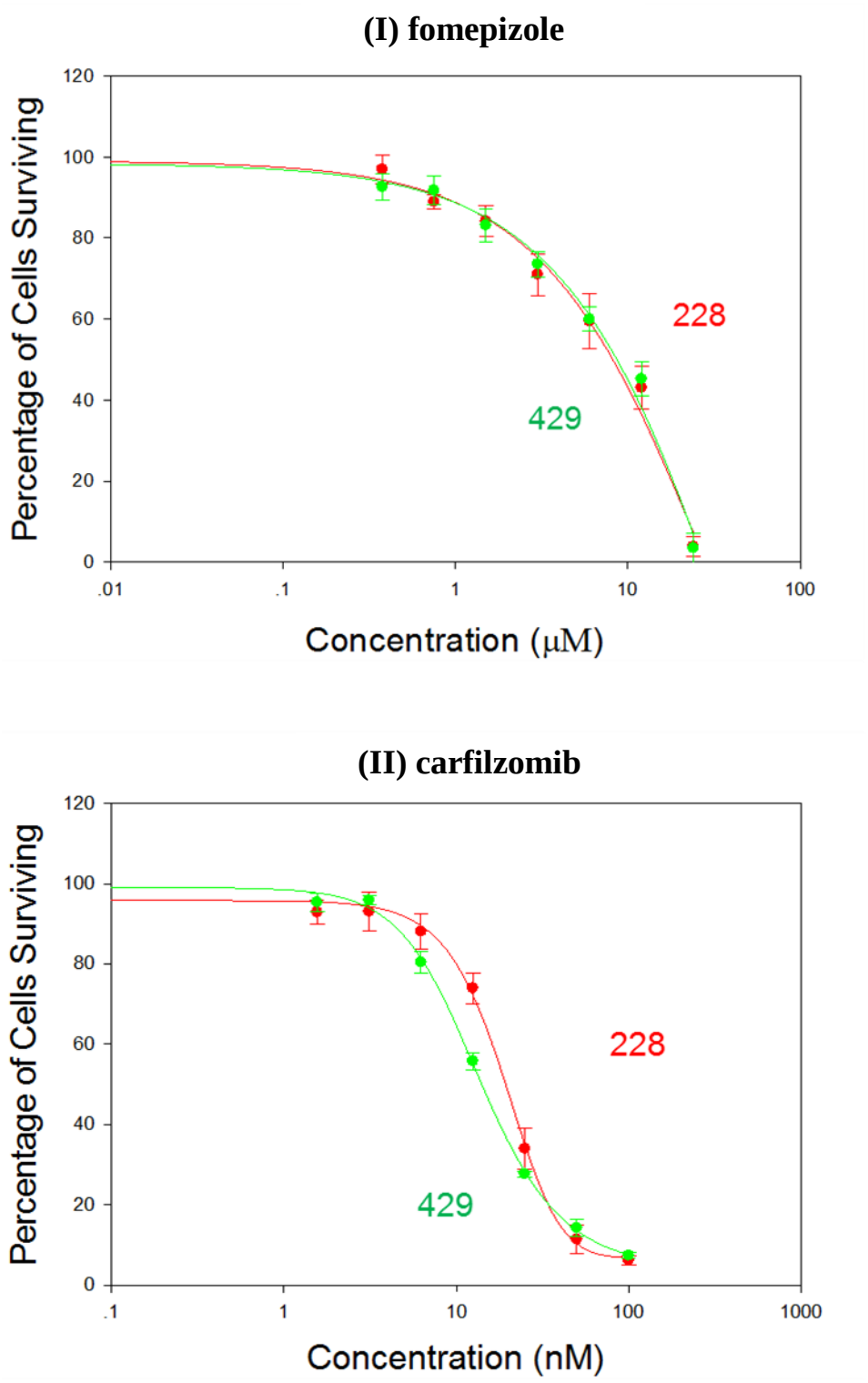

Figure S1.6. Validating of fomepizole, and carfilzomib on GUMC-429 and GUMC-228 cells. Dose–response curves for (I) fomepizole, (II) carfilzomib.

(I) flavopiridol

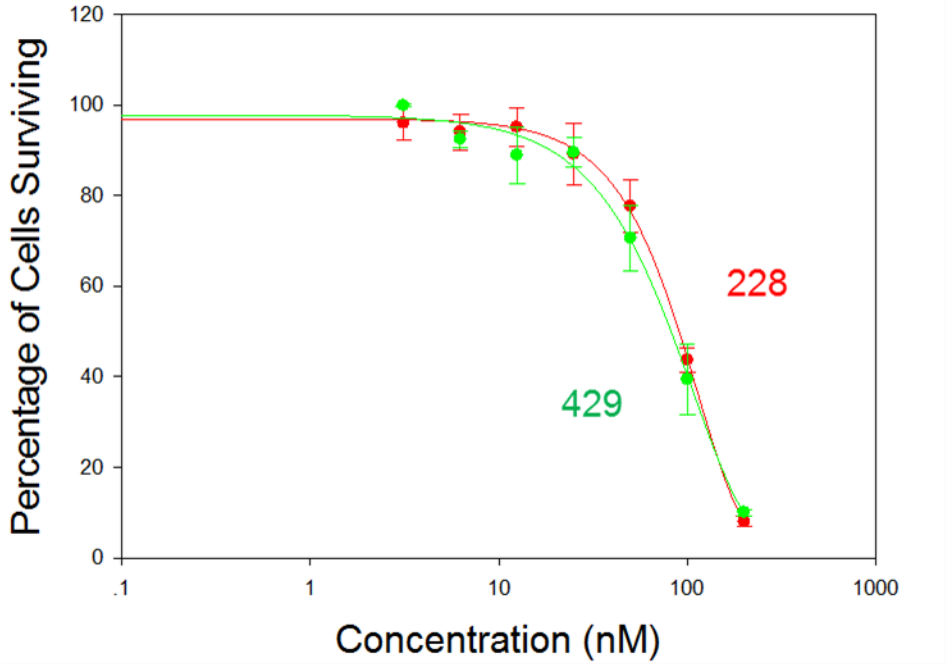

(II) AT-7519

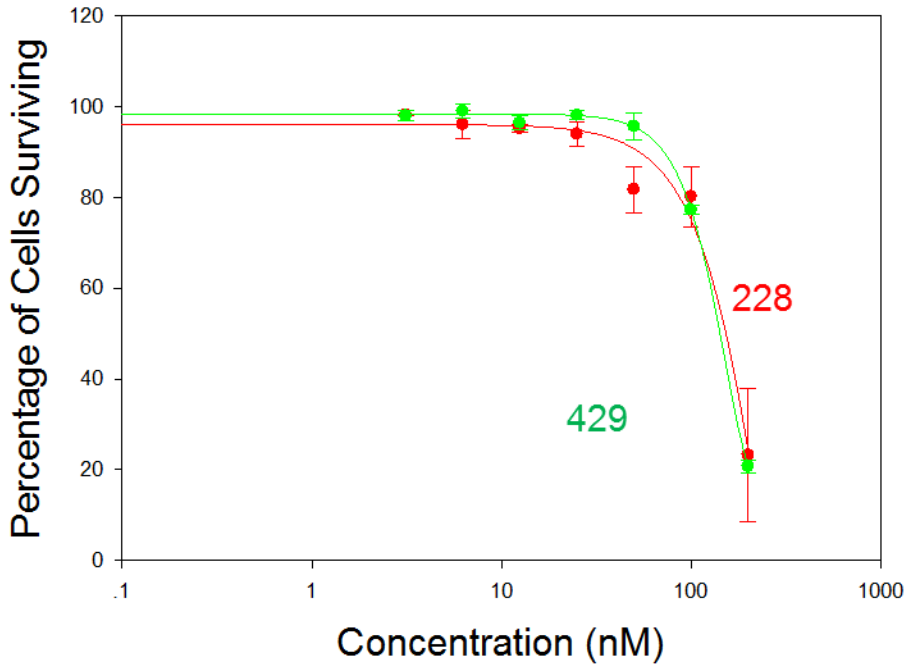

Figure S1.7. Validating of flavopiridol, and AT-7519 on GUMC-429 and GUMC-228 cells. Dose–response curves for (I) flavopiridol, (II) AT-7519.

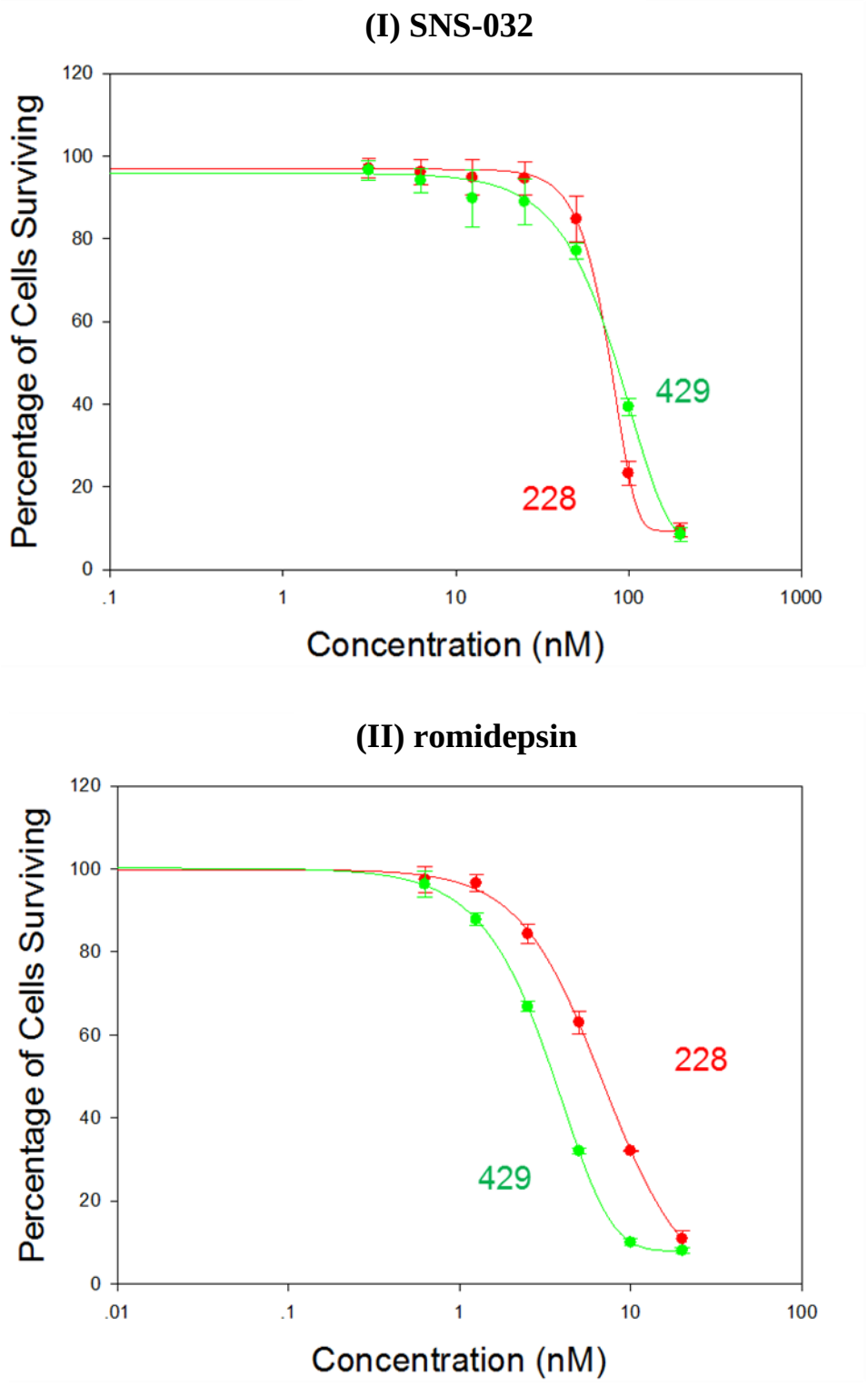

Figure S1.8. Validating of SNS-032, and romidepsin on GUMC-429 and GUMC-228 cells. Dose–response curves for (I) SNS-032, (II) romidepsin.

(I) PF-04691502

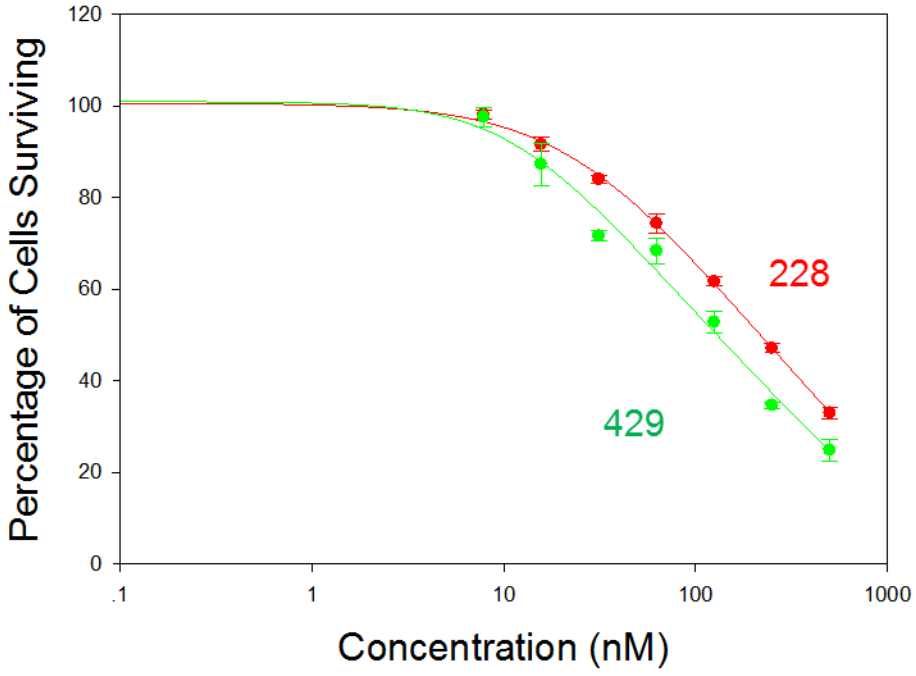

(II) sertindole

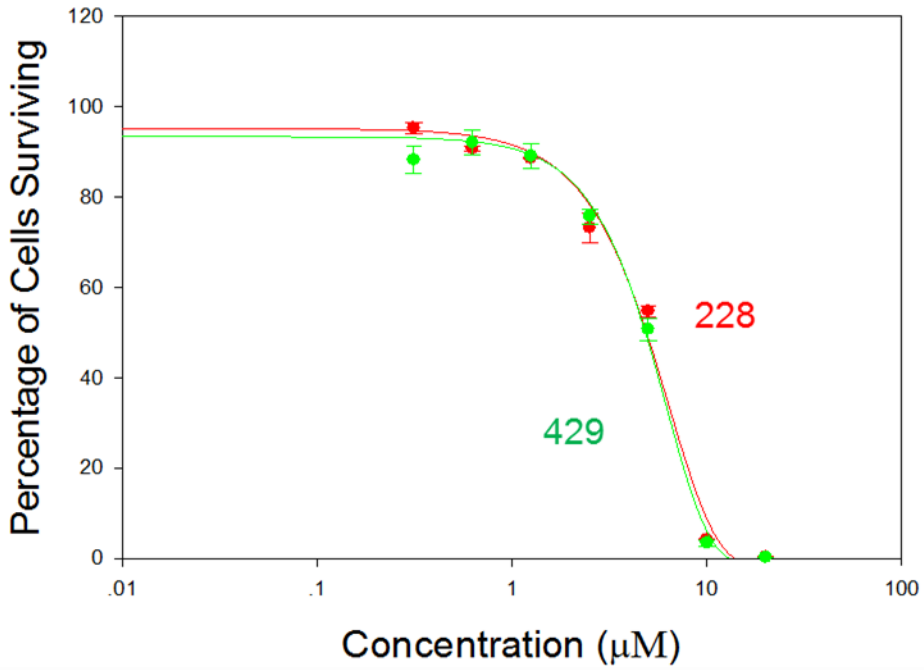

(III) crenolanib

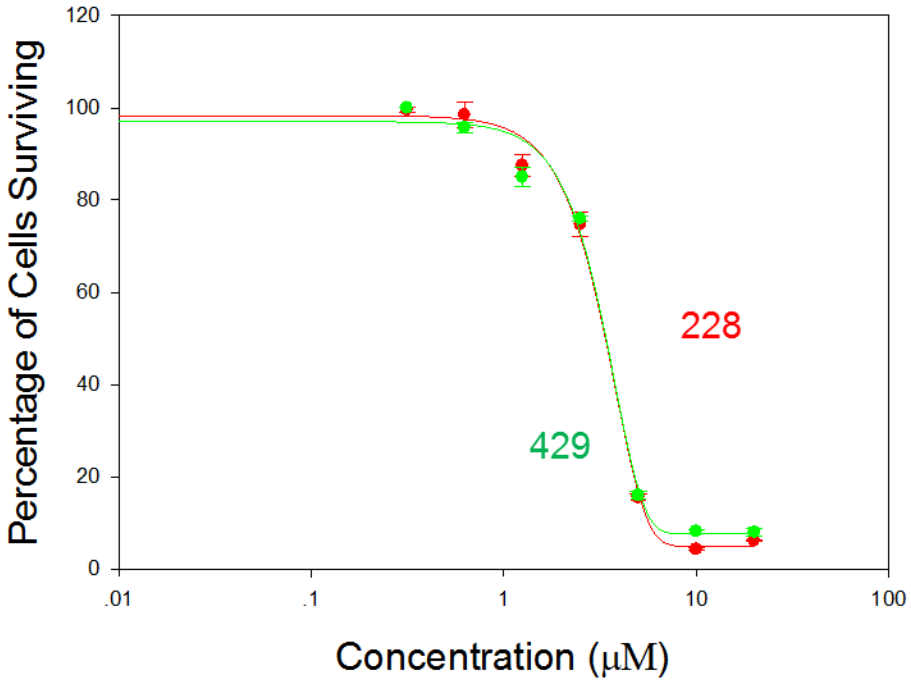

Figure S1.9. Validating of PF-04691502, sertindole, and crenolanib on GUMC-429 and GUMC-228 cells. Dose–response curves for (I) PF-04691502, (II) sertindole, and (III) crenolanib.

Table S1.1. The best 45 drugs from NCATS analysis.

Drugs	Name	Mode of Action	IC50 (uM)
Drug 1	Idarubicin hydrochloride	DNA Topoisomerase II Inhibitors	2.3485
Drug 2	Sepantronium bromide	Survivin inhibitor	0.186548
Drug 3	Flavopiridol	CDK1/2/4/6/7/9 Inhibitor	0.132066
Drug 4	Proscillaridin	Steroid	0.016626
Drug 5	NCGC00188382-01	ITK inhibitor	0.934955
Drug 6	WYE-354	mTORC1/2 inhibitor	0.026351
Drug 7	BX-795	IKK-epsilon Inhibitor	10.49036
Drug 8	PHA-793887	CDK1,2,3,4,5 Inhibitor	1.481803
Drug 9	AT7519	CDK 1 & 2 inhibitor	1.049036
Drug 10	A-674563	Akt1/PKA Inhibitor	2.63506
Drug 11	CAY10626	PI3Kalpha inhibitor	0.117704
Drug 12	PHA-690509	CDK2/Cyclin A Inhibitor	0.331734
Drug 13	Fomepizole	Alcohol Dehydrogenase Inhibitor	1.662611
Drug 14	Daunorubicin	Antineoplastic Antibiotics	0.372212
Drug 15	Bortezomib	Proteasome Inhibitor	0.263506
Drug 16	Romidepsin	Histone Deacetylase (HDAC) Inhibitor	0.104904
Drug 17	BS-194	CDK1/2/5/9 inhibitor	0.372212
Drug 18	RGB-286147	CDK1/2/3/7/9 inhibitor	0.132066
Drug 19	GNE-493	PI3K Inhibitor	0.14818
Drug 20	PF-3758309	p21-Activated Kinase 4 (PAK4) Inhibitors	3.722122
Drug 21	Carfilzomib	Proteasome Inhibitor	1.049036
Drug 22	Verteporfin	photosensitizer	0.661897
Drug 23	GSK-615	PI3Kalpha inhibitor	0.23485

Drug 24	Racecadotril	Neprilysin (Enkephalinase, Neutral Endopeptidase, NEP) Inhibitors	1.177038
Drug 25	Fostamatinib disodium	Syk Kinase inhibitor	0.934955
Drug 26	SNS-032	CDK2,7,9 Inhibitor	0.468587
Drug 27	Echinomycin	Antineoplastic Antibiotics	0.020931
Drug 28	Dinaciclib (SCH727965)	CDK1/2/5/9 inhibitor	0.046859
Drug 29	CUDC-907	PI3K Inhibitor	1.049036
Drug 30	Crenolanib	PDGFR beta inhibitor	0.01049
Drug 31	Triptolide	Inhibition of RNA polymerase II?mediated transcription	0.033173
Drug 32	PF-04691502	PI3K Inhibitor	0.263506
Drug 33	BAY-80-6946	PI3K alpha/delta Inhibitor	0.064504
Drug 34	BMS-536924	IGF-1R Inhibitor	0.23485
Drug 35	7-Hydroxystaurosporine	CDK1/2/4/6	1.481803
Drug 36	NVP-TAE226	Focal Adhesion Kinase (FAK) Inhibitor	1.481803
Drug 37	A-443654	PKB alpha/Akt1 Inhibitors	1.86548
Drug 38	HMSL10084	FLT3	2.956586
Drug 39	PIK-75	PI3K Inhibitor	0.023485
Drug 40	Nemorubicin	Topoisomerase I inhibitor	0.021136
Drug 41	Sertindole	5-HT2 serotonin and D2 dopamine receptor antagonist and antipsychotic.	2.660862
Drug 42	Carfilzomib	Proteasome Inhibitor	1.188564
Drug 43	Cantharidin	PP-1 Inhibitors;PP-2A Inhibitors	3.349827
Drug 44	Bortezomib	Proteasome Inhibitor	0.149631
Drug 45	Forskolin	ubiquitous activator of eukaryotic adenylyl cyclase	1.678891

Appendix B: Chapter Two Supplementary Figures and Data

Supplementary Methods

Another source for tissue, a strip of scrotal skin, was processed to isolate keratinocytes and fibroblasts using conditional reprogramming condition. Keratinocytes growth (GUMC-100) was tested in different conditions (i) In co-culture with irradiated 3T3 fibroblasts (J2 strain) in F media with 10 uM Y-27632 Rho-kinase inhibitor (Enzo Life Sciences), (ii) In F media with 10 uM Y-27632 with no J2, (iii) In CnT-09 media supplemented with A and B supplements (CELLnTEC, Switzerland) with or without 10 uM Y-27632, (iv) In Keratinocyte Serum-Free Medium (KSFM) supplemented with Bovine Pituitary Extract (BPE) and Epidermal Growth Factor 1-53 (EGF 1-53) (KSFM; Invitrogen) with 10 uM Y-27632. FACS analysis of human keratinocytes (HFK) and mouse fibroblasts (j2) using pan-cytokeratin antibody. Immunohistochemistry validation of CK-14 antibody for equine tissues.

Supplementary Results

In order to ensure the reproducibility of our work a strip of scrotal skin was processed to generate keratinocytes. Cells were established, termed GUMC-100, and were tested in different growth conditions. Similar to GUMC-1547, GUMC-100 grew in F+Y+feeders, F+Y and CNT+Y but not in CNT or KGM+Y (Supplementary figure 2.1). To validate the specificity of Pan-cytokeratin antibody, HFKs and fibroblasts were tested and only HFKs were positive to Pan-cytokeratin antibody (Supplementary figure 2.2). Moreover, specificity and reactivity of CK-14 were tested by using diluted concentration of CK14 or no antibody in breast cancer tissue (positive control) and equine skin tissue respectively with clear staining in the epidermal part of the tissue indicating specificity for keratinocytes over fibroblasts (Supplementary figure 2.3).

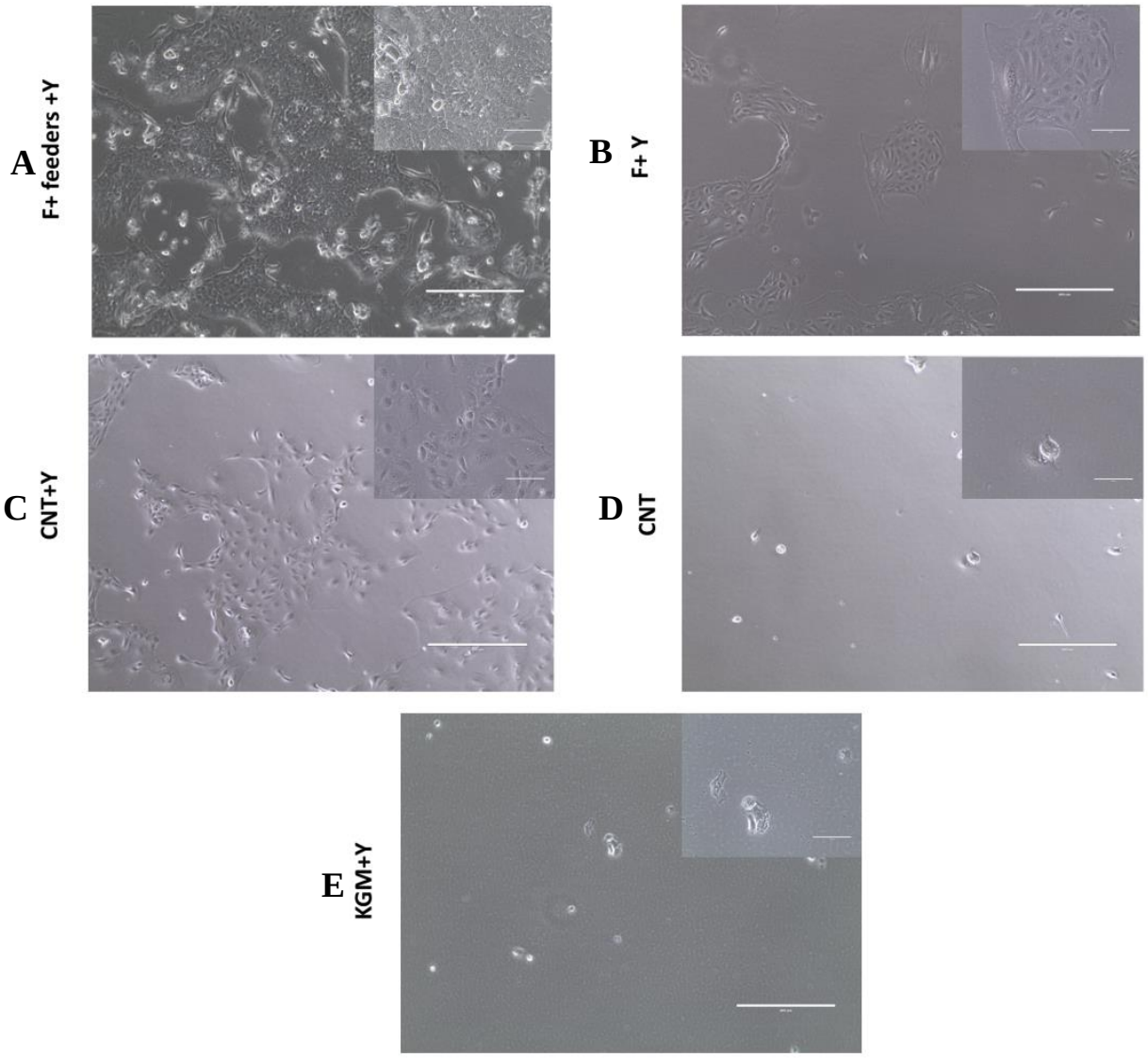

Figure S2.1. Equine keratinocytes (EK-100) were cultured in various culture conditions. Representative phase contrast images of primary equine keratinocytes (EK-100) cultured in (A) co-culture with irradiated fibroblasts+10 uM Y-27632,(B) F +10 uM Y-27632 (C,D) CNT with or without 10 uM Y-27632 and (e)KSFM+ 10 uM. All images were taken on and day7 following initial culture without passage (10X magnification. Size bars= 400µm). Top right images show enlarged magnification (40X magnification, size bars= 100µm).

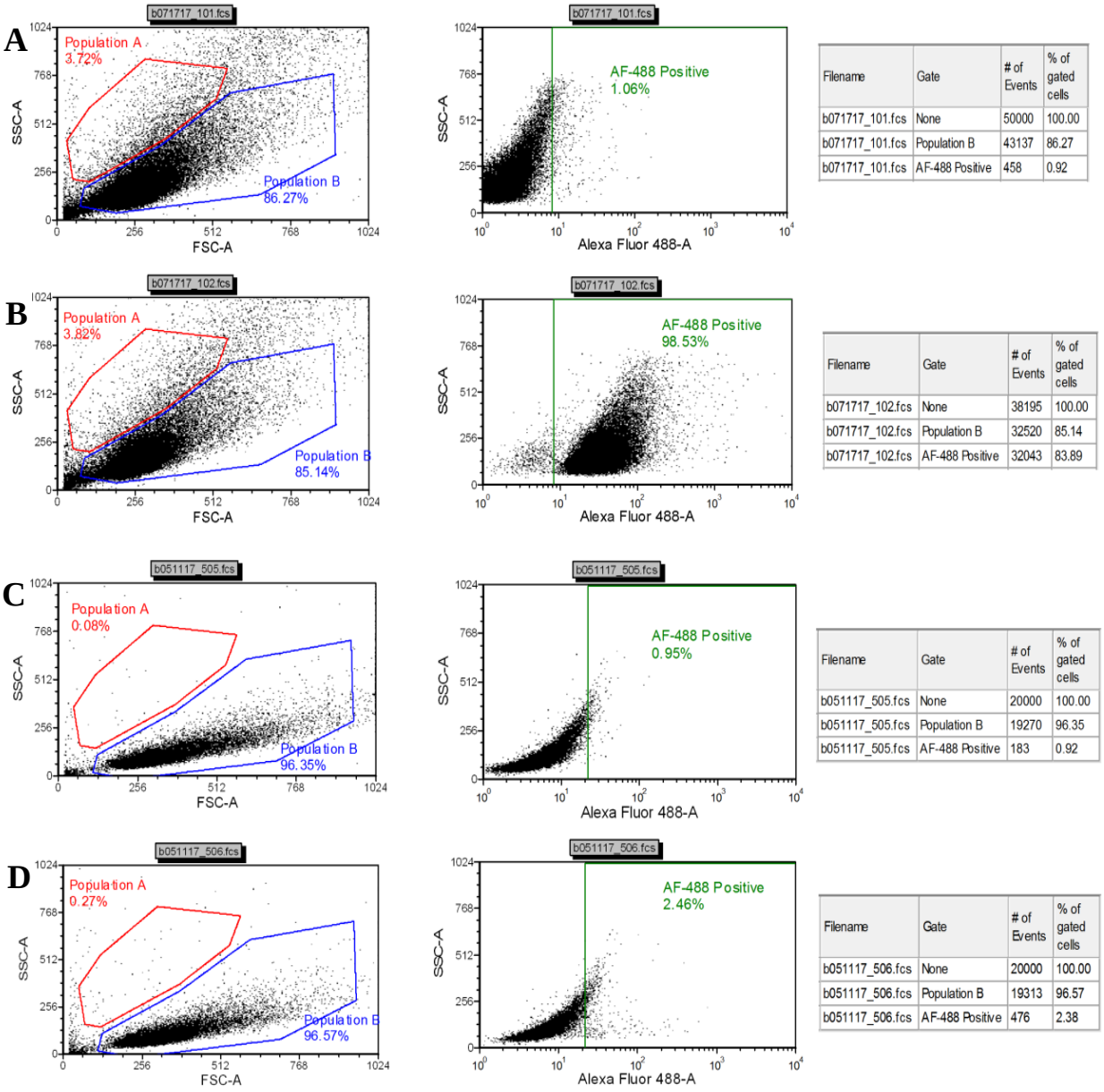

Filename	Gate	# of Events	% of gated cells
b071717_101.fcs	None	50000	100.00
b071717_101.fcs	Population B	43137	86.27
b071717_101.fcs	AF-488 Positive	458	0.92

Filename	Gate	# of Events	% of gated cells
b071717_102.fcs	None	38195	100.00
b071717_102.fcs	Population B	32520	85.14
b071717_102.fcs	AF-488 Positive	32043	83.89

Filename	Gate	# of Events	% of gated cells
b051117_505.fcs	None	20000	100.00
b051117_505.fcs	Population B	19270	96.35
b051117_505.fcs	AF-488 Positive	183	0.92

Filename	Gate	# of Events	% of gated cells
b051117_506.fcs	None	20000	100.00
b051117_506.fcs	Population B	19313	96.57
b051117_506.fcs	AF-488 Positive	476	2.38

Figure S2.2. Fluorescence-activated cell sorting (FACS) analysis of human keratinocytes (HFK) and mouse fibroblasts (j2) using Pan-cytokeratin antibody. HFK cells were incubated without (A) Pan-CK antibody or (B) with Pan-CK antibody, (C) J2 fibroblasts without Pan-CK antibody, or (D) with Pan-CK antibody.

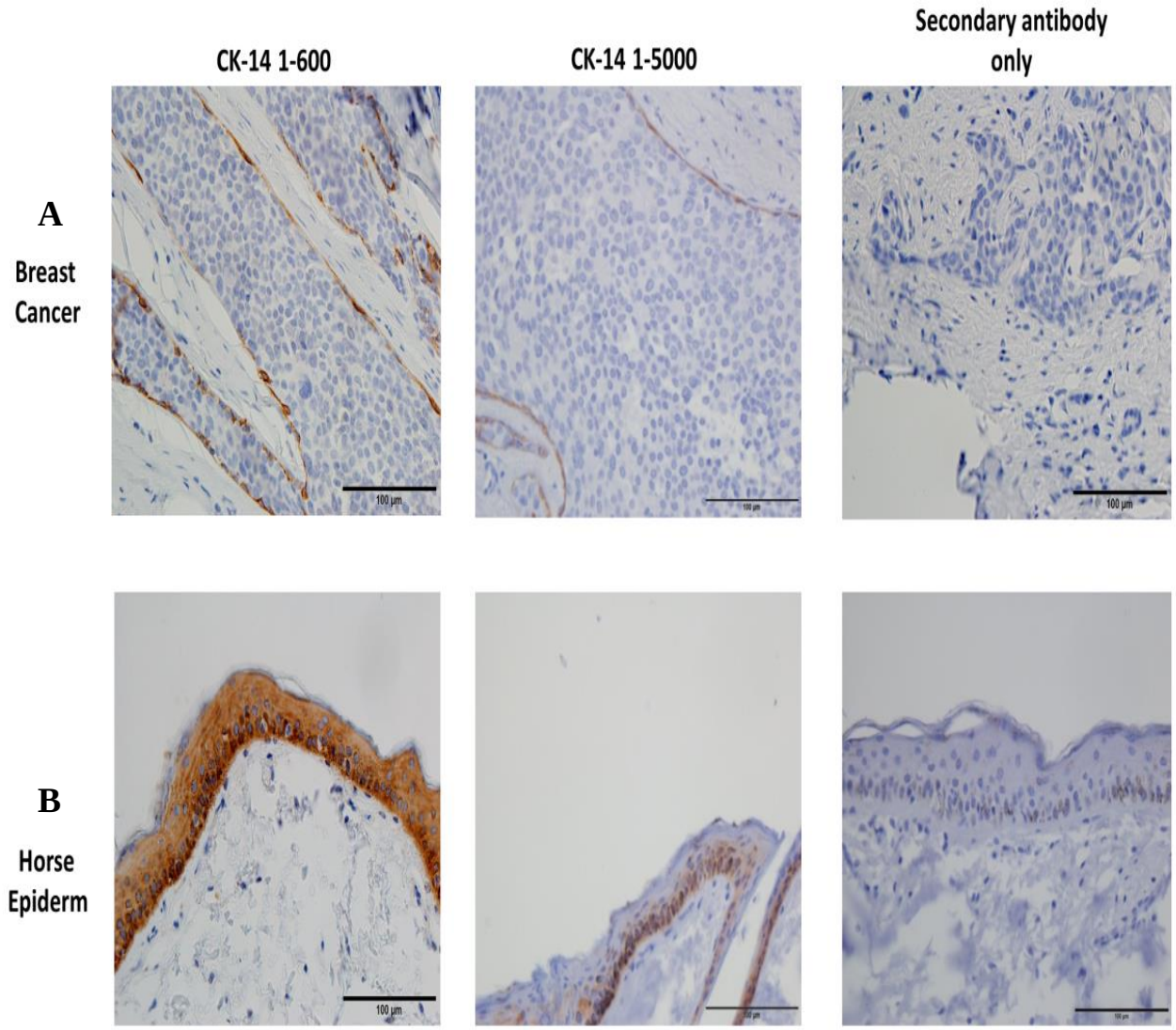

Figure S2.3. Validation of antibodies for equine tissues. Specificity and reactivity of CK-14 was tested by using diluted concentration of CK14 1:600, 1:5000 and no antibody respectively in (A) breast cancer tissue and (B) equine skin tissue. All images (40x magnification, scale bar= 100µm) are representative of three experimental repeats.

REFERENCES

1. Scherer, William F., Jerome T. Syverton, and George O. Gey. 1953. Studies of the propagation in vitro of poliomyelitis virus. The Journal of experimental medicine 97 (5): 695–710.

2. Levenson a S, Jordan VC. MCF-7: the first hormone-responsive breast cancer cell line. Cancer research. 1997.

3. Lippman ME, Bolan G. Oestrogen-responsive human breast cancer in long term tissue culture. Nature. 1975.

4. Masters JRW. Cell line misidentification: The beginning of the end. Nature Reviews Cancer. 2010.

5. Lorsch JR, Collins FS, Lippincott-Schwartz J. Fixing problems with cell lines. Science. 2014.

6. Horbach SPJM, Halffman W. The ghosts of HeLa: How cell line misidentification contaminates the scientific literature. PLoS ONE. 2017.

7. Pan C, Kumar C, Bohl S, Klingmueller U, Mann M. Comparative Proteomic Phenotyping of Cell Lines and Primary Cells to Assess Preservation of Cell Type-specific Functions. Molecular & Cellular Proteomics. 2009.

8. Borrell B. How accurate are cancer cell lines? Nature. 2010.

9. Liu X, Ory V, Chapman S, Yuan H, Albanese C, Kallakury B, et al. ROCK inhibitor and feeder cells induce the conditional reprogramming of epithelial cells. American Journal of Pathology. 2012;180:599–607.

10. Gordon K, Clouaire T, Bao XX, Kemp SE, Xenophontos M, De Las Heras JI, et al. Immortality, but not oncogenic transformation, of primary human cells leads to epigenetic reprogramming of DNA methylation and gene expression. Nucleic Acids Research. 2014.

11. Belgiovine C, Chiodi I, Mondello C. Telomerase: Cellular immortalization and neoplastic transformation. Multiple functions of a multifaceted complex. Cytogenetic and Genome Research. 2009.

12. Koli K, Keski-Oja J. Cellular senescence. . Annals of Medicine. 1992.

13. Münger K, Phelps WC, Bubb V, Howley PM, Schlegel R. The E6 and E7 genes of the human papillomavirus type 16 together are necessary and sufficient for transformation of primary human keratinocytes. Journal of virology. 1989.

14. Chapman S, Liu X, Meyers C, Schlegel R, McBride AA. Human keratinocytes are efficiently immortalized by a Rho kinase inhibitor. Journal of Clinical Investigation. 2010;120:2619–26.

15. Hawley-Nelson P, Vousden KH, Hubbert NL, Lowy DR, Schiller JT. HPV16 E6 and E7 proteins cooperate to immortalize human foreskin keratinocytes. The EMBO journal. 1989.

16. A.J. Ridley, H.F. Paterson, M. Noble, H. Land, Ras-mediated cell cycle arrest is altered by nuclear oncogenes to induce Schwann cell transformation., The EMBO Journal. (1988).

17. Rheinwald JG, Green H. Serial Cultivation of Strains of Human Epidermal Keratinocytes: the Formation of Keratinizing Colonies from Single Cells. Cell. 1975;6:331–44.

18. Liu X, Krawczyk E, Suprynowicz FA, Palechor-Ceron N, Yuan H, Dakic A, et al. Conditional reprogramming and long-term expansion of normal and tumor cells from human biospecimens. Nature Protocols. 2017;12:439–51. doi:10.1038/nprot.2016.174.

19. Guo R, Ye X, Yang J, Zhou Z, Tian C, Wang H, et al. Feeders facilitate telomere maintenance and chromosomal stability of embryonic stem cells. Nature Communications. 2018.

20. Palechor-Ceron, Nanc1. Palechor-Ceron, N. et al. Radiation induces diffusible feeder cell factor(s) that cooperate with ROCK inhibitor to conditionally reprogram and immortalize epithelial cells. Am. J. Pathol. 183 1862–1870 (2013).y, Suprynowicz FA, Upadhyay G, Dakic

A, Minas T, Simic V, et al. Radiation induces diffusible feeder cell factor(s) that cooperate with ROCK inhibitor to conditionally reprogram and immortalize epithelial cells. American Journal of Pathology. 2013;183:1862–70.

21. Alamri AM, Liu X, Blancato JK, Haddad BR, Wang W, Zhong X, et al. Expanding primary cells from mucoepidermoid and other salivary gland neoplasms for genetic and chemosensitivity testing. Disease Models & Mechanisms. 2018;11:dmm031716. doi:10.1242/dmm.031716.

22. Saeed K, Rahkama V, Eldfors S, Bychkov D, Mpindi JP, Yadav B, et al. Comprehensive Drug Testing of Patient-derived Conditionally Reprogrammed Cells from Castration-resistant Prostate Cancer. European Urology. 2017;71:319–27.

23. Riento K, Ridley AJ. Rocks: Multifunctional kinases in cell behaviour. Nature Reviews Molecular Cell Biology. 2003.

24. Watanabe K, Ueno M, Kamiya D, Nishiyama A, Matsumura M, Wataya T, et al. A ROCK inhibitor permits survival of dissociated human embryonic stem cells. Nature Biotechnology. 2007;25:681–6.

25. Terunuma A, Limgala RP, Park CJ, Choudhary I, Vogel JC. Efficient procurement of epithelial stem cells from human tissue specimens using a Rho-associated protein kinase inhibitor Y-27632. Tissue engineering Part A. 2010;16:1363–8.

26. Suprynowicz FA, Upadhyay G, Krawczyk E, Kramer SC, Hebert JD, Liu X, et al. Conditionally reprogrammed cells represent a stem-like state of adult epithelial cells. Proceedings of the National Academy of Sciences. 2012;109:20035–40. doi:10.1073/pnas.1213241109.

27. Hughes JP, Rees S, Kalindjian SB, Philpott KL. Principles of early drug discovery. British journal of pharmacology. 2011.

28. Morgan S, Grootendorst P, Lexchin J, Cunningham C, Greyson D. The cost of drug development: A systematic review. Health Policy. 2011.

29. Federsel H-J. Handing over the baton: connecting medicinal chemistry with process R&D. Drug news & perspectives. 2008.

30. DiMasi JA, Feldman L, Seckler A, Wilson A. Trends in risks associated with new drug development: success rates for investigational drugs. Clin Pharmacol Ther. 2010.

31. Tobinick EL. The value of drug repositioning in the current pharmaceutical market. Drug News & Perspectives. 2009.

32. Ashburn TT, Thor KB. Drug repositioning: identifying and developing new uses for existing drugs. Nature Reviews Drug Discovery. 2004;3:673–83. doi:10.1038/nrd1468.

33. Novac N. Challenges and opportunities of drug repositioning. Trends in Pharmacological Sciences. 2013.

34. Jameson JL, Longo DL. Precision Medicine — Personalized, Problematic, and Promising. New England Journal of Medicine. 2015.

35. Dance A. Medical histories. Nature. 2016.

36. Kwak EL, Bang YJ, Camidge DR, Shaw AT, Solomon B, Maki RG, et al. Anaplastic Lymphoma Kinase Inhibition in Non-Small-Cell Lung Cancer. New England Journal of Medicine. 2010.

37. Hudis CA. Trastuzumab — Mechanism of Action and Use in Clinical Practice. New Engl J Med. 2007.

38. Ribas A. Tumor Immunotherapy Directed at PD-1. New England Journal of Medicine. 2012.

39. Porter DL, Levine BL, Kalos M, Bagg A, June CH. Chimeric antigen receptor-modified T cells in chronic lymphoid leukemia. The New England journal of medicine. 2011.

40. Mason C, Dunnill P. A brief definition of regenerative medicine. Regenerative Medicine. 2008.

41. Kaiser L. The future of multihospital systems. Topics in health care financing. 1992.

42. Sampogna G, Guraya SY, Forgione A. Regenerative medicine: Historical roots and potential strategies in modern medicine. Journal of Microscopy and Ultrastructure. 2015.

43. Aida L. Alexis Carrel (1873–1944): Visionary vascular surgeon and pioneer in organ transplantation. Journal of Medical Biography. 2014.

44. Schold JD, Srinivas TR, Sehgal AR, Meier-Kriesche HU. Half of kidney transplant candidates who are older than 60 years now placed on the waiting list will die before receiving a deceased-donor transplant. Clinical Journal of the American Society of Nephrology. 2009.

45. Atala A. Regenerative medicine strategies. Journal of Pediatric Surgery. 2012.

46. Ilic D, Polak JM. Stem cells in regenerative medicine: Introduction: British Medical Bulletin. 2011.

47. Fusconi M, Grasso M, Greco a, Gallo a, Campo F, Remacle M, et al. Recurrent respiratory papillomatosis by HPV: review of the literature and update on the use of cidofovir. Acta otorhinolaryngologica Italica : organo ufficiale della Societa italiana di otorinolaringologia e chirurgia cervico-facciale. 2014.

48. de Villiers EM. Cross-roads in the classification of papillomaviruses. Virology. 2013.

49. Vinzón SE, Rösl F. HPV vaccination for prevention of skin cancer. Human Vaccines and Immunotherapeutics. 2015.

50. Baseman JG, Koutsky LA. The epidemiology of human papillomavirus infections. Journal of Clinical Virology. 2005.

51. Bernard HU, Calleja-Macias IE, Dunn ST. Genome variation of human papillomavirus types:

Phylogenetic and medical implications. International Journal of Cancer. 2006.

52. Handler MZ, Handler NS, Majewski S, Schwartz RA. Human papillomavirus vaccine trials and tribulations Clinical perspectives. Journal of the American Academy of Dermatology. 2015.

53. Palefsky JM, Holly EA. Molecular Virology and Epidemiology of Human Papillomavirus and Cervical Cancer1. Cancer. 1995;4:5–428.

54. Forcier M, Musacchio N. An overview of human papillomavirus infection for the dermatologist: Disease, diagnosis, management, and prevention. Dermatologic Therapy. 2010.

55. Duensing S, M??nger K. Mechanisms of genomic instability in human cancer: Insights from studies with human papillomavirus oncoproteins. International Journal of Cancer. 2004.

56. Smith JA, Haberstroh FS, White EA, Livingston DM, DeCaprio JA, Howley PM. SMCX and components of the TIP60 complex contribute to E2 regulation of the HPV E6/E7 promoter. Virology. 2014.

57. Dunne EF, Park IU. HPV and HPV-associated diseases. Infectious Disease Clinics of North America. 2013.

58. Schiffman M, Clifford G, Buonaguro FM. Classification of weakly carcinogenic human papillomavirus types: Addressing the limits of epidemiology at the borderline. Infectious Agents and Cancer. 2009.

59. Munoz N, Bosch FX, de Sanjose S, Herrero R, Castellsague X, Shah K V, et al. Epidemiologic classification of human papillomavirus types associated with cervical cancer. N Engl J Med. 2003.

60. Dickens P, Srivastava G, Loke SL, Larkin S. Human papillomavirus 6, 11, and 16 in laryngeal papillomas. The Journal of Pathology. 1991.

61. Larson D a, Derkay CS. Epidemiology of recurrent respiratory papillomatosis. APMIS : acta

pathologica, microbiologica, et immunologica Scandinavica. 2010.

62. Xue Q, Wang H, Wang J. Recurrent respiratory papillomatosis: an overview. European journal of clinical microbiology & infectious diseases : official publication of the European Society of Clinical Microbiology. 2010.

63. Soldatski IL, Onufrieva EK, Steklov AM, Schepin N V. Tracheal, bronchial, and pulmonary papillomatosis in children. Laryngoscope. 2005.

64. Bonagura VR, Hatam LJ, Rosenthal DW, De Voti JA, Lam F, Steinberg BM, et al. Recurrent respiratory papillomatosis: A complex defect in immune responsiveness to human papillomavirus-6 and -11. APMIS. 2010.

65. Bonagura VR, Vambutas A, DeVoti J a, Rosenthal DW, Steinberg BM, Abramson AL, et al. HLA alleles, IFN-gamma responses to HPV-11 E6, and disease severity in patients with recurrent respiratory papillomatosis. Human immunology. 2004.

66. Bonagura VR, Siegal FP, Abramson AL, Santiago-Schwarz F, O'Reilly ME, Shah K, et al. Enriched HLA-DQ3 phenotype and decreased class I major histocompatibility complex antigen expression in recurrent respiratory papillomatosis. Clinical and diagnostic laboratory immunology. 1994.

67. Bonagura VR, Du Z, Ashouri E, Luo L, Hatam LJ, DeVoti JA, et al. Activating killer cell immunoglobulin-like receptors 3DS1 and 2DS1 protect against developing the severe form of recurrent respiratory papillomatosis. Human Immunology. 2010.

68. Rabah R, Lancaster WD, Thomas R, Gregoire L. Human papillomavirus-11-associated recurrent respiratory papillomatosis is more aggressive than human papillomavirus-6-associated disease. Pediatric and Developmental Pathology. 2001.

69. Ivancic R, Iqbal H, deSilva B, Pan Q, Matrka L. Current and future management of recurrent

respiratory papillomatosis. Laryngoscope Investigative Otolaryngology. 2018.

70. Chesson HW, Forhan SE, Gottlieb SL, Markowitz LE. The potential health and economic benefits of preventing recurrent respiratory papillomatosis through quadrivalent human papillomavirus vaccination. Vaccine. 2008.

71. Theoret CL, Wilmink JM. Aberrant wound healing in the horse: Naturally occurring conditions reminiscent of those observed in man. Wound Repair and Regeneration. 2013.

72. Owen KR, Singer ER, Clegg PD, Ireland JL, Pinchbeck GL. Identification of risk factors for traumatic injury in the general horse population of north-west England, Midlands and north Wales. Equine Veterinary Journal. 2012.

73. Inness CM, Morgan KL. Polo pony injuries: Player-owner reported risk, perception, mitigation and risk factors. Equine Veterinary Journal. 2015.

74. Theoret CL, Bolwell CF, Riley CB. A cross-sectional survey on wounds in horses in New Zealand. New Zealand Veterinary Journal. 2016.

75. Sole A, Bolwell CF, Dart A, et al. A cross-sectional survey of wounds
in horses in Australia. Aust Eq Vet 2015; 34: 68.

76. Perkins NR, Reid SWJ, Morris RS. Profiling the New Zealand thoroughbred racing industry. 2. Conditions interfering with training and racing. New Zealand Veterinary Journal. 2004.

77. De Groot PG, Urbanus RT, Roest M. Platelet interaction with the vessel wall. Handbook of Experimental Pharmacology. 2012.

78. Theoret CL. 1. Physiology of Wound Healing. In: Equine Wound Management: Third Edition. 2017. p. 1–13.

79. Wulff BC, Wilgus TA. Mast cell activity in the healing wound: More than meets the eye? Experimental Dermatology. 2013.

80. Wong VW, Gurtner GC, Longaker MT. Wound healing: A paradigm for regeneration. In: Mayo Clinic Proceedings. 2013.

81. Theoret C. Tissue engineering in wound repair: The three “r”s - Repair, replace, regenerate. Veterinary Surgery. 2009.

82. Armstrong LR, Derkay CS, Reeves WC. Initial results from the national registry for juvenile-onset recurrent respiratory papillomatosis. RRP Task Force. Archives of Otolaryngology -- Head & Neck Surgery. 1999;125:743–8.

83. Fortes HR, von Ranke FM, Escuissato DL, Araujo Neto CA, Zanetti G, Hochhegger B, et al. Recurrent respiratory papillomatosis: A state-of-the-art review. Respiratory Medicine. 2017;126:116–21.

84. Dyrstad SW, Rao K a. Recurrent Respiratory Papillomatosis (RRP)-Juvenile Onset. Clinical medicine Oncology. 2008;2:481–6.

85. Derkay CS. Task Force on Recurrent Respiratory Papillomas: A Preliminary Report. Archives of Otolaryngology--Head and Neck Surgery. 1995;121:1386–91.

86. Goon P, Sonnex C, Jani P, Stanley M, Sudhoff H. Recurrent respiratory papillomatosis: an overview of current thinking and treatment. Eur Arch Otorhinolaryngol. 2008;265:147–51.

87. Derkay CS, Wiatrak B. Recurrent Respiratory Papillomatosis: A Review. The Laryngoscope. 2008;118:1236–47. doi:10.1097/MLG.0b013e31816a7135.

88. Rodman R, Mutasa S, Dupuis C, Spratt H, Underbrink M. Genetic dysregulation in recurrent respiratory papillomatosis. In: Laryngoscope. 2014.

89. Mahajan AS, Sugita BM, Duttargi AN, Saenz F, Krawczyk E, McCutcheon JN, et al. Genomic comparison of early-passage conditionally reprogrammed breast cancer cells to their corresponding primary tumors. PLoS ONE. 2017;12.

90. Correa BRS, Hu J, Penalva LOF, Schlegel R, Rimm DL, Galante PAF, et al. Patient-derived conditionally reprogrammed cells maintain intra-tumor genetic heterogeneity. Scientific Reports. 2018;8.

91. Yuan H, Myers S, Wang J, Zhou D, Woo JA, Kallakury B, et al. Use of reprogrammed cells to identify therapy for respiratory papillomatosis. The New England journal of medicine. 2012;367:1220–7. doi:10.1056/NEJMoa1203055.

92. Celik H, Hong S-H, Colon-Lopez DD, Han J, Kont YS, Minas TZ, et al. Identification of Novel Ezrin Inhibitors Targeting Metastatic Osteosarcoma by Screening Open Access Malaria Box. Molecular Cancer Therapeutics. 2015;14:2497–507. doi:10.1158/1535-7163.MCT-15-0511.

93. Huang R, Southall N, Wang Y, Yasgar A, Shinn P, Jadhav A, et al. The NCGC pharmaceutical collection: A comprehensive resource of clinically approved drugs enabling repurposing and chemical genomics. Science Translational Medicine. 2011;3.

94. Heske CM, Davis MI, Baumgart JT, Wilson K, Gormally M V., Chen L, et al. Matrix screen identifies synergistic combination of PARP inhibitors and nicotinamide phosphoribosyltransferase (NAMPT) inhibitors in Ewing sarcoma. Clinical Cancer Research. 2017;23:7301–11.

95. Williams VM, Filippova M, Soto U, Duerksen-Hughes PJ. HPV-DNA integration and carcinogenesis: putative roles for inflammation and oxidative stress. Future Virology. 2011;6:45–57. doi:10.2217/fvl.10.73.

96. Kusumoto-Matsuo R, Kanda T, Kukimoto I. Rolling circle replication of human papillomavirus type 16 DNA in epithelial cell extracts. Genes Cells. 2011;16:23–33. doi:10.1111/j.1365-2443.2010.01458.x.

97. Hall A. The cytoskeleton and cancer. Cancer and Metastasis Reviews. 2009;28:5–14.

98. Inglese J, Auld DS, Jadhav A, Johnson RL, Simeonov A, Yasgar A, et al. Quantitative high-throughput screening: A titration-based approach that efficiently identifies biological activities in large chemical libraries. Proceedings of the National Academy of Sciences. 2006;103:11473–8. doi:10.1073/pnas.0604348103.

99. Friedrich J, Seidel C, Ebner R, Kunz-Schughart LA. Spheroid-based drug screen: Considerations and practical approach. Nature Protocols. 2009;4:309–24.

100. Chen C, Choudhury S, Wangsa D, Lescott CJ, Wilkins DJ, Sripadhan P, et al. A multiplex preclinical model for adenoid cystic carcinoma of the salivary gland identifies regorafenib as a potential therapeutic drug. Scientific Reports. 2017;7.

101. Li YY, Jones SJM. Drug repositioning for personalized medicine. Genome Medicine. 2012;4.

102. (FDA) USF& D administration. Press Announcements - FDA approves Farydak for treatment of multiple myeloma. U.S. Department of Health and Human Services. 2015. https://www.fda.gov/NewsEvents/Newsroom/PressAnnouncements/ucm435296.htm%0Ahttp://www.fda.gov/NewsEvents/Newsroom/PressAnnouncements/ucm435296.htm.

103. Vandermolen KM, McCulloch W, Pearce CJ, Oberlies NH. Romidepsin (Istodax, NSC 630176, FR901228, FK228, depsipeptide): A natural product recently approved for cutaneous T-cell lymphoma. Journal of Antibiotics. 2011;64:525–31.

104. Jones SF, Bendell JC, Infante JR, Spigel DR, Thompson DS, Yardley D a, et al. A phase I study of panobinostat in combination with gemcitabine in the treatment of solid tumors. Clinical advances in hematology & oncology : H&O. 2011;9:225–30. http://www.ncbi.nlm.nih.gov/pubmed/21475129.

105. Singh A, Patel P, Jageshwar, Patel VK, Jain DK, Kamal M, et al. The Safety, Efficacy and Therapeutic Potential of Histone Deacetylase Inhibitors with Special Reference to Panobinostat in Gastrointestinal Tumors: A Review of Preclinical and Clinical Studies. Current cancer drug targets. 2017;:1–17.

106. Johnson AJ, Yeh YY, Smith LL, Wagner AJ, Hessler J, Gupta S, et al. The novel cyclin-dependent kinase inhibitor dinaciclib (SCH727965) promotes apoptosis and abrogates microenvironmental cytokine protection in chronic lymphocytic leukemia cells. Leukemia. 2012;26:2554–7.

107. Desai BM, Villanueva J, Nguyen TTK, Lioni M, Xiao M, Kong J, et al. The Anti-Melanoma Activity of Dinaciclib, a Cyclin-Dependent Kinase Inhibitor, Is Dependent on p53 Signaling. PLoS ONE. 2013;8.

108. Fu W, Ma L, Chu B, Wang X, Bui MM, Gemmer J, et al. The cyclin-dependent kinase inhibitor SCH 727965 (dinacliclib) induces the apoptosis of osteosarcoma cells. Molecular cancer therapeutics. 2011;10:1018–27.

109. Feldmann G, Mishra A, Bisht S, Karikari C, Garrido-Laguna I, Rasheed Z, et al. Cyclin-dependent kinase inhibitor dinaciclib (SCH727965) inhibits pancreatic cancer growth and progression in murine xenograft models. Cancer Biology and Therapy. 2011;12:598–609.

110. Knudsen ES, Wang JYJ. Targeting the RB-pathway in cancer therapy. Clinical Cancer Research. 2010;16:1094–9.

111. Whittaker SR, Mallinger A, Workman P, Clarke PA. Inhibitors of cyclin-dependent kinases as cancer therapeutics. Pharmacology and Therapeutics. 2017;173:83–105.

112. Almenara J, Rosato R, Grant S. Synergistic induction of mitochondrial damage and apoptosis in human leukemia cells by flavopiridol and the histone deacetylase inhibitor

suberoylanilide hydroxamic acid (SAHA). Leukemia. 2002;16:1331–43.

113. Heijkants R, Willekens K, Schoonderwoerd M, Teunisse A, Nieveen M, Radaelli E, et al. Combined inhibition of CDK and HDAC as a promising therapeutic strategy for both cutaneous and uveal metastatic melanoma. Oncotarget. 2018;9. doi:10.18632/oncotarget.23485.

114. Shen YH, Xu YL. Two new diterpenoids from coleus forskohlii. Journal of Asian Natural Products Research. 2005;7:811–5.

115. Godard MP, Johnson BA, Richmond SR. Body composition and hormonal adaptations associated with forskolin consumption in overweight and obese men. Obesity Research. 2005;13:1335–43.

116. González-Sánchez R, Trujillo X, Trujillo-Hernández B, Vásquez C, Huerta M, Elizalde A. Forskolin versus sodium cromoglycate for prevention of asthma attacks: A single-blinded clinical trial. Journal of International Medical Research. 2006;34:200–7.

117. Majeed M, Nagabhushanam K, Natarajan S, Vaidyanathan P, Karri SK, Jose JA. Efficacy and safety of 1% forskolin eye drops in open angle glaucoma - An open label study. Saudi Journal of Ophthalmology. 2015;29:197–200.

119. Agarwal KC, Parks RE. Forskolin: A potential antimetastatic agent. International Journal of Cancer. 1983;32:801–4.

120. McEwan DG, Brunton VG, Baillie GS, Leslie NR, Houslay MD, Framee MC. Chemoresistant KM12C colon cancer cells are addicted to low cyclic AMP levels in a phosphodiesterase 4-regulated compartment via effects on phosphoinositide 3-kinase. Cancer Research. 2007;67:5248–57.

121. Mathews Griner LA, Zhang X, Guha R, McKnight C, Goldlust IS, Lal-Nag M, et al. Large-scale pharmacological profiling of 3D tumor models of cancer cells. Cell Death and Disease.

2016;7.

121. Alkhilaiwi Faris, Wang Liqing, Zhou Dan, Raudsepp Terje GS, Siddartha Paul, et al. Long-term Expansion of Primary Equine Keratinocytes that Maintain the Ability to Differentiate into Stratified Epidermis. Stem Cell Research & Therapy. 2018;:1–12. https://stemcellres.biomedcentral.com/articles/10.1186/s13287-018-0918-x.

122. Outram AK, Stear NA, Bendrey R, Olsen S, Kasparov A, Zaibert V, et al. The Earliest Horse Harnessing and Milking. Science. 2009;323:1332–5. doi:10.1126/science.1168594.

123. OGOREVC J, LAPANJA T, POKLUKAR K, TOMINŠEK N, DOVČ P. Establishment of primary keratinocyte culture from horse tissue biopsates. Acta agriculturae Slovenica. 2015;106:87–91. doi:10.14720/aas.2015.106.2.3.

124. Madewell, B.R. Cancer. UC Davis Book of Horses, Ed: M. Siegal. 339–345 (1996).

125. Stannard, A.A. and Barlough, J. The Skin and Various Disorders. UC Davis Book of Horses. 164-167 (1996).

126. Bertone AL. Management of exuberant granulation tissue. The Veterinary clinics of North America Equine practice. 1989;5:551–62. http://europepmc.org/abstract/MED/2691030/reload=0.

127. Theoret CL, Barber SM, Moyana TN, Gordon JR. Preliminary observations on expression of transforming growth factors beta1 and beta3 in equine full-thickness skin wounds healing normally or with exuberant granulation tissue. Veterinary surgery : VS : the official journal of the American College of Veterinary Surgeons. 2002;31:266–73.

128. Steel CM, Robertson ID, Thomas J, Yovich J V. Effect of topical rh-TGF-beta 1 on second intention wound healing in horses. Australian veterinary journal. 1999;77:734–7. http://www.ncbi.nlm.nih.gov/pubmed/10685169.

129. Dart AJ, Cries L, Jeffcott LB, Hodgson DR, Rose RJ. The effect of equine recombinant growth hormone on second intention wound healing in horses. Veterinary Surgery. 2002;31:314–9.

130. Cochrane CA. Models in vivo of wound healing in the horse and the role of growth factors. Veterinary Dermatology. 1997;8:259–72.

131. Cyranoski D. Stem cells boom in vet clinics. Nature. 2013;496:148–9.

132. Guest DJ, Smith MRW, Allen WR. Equine embryonic stem-like cells and mesenchymal stromal cells have different survival rates and migration patterns following their injection into damaged superficial digital flexor tendon. Equine Veterinary Journal. 2010;42:636–42.

133. Becerra P, Valdés Vázquez MA, Dudhia J, Fiske-Jackson AR, Neves F, Hartman NG, et al. Distribution of injected technetium99m-labeled mesenchymal stem cells in horses with naturally occurring tendinopathy. Journal of Orthopaedic Research. 2013;31:1096–102.

134. Nagy K, Sung HK, Zhang P, Laflamme S, Vincent P, Agha-Mohammadi S, et al. Induced pluripotent stem cell lines derived from equine fibroblasts. Stem Cell Rev. 2011;7:693–702. doi:10.1007/s12015-011-9239-5.

135. Breton A, Sharma R, Diaz AC, Parham AG, Graham A, Neil C, et al. Derivation and Characterization of Induced Pluripotent Stem Cells from Equine Fibroblasts. Stem Cells and Development. 2013;22:611–21. doi:10.1089/scd.2012.0052.

136. Whitworth DJ, Ovchinnikov D a, Sun J, Fortuna PRJ, Wolvetang EJ. Generation and characterization of leukemia inhibitory factor-dependent equine induced pluripotent stem cells from adult dermal fibroblasts. Stem cells and development. 2014;23:1515–23. doi:10.1089/scd.2013.0461.

137. Aguiar C, Therrien J, Lemire P, Segura M, Smith LC, Theoret CL. Differentiation of equine

induced pluripotent stem cells into a keratinocyte lineage. Equine Veterinary Journal. 2016;48:338–45.

138. Dahm a M, de Bruin a, Linat a, von Tscharner C, Wyder M, Suter MM. Cultivation and characterisation of primary and subcultured equine keratinocytes. Equine veterinary journal. 2002;34:114–20.

139. Visser MB, Pollitt CC. Characterization of extracellular matrix macromolecules in primary cultures of equine keratinocytes. BMC veterinary research. 2010;6:16. doi:10.1186/1746-6148-6-16.

140. Kesmen Z, Sahin F, Yetim H. PCR assay for the identification of animal species in cooked sausages. Meat Science. 2007;77:649–53.

141. Hrdlickova R, Nehyba J, Bose HR. Alternatively Spliced Telomerase Reverse Transcriptase Variants Lacking Telomerase Activity Stimulate Cell Proliferation. Molecular and Cellular Biology. 2012;32:4283–96. doi:10.1128/MCB.00550-12.

142. Raudsepp T, Chowdhary BP. FISH for mapping single copy genes. Methods in molecular biology (Clifton, NJ). 2008;422:31–49. doi:10.1007/978-1-59745-581-7_3.

143. Arrighi FE, Hsu TC. Localization of heterochromatin in human chromosomes. Cytogenetic and Genome Research. 1971;10:81–6. doi:10.1159/000130130.

144. Seabright M. A RAPID BANDING TECHNIQUE FOR HUMAN CHROMOSOMES. The Lancet. 1971;298:971–2.

145. Shamir ER, Ewald AJ. Three-dimensional organotypic culture: Experimental models of mammalian biology and disease. Nature Reviews Molecular Cell Biology. 2014;15:647–64.

146. Knottenbelt DC. Equine wound management: Are there significant differences in healing at different sites on the body? Veterinary Dermatology. 1997;8:273–90.

147. Sharma R, Barakzai SZ, Taylor SE, Donadeu FX. Epidermal-like architecture obtained from equine keratinocytes in three-dimensional cultures. Journal of Tissue Engineering and Regenerative Medicine. 2016;10:627–36.

148. Dakic A, DiVito K, Fang S, Suprynowicz F, Gaur A, Li X, et al. ROCK inhibitor reduces Myc-induced apoptosis and mediates immortalization of human keratinocytes. Oncotarget. 2016;7:66740–53. doi:10.18632/oncotarget.11458.

149. Staiger EA, Al Abri MA, Pflug KM, Kalla SE, Ainsworth DM, Miller D, et al. Skeletal variation in Tennessee Walking Horses maps to the LCORL/NCAPG gene region. Physiological Genomics. 2016;48:325–35.

150. Ghosh S, Qu Z, Das PJ, Fang E, Juras R, Cothran EG, et al. Copy Number Variation in the Horse Genome. PLoS Genetics. 2014;10.

151. F. Coutlée, H. Trottier, S. Gagnon, A. Koushik, H. Richardson, M. Roger, A.S. Ferenczy,E.L. Franco. Low-risk human papillomavirus type 6 DNA load and integration in cervical samples from women with squamous intraepithelial lesions. Journal of ClinicalVirology. 2009. doi:10.1016/j.jcv.2009.03.019.